

Bristol Composites Institute

DOCTORAL RESEARCH SYMPOSIUM

April 2023 University of Bristol

POSTER BOOKLET

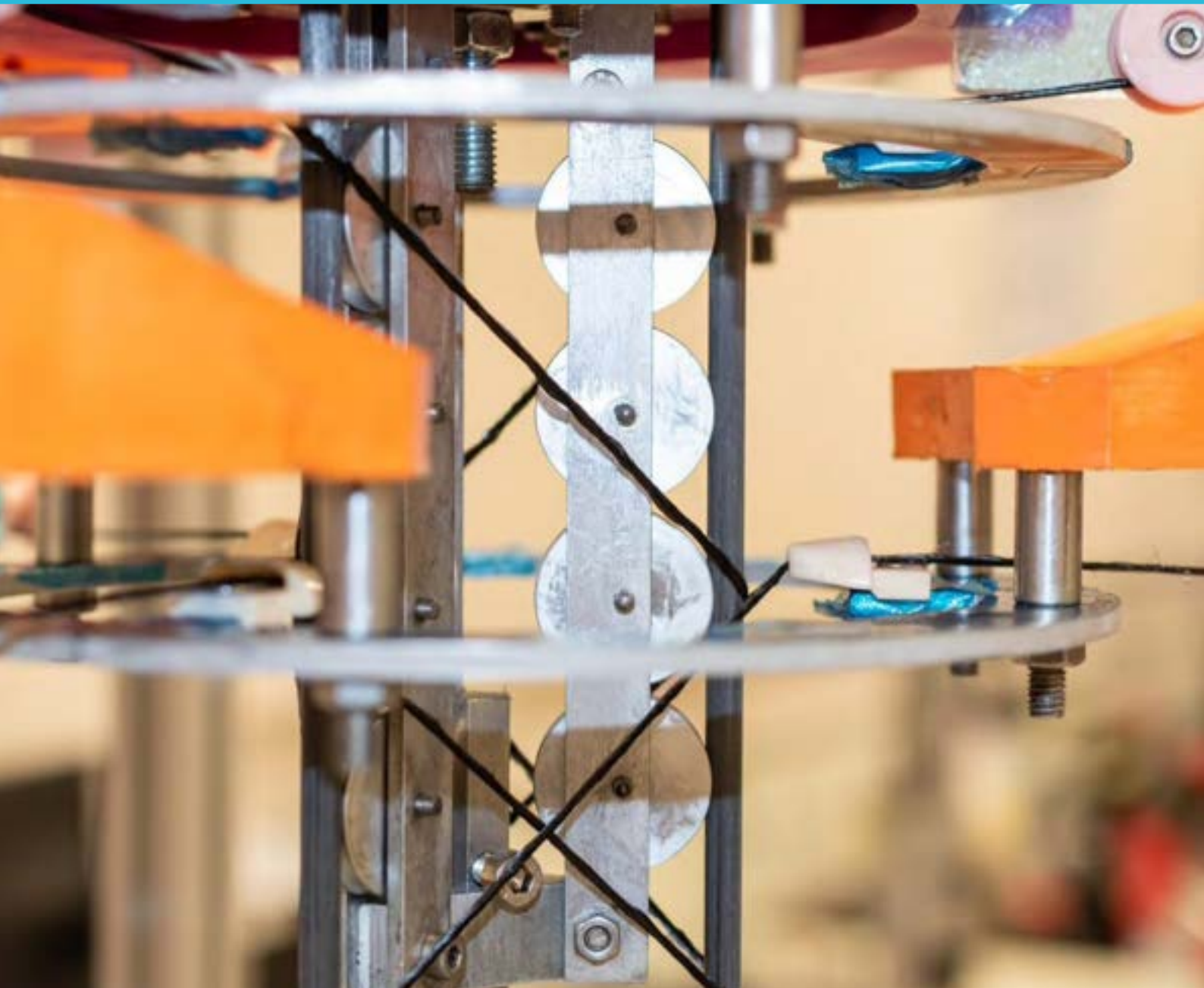


Photo credits: Cover: Francescogiuseppe Morabito



EPSRC Centre for Doctoral
Training in Composites Science,
Engineering and Manufacturing



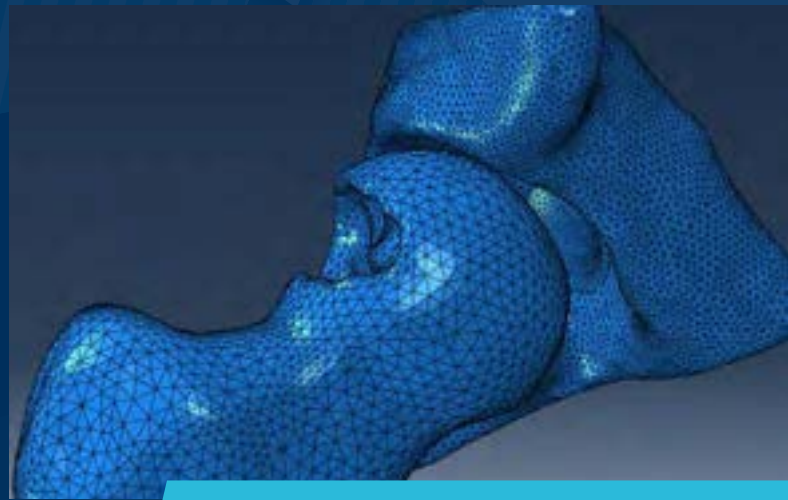
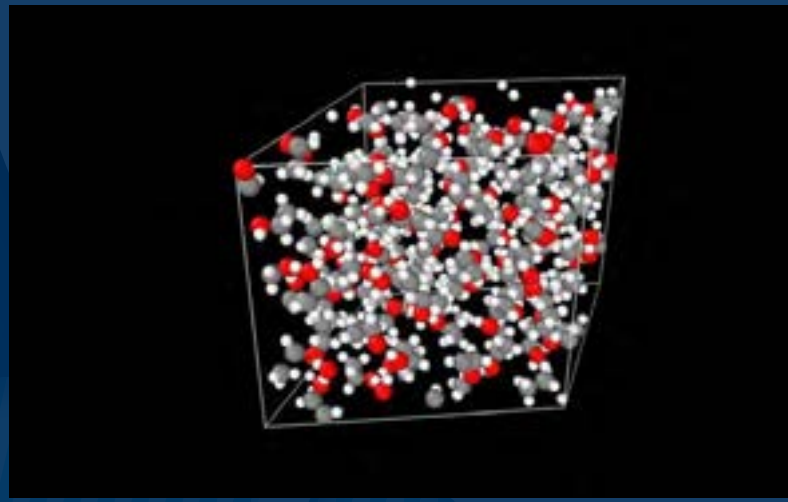
EPSRC Centre for Doctoral Training
in Advanced Composites
for Innovation and Science



Bristol Composites Institute



Engineering and
Physical Sciences
Research Council



MATERIALS

Recycling of FRP wind blade waste material in concrete

Meiran Abdo, Eleni Toumpanaki, Andrea Diambra, Lawrence C. Bank, Gianni Comandini, Stephen Eichhorn

Aims: presenting a new type of discrete reinforcing elements for concrete produced from either waste or new pultruded fibre-reinforced polymer (FRP) composite materials. The FRP-Needles were derived from a reclaimed wind turbine blade made of GFRP and had a nominal thickness of 6 mm and a length of 50 mm (aspect ratio = 8.33). FRP- Needles will be incorporated in concrete to replace 2.5%, 5% and 10% of coarse natural aggregate (NA) by volume. The concrete compressive and splitting tensile strength of the mixes were compared with control specimens.

Materials: A recycled Glass fibre length = 50 mm with [Tensile Strength MPa = 3530, Density(kg.m-3) = 1760, and E (GPa)=230], coarse aggregate a crushed stone average size of 20-22 mm, and an Ordinary Portland Cement.

Results

1. Testing

For analyses simplicity, all specimens in this study were tested in accordance with ASTM C39 and ASTM C496 standards for compressive strength and split tensile strength, respectively see Fig1. The Instron 600DX machine was used for testing all samples, Alicona machine was used to obtain a surface roughness measurement for the FRP Needles.

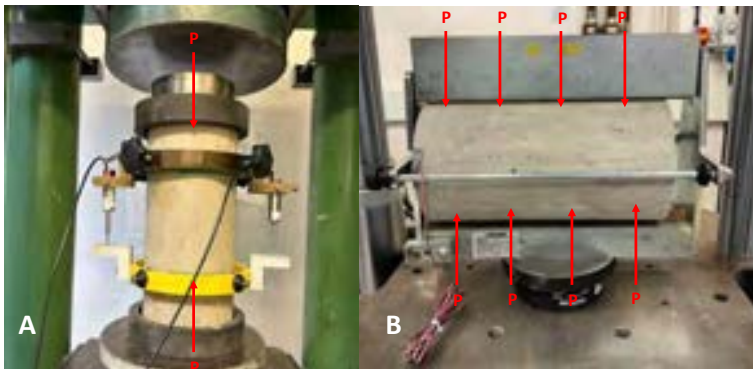


Figure 1: A) compressive test (ASTM C39) . B) split tensile test (ASTM C496).

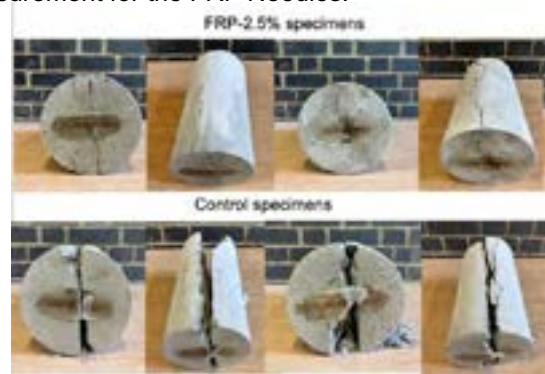


Figure 2: Splitting fracture Pattern types .

2. Fracture Patterns : The fracture patterns have been identified for the split tensile test of the cylinder concrete at age 14 days in Fig.2 which shows an improvement in the impact strength for samples with 2.5% FRP while no improvement was observed for the post peak. All fracture patterns were reported based on ASTM C39 standard.

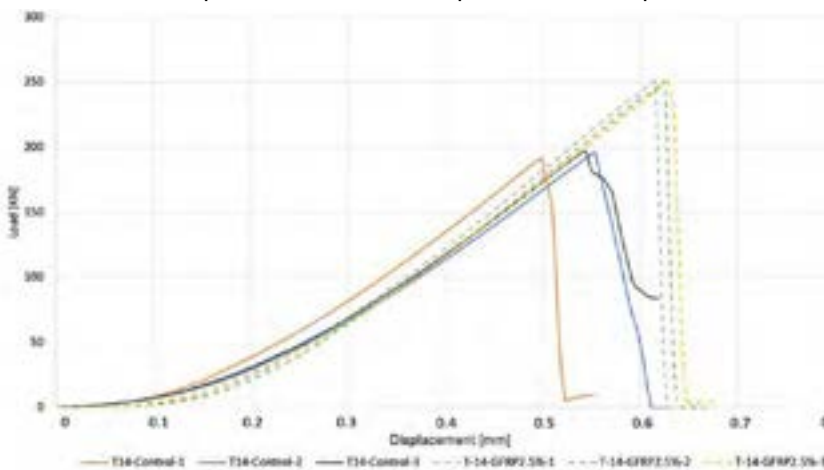


Figure 3: Split Tensile Strength load vs displacement.

Conclusions :

- The results in Fig.3 shows that: Adding 2.5% replacement of FRP leads to improvement of the tensile strength by 26.09% compared with control specimens.
- Adding 2.5% replacement FRP leads to compressive strength reduction by 6.73% compared with control specimens. However, they are still in above 30 MPa and adequate for design of structural members

3. FRP Needles surface analysis: studying the surface roughness is a very important element for improving the surface bonding between FRP and cement in the mix. The Alicona machine is used to compare the roughness of the needles before and after sandblasting.

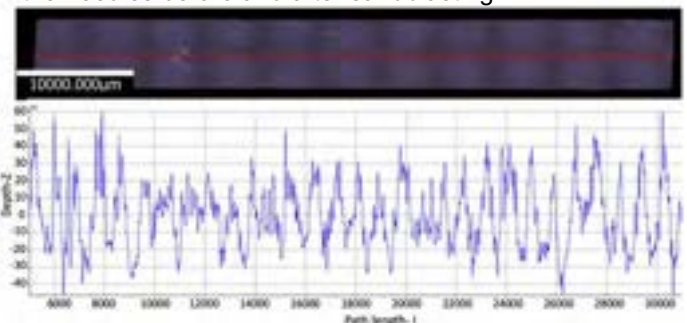


Figure 4: FRP Needles surface roughness measurement after sandblasting.

Further developments:

- Implementing 5% and 10% FRP Replacement.
- Improving the surface bonding between FRP and cement in the mix.
- Finding optimum needles geometry.
- Studying the long-term mechanical performance of FRPcrete for structural applications considering different variables.

Mycelium Composites as a Sustainable Alternative for Developing Countries



Stefania Akromah, Neha Chandarana, Stephen J. Eichhorn

Background

To drive socio-economic development, Africa and other developing countries need cost-effective sustainable solutions that can increase agricultural productivity, revenue, and employment^{1,2}. In this regard, mycelium composites, a novel class of bio-based materials made of agricultural waste particles bound in fungal mycelium, represent a promising material. They are cost- and energy-efficient; they add value to and provide an eco-friendly waste management route for agricultural waste; they are biocompatible, biodegradable, and compostable. However, the low strength and stiffness of the mycelium binder limits their applications³.

Aim:

To improve strength and stiffness of mycelium matrix via approaches inspired by work done with "SuperWood"⁴.

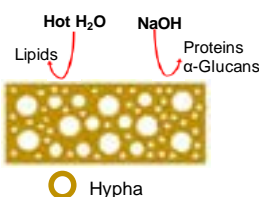
Objectives:

1. To control and improve orientation of mycelium hyphae
2. To partially dissolve weak cell wall components to increase interfacial bond sites
3. To improve the stiffness of mycelium by additional chemical treatment followed by hot-pressing
4. To assess the sustainability of mycelium composites as alternatives for developing countries

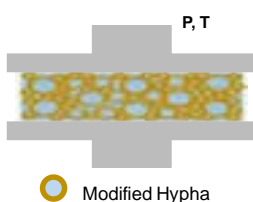
1. Orientation



2. Chemical Treatment



3. Hot-Press



4. Sustainability

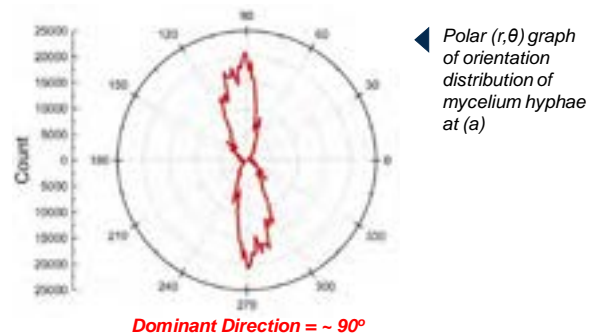


Experiments

Orientation



◀ Oriented mycelium culture on agar plate



◀ Polar (r,θ) graph of orientation distribution of mycelium hyphae at (a)

Key findings

Oriented growth can be achieved by exploiting the natural growth mechanisms of fungi (i.e., negative autotropism & positive nutrient chemotropism).

What's next...

1. Oriented growth optimization
2. Chemical analysis by Raman Spectroscopy
3. Characterization of tensile properties

References

1. SDG/A. Africa 2030: SDGs within social boundaries – Leave no one behind Outlook. <https://sdg.africa/> (2021).
2. African Development Bank Group. Feed Africa: Strategy for Agricultural Transformation in Africa 2016-2025. (2016).
3. Jones, M., Maitiner, A., Luenco, S., Bismark, A. & John, S. Engineered Mycelium Composite Construction Materials from Fungal Biorefineries: A Critical Review. *Mater Des* **187**, 108397 (2020).
4. Song, J., Chen, C., Zhu, S. et al. Processing bulk natural wood into a high-performance structural material. *Nature* **554**, 224–228 (2018). <https://doi.org/10.1038/nature26476>

Figures

1. Stack of mycelium composites obtained from: <https://www.frontiersin.org/articles/10.3389/fmats.2021.737377/full>
2. SDG Africa image obtained from: <https://africa.com/2021/09/21/new-portal-drives-sdg-in-africa/>



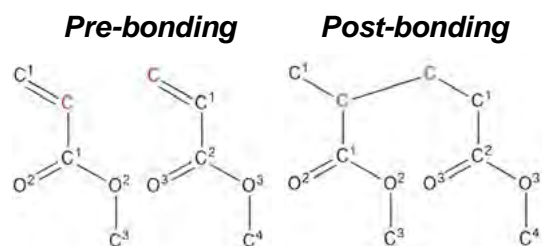
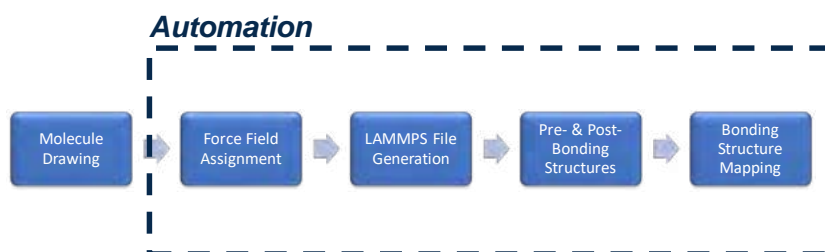
Automating Modelling for Digital Materials Science

Matthew A. Bone, Terence Macquart, Brendan J. Howlin, Ian Hamerton

Model Pre-Processing Automation

Molecular dynamics (MD) is an atomistic scale simulation tool that enables virtual characterisation of key material and manufacturing properties. Through computational chemistry, new polymer matrices can be screened for glass transition temperature (T_g), melting temperature, viscosity, Young's modulus and many more. This saves researchers time and money by reducing the volume of laboratory experiments needed to discover new materials. It is also a more sustainable way of doing research, as no waste disposal is needed for simulation!

One of the key issues when simulating polymers with computational chemistry is the model setup. Extensive pre-processing is required to parameterise monomers and allow them to bond. This PhD project has developed a suite of tools to automate the pre-processing required. Using chemical graph theory, we can map atoms in a molecule before and after a reaction has happened. This allows the user to simply draw the molecules and then begin polymerisation, significantly speeding up model setup.



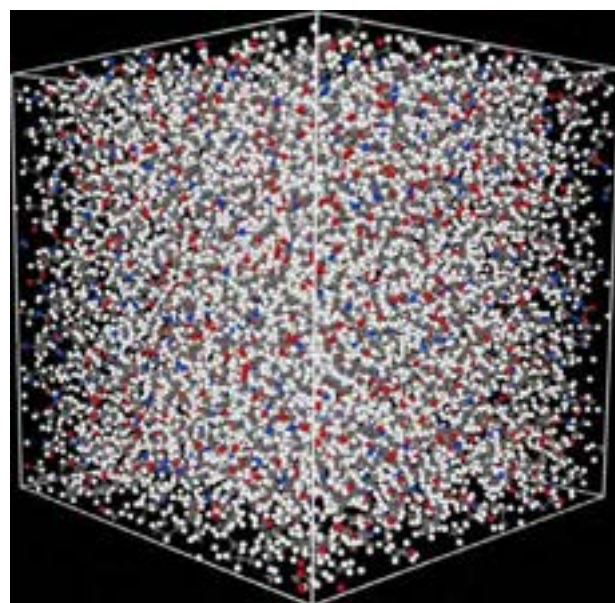
Rapid Surrogate Models with AI

MD simulations come with high computational cost – determining the T_g of a polymer can take 24 – 36 hrs on a supercomputer node.

A simple neural network model trained on features representing the local chemical environment of a polymer has been shown to predict the T_g to within 10 – 20 K mean absolute error. The concept of AI surrogate models with atomistic simulation is now being explored further.



Molydyn is commercialising this technology with its web platform Atlas, designed to help beginners and experts access valuable simulation data.



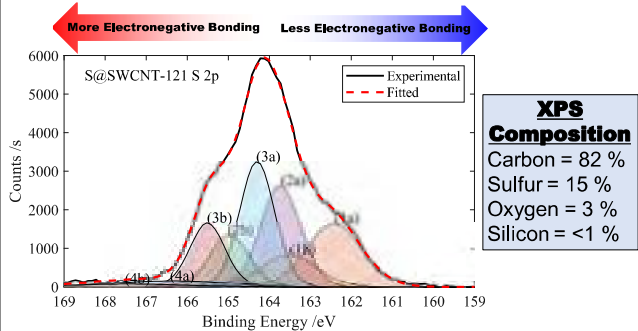
Magnetization Measurements of S@SWNCT Nanocomposites in a Hydrogen Atmosphere

Charles D. Brewster[†], Lui R. Terry, Sebastien Rochat, Valeska P. Ting

Carbon/sulfur[1,2] and carbon/sulfur/hydrogen[3] composites are of increasing interest within the energy sector for **hydrogen storage**[1] and **hydrogen-based superconductivity**[2,3]. Here we study the magnetic properties of **sulfur-encapsulated single-walled carbon nanotubes (S@SWCNTs)** under vacuum and **100 mbar of hydrogen** down to 2 K. We show the magnetic moment of the composite can be **altered by exposure to hydrogen** at cryogenic temperatures. Although **superconductivity was not observed** in this system, our findings demonstrate the potential for hydrogen as a strategy for **tuning the magnetic properties** of S@SWCNTs with envisioned applications in **magnetic hydrogen technologies**[4] and **spintronics**.

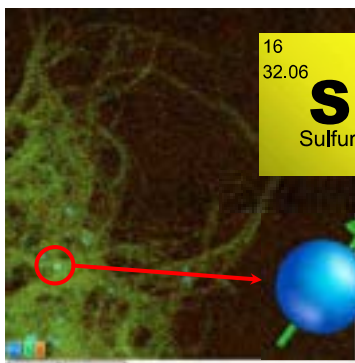


Sulfur Speciation



- Peaks 1a/1b suggest **confined polysulfide species** within the sample. Further confirmed by **Raman spectroscopy**[5].
- Peaks 2a/2b show small **polysulfide motifs** (S_x ($2 < x < 8$)).

Morphology



Sulfur
Sulfur is **spatially coincidental** with carbon, implying sulfur is located in/on the carbon nanotubes.

Cobalt Impurities
Single-domain ferromagnetic **cobalt nanoparticles** present from synthesis (despite additional removal steps)

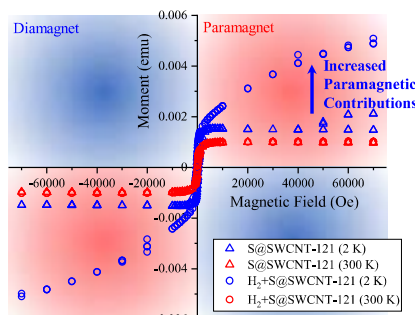
Conclusion

- The presence of **ferromagnetic nanoparticulate impurities** dominates the likely weak diamagnetic response of S@SWCNTs.
- Interactions of hydrogen with the S@SWCNT composite show **hysteretic magnetization properties**.
- Potential applications for **magnetic hydrogen technologies** at cryogenic temperatures.

Future Work

- Modelling and subtraction of the magnetic moment of cobalt with the **Langevin function**.
- Experimentation of different **porous carbon/sulfur composites** to determine the effect of pore morphology.

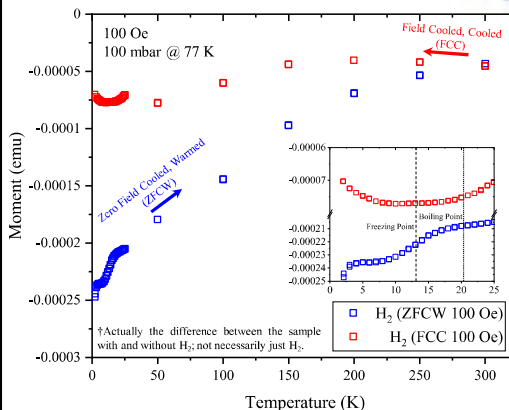
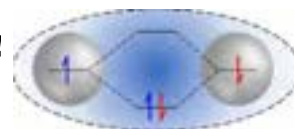
Magnetic Measurements



- Magnetic moment of S@SWCNT is largely dominated by the **superparamagnetic response** of cobalt nanoparticles.
- Enhanced paramagnetic contribution** from interactions with hydrogen.
- Enhancement **limited to cryogenic conditions**

SOMETHING UNEXPECTED!

Molecular hydrogen (H_2) has **no unpaired electrons** therefore, should be diamagnetic!



H₂ Adsorption Properties of S@SWCNTs



- Phase changes** of hydrogen are clearly visible by **abrupt changes in magnetic moment**.
- Adsorption of hydrogen ($T > 20$ K)** results in greater diamagnetic moment.
- Cooling the sample in an external field **"locks" spin states** of hydrogen interacting with the sample.
- Solid- H_2 phase transition in the presence of an external magnetic field shows **hysteretic paramagnetic behaviour**.

References

- J. P. Paraknowitsch and A. Thomas, *Energy & Environmental Science*, 2013, **6**, 2839-2855.
- I. Felner, *Magnetochemistry*, 2016, **2**, 34.
- A. P. Drozdov, M. I. Erements, I. A. Troyan, V. Ksenofontov and S. I. Shylin, *Nature*, 2015, **525**, 73-76.
- P. V. Shinde and C. S. Rout, *Nanoscale Advances*, 2021, **3**, 1551-1568.
- C. D. Brewster, L. R. Terry, H. V. Doan, S. Rochat and V. P. Ting, *Energy Advances*, 2023, DOI: 10.1039/D2YA00242F.

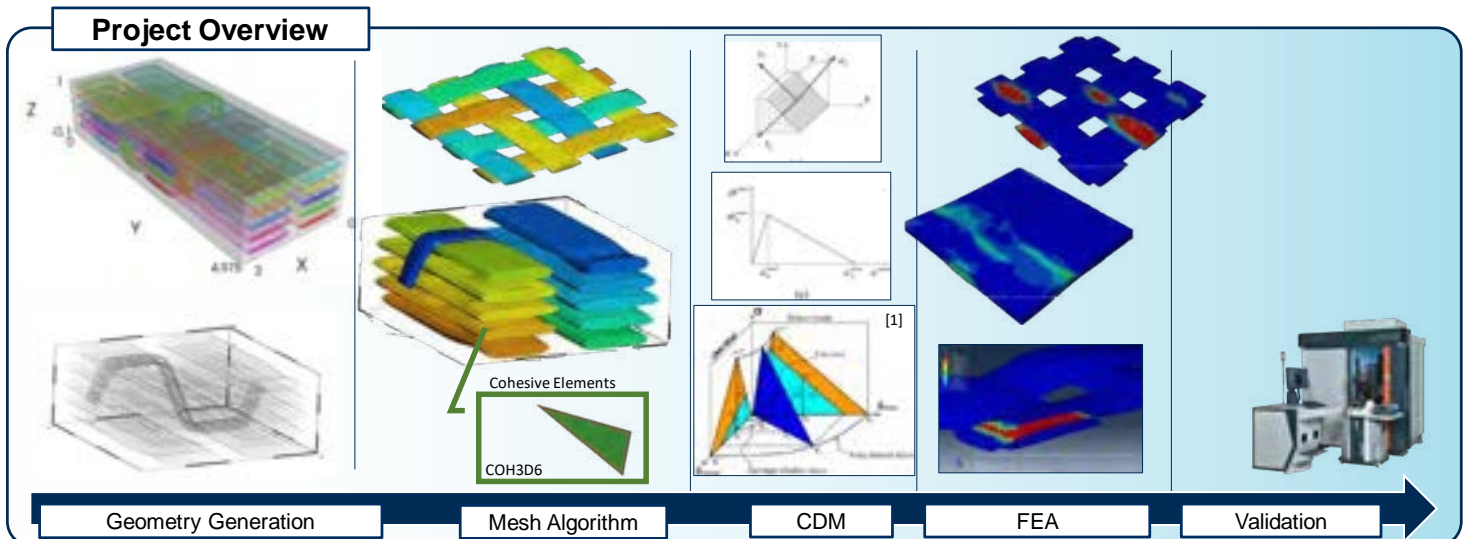


Advanced High-Fidelity Modelling of Woven Composites

Ruggero Filippone, Dr. Bassam El Said, Dr. Adam Thompson, Dr. Peter Foster and Prof. Stephen Hallett

This research aims to develop state-of-the-art modelling capabilities for meso-scale damage modelling in woven textile composites. In particular, 3D woven composites debonding is one of the key damage mechanisms that have been extensively observed via experimental test studies. In the absence of debonding models, Matrix cracks can progress directly from matrix to yarn materials, resulting in a premature prediction of failure.

Here, a dedicated meshing framework is proposed to include reliable debonding failure detection in the meso-scale models of textile composites. In this first stage of research, a dedicated model has been implemented to generate a structured mesh of woven composites. It can automatically generate the geometry of the RUC (Representative Unit Cell) of a tessellated woven fabric embedded into the matrix, generating a tailored structured mesh for both of yarns and matrix. Furthermore, the cohesive elements are generated into the interfaces region to investigate how the stress/strain state in these regions generate the debonding defect, leading to an anticipated failure.



Advanced H-F Modelling

A dedicated algorithm has been implemented to generate a high-fidelity model of a 2D or 3D Woven fabric at Meso-Scale. The output file can be read by FE Software to run the analysis.

Main Features:

- Selectable Geometry
- High fidelity of contact surfaces between yarn and matrix.
- Conformal Mesh generation.
- Possibility to generate Cohesive Elements around the yarns.
- Kinematic simulation
- High resolution of interface regions between yarns and Matrix

CDM

VUMAT subroutines:

- Yarn** [2] *Puck's theory*
Matrix cracking under transverse compression

$$\left(\frac{\tau_T}{S_T - \mu_T \sigma_N}\right)^2 + \left(\frac{\tau_L}{S_L - \mu_L \sigma_N}\right)^2 = 1$$

- Yarn Interface** [1]
Quadratic damage initiation criterion
under a multi-axial stress state

$$\left(\frac{\sigma_1}{\sigma_{1c}}\right)^2 + \left(\frac{\sigma_2}{\sigma_{2c}}\right)^2 = 1$$

Failure Criterion

$$\left(\frac{\sigma_1}{\sigma_{1c}}\right)^2 + \left(\frac{\sigma_2}{\sigma_{2c}}\right)^2 = 1$$

- Matrix pockets**
Drucker-Prager Linear Hardening

$\beta = \arctg \frac{3 - 3r}{1 + r}$	E_m	3GPa
$r = \frac{\sigma_1}{\sigma_2}$	ν	0.855
$\varphi = \arctg \frac{3(1 - 2\nu\beta)}{2(1 + \nu\beta)}$	$\nu\beta^2$ ($\nu = 0.03$)	0.5
	β	13.2
	φ	0 plastic incompressibility

Hexply IM7/8552

Results and Future Work

To date, the FEAs show a high quality of results in terms of stress gradients and prediction of failures in the matrix. Furthermore, the Cohesive elements increased the investigation spectrum of the Damage mechanics onset in Woven Fabrics, showing a correlation between delamination and crack initiation on the matrix.

Next works will observe the crack onset of the tested coupon, in order to validate the model with 3D woven composites. For this purpose, a dedicated CDM VUMAT will be developed for viscoelastic materials.

[1] Wen-Guang Jiang, Stephen R. Hallett (2007)
[2] Supraticket, Ali (2019)

Towards more sustainable fibre composites with improved compressive performance

Eleni Georgiou^a, Gustavo Quino^{a,b}, Ian Hamerton^a, Richard Trask^a

^a BCI, University of Bristol, ^b Department of Aeronautics, Imperial College London

Longitudinal compression failure is a design limiting factor for continuous fibre reinforced polymers (FRPs), with compression strength being up to 60% lower than the tensile strength for a given composite material. To develop more sustainable material systems with enhanced compressive performance, reliable and repeatable methodologies for materials characterisation are essential. Various challenges arise when testing under uniaxial direct compression, including complex specimen preparation, sensitivity to specimen alignment, stress concentrations at gripped regions, the need to avoid global buckling and high variability in results. In this work, the compression side of a PMMA beam under bending is used to test high modulus carbon/epoxy pultruded rods, consistently achieving acceptable compressive failures within the gauge section. Carbon/epoxy has been chosen for this testing campaign since this material is relatively well understood in compression, and so can be used to experimentally validate the methodology before it is applied to more sustainable fibre composites, such as basalt fibre.

PhD Project Motivation and Aims:

- The superior tensile and compressive properties of basalt fibre composites (BFCs) when compared to E-glass, coupled with their cost effectiveness, low moisture content (<0.1%) and high thermal stability, means that BFCs have high potential for structural applications
- Industry adoption of BFCs is currently limited due to a lack of extensive materials characterisation, and therefore confidence, in mechanical properties
- This project aims to characterise and increase the mechanical performance of BFCs, focusing on the compressive strength, which is a critical design limiting factor for FRPs, and the damage mechanisms associated with failure

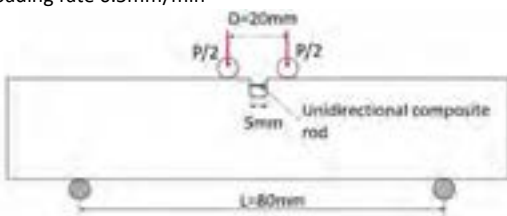


Current Objectives:

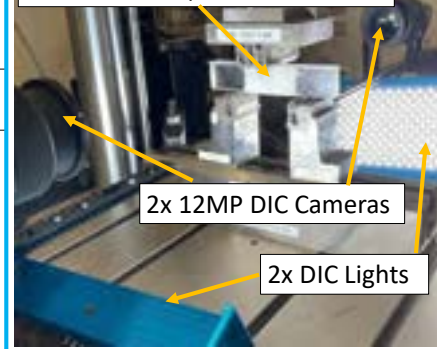
- To adapt a 4 point bend test methodology [1] to reliably and repeatably characterise the compressive properties of pultruded composite rods
- To apply the test methodology to BFCs to establish the underlying damage mechanisms associated with their compression failure

Materials & Experimental Setup:

- 4 point bend test setup
- High modulus carbon fibre pultruded circular rods, $\phi 0.7\text{mm}$
- Gauge length 5mm
- 2D Digital Image Correlation (DIC) with 2 cameras
- Loading rate 0.5mm/min

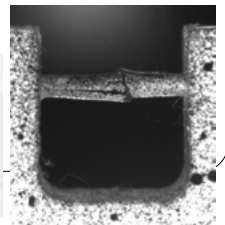
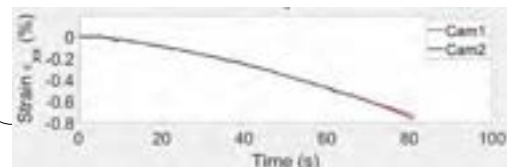


PMMA beam with carbon/epoxy rod loaded in 4 point bend fixture



Results:

- 0.87% \pm 0.2 mean failure strain
- Kink band formation
- Longitudinal splitting occurred suddenly and concurrently with final failure



Future Work:

- Characterise fibre alignment in rods using optical microscopy
- Develop an FEA model to validate current and future experimental results
- Improve Digital Image Correlation (DIC) setup by improving camera field of view, using finer speckle pattern for finer strain resolution and improving specimen alignment
- Repeat experiments with improved setup to validate methodology with reduced variability in strain results
- Apply test to other materials systems for compression characterisation

Cryogenic Thermal Shock of Epoxy Nanocomposites

James Griffith^a, Dr. Karthik Ram Ramakrishnan^{a, b}, Dr. Marcus Walls-Bruck^b, Dr. Sebastien Rochat^c, Prof. Valeska Ting^a, Prof. Ian Hamerton^{a, b}

Liquid Hydrogen (LH₂) for Civil Aviation

Liquid hydrogen (LH₂) is hydrogen gas cooled down to **20 K (-253°C)**. It is widely considered the best zero carbon emission alternative to kerosene to service the majority of the aircraft market, with a **better payload and range** than:

- Batteries, which have low gravimetric energy efficiency
- Gaseous H₂, which requires a larger tank mass for lower density and higher pressure storage
- Ammonia, which has environmental concerns and high fuel system mass

However, there are numerous challenges to overcome, with the Aerospace Technology Institutes 2022 Technology Strategy stating "The biggest research and technology challenges concern the safe storage and use of cryogenic hydrogen as a fuel on aircraft..."¹

LH₂ Storage Challenges

While composite tanks offer a predicted 43-47% mass saving over metallic tanks, which can translate to considerable lifelong cost savings of \$2000/kg², carbon fibre reinforced polymers (CFRP) are susceptible to matrix microcracking in cryogenic environments.

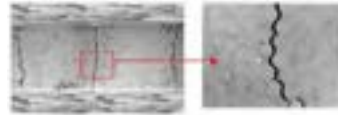


Figure 1: Microcracking in composites due to transverse stress³

This can lead to:

- Increasing LH₂ and H₂ permeation
- Decrease in tank stability
- Potential delamination or tank rupture if the LH₂ in cracks boils off during thermal cycling

Causes of Cryogenic Matrix Microcracking

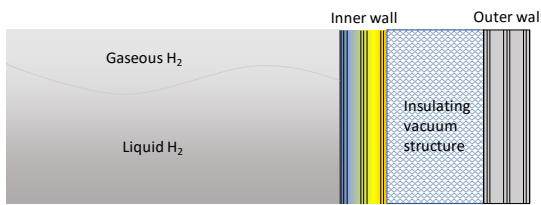


Figure 2: Schematic of inner wall CFRP thermal shock

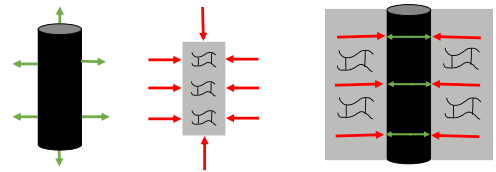


Figure 3: Co-efficient of thermal expansion (CTE) mismatch in constituents

Thermal shock of the composite material through exposure to cryogen

Temperature gradient across material

Build up of transient residual stresses

Micro-cracking

Build-up of compressive stress at the fibre-matrix interface

Opposing expansion and contraction of constituents

Constituent CTE Mismatch⁴

Research Questions

1. Without the issue of CTE mismatch, will microcracking occur in the epoxy matrix alone due to thermal shock from cryogenic cycling?
2. Can microcracking be prevented by matrix toughening and how do the physical properties of the matrix change during cryogenic cycling?

Results

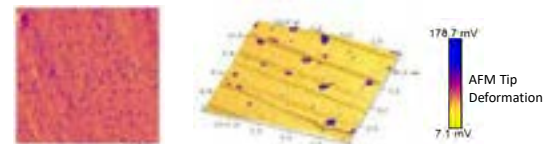


Figure 6: Atomic Force Microscopy (AFM) depicting softer particles within the stiffer matrix of the particle and thermoplastic-particle toughened material after cryogenic cycling

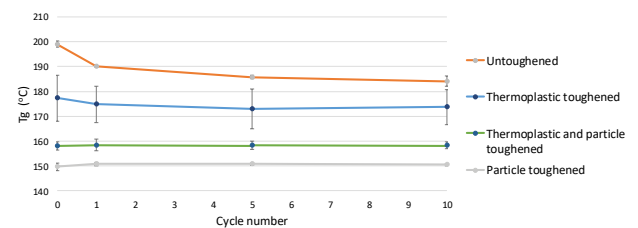


Figure 7: Change in glass transition temperature (T_g) with cryogenic cycling

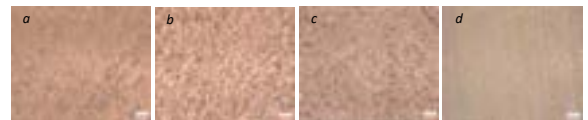


Figure 8: Optical microscopy of a) untoughened b) thermoplastic toughened c) particle toughened and d) thermoplastic and particle toughened epoxies after 10 cryogenic cycles, exhibiting no microcracking

Materials and Methods

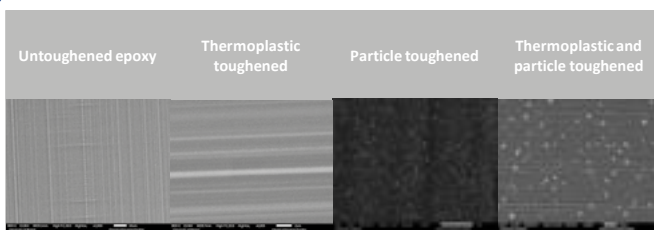


Figure 4: SEM cross-section of matrix materials investigated



Figure 5: Cryogenic cycling method. Liquid nitrogen was used due to availability and safety issues with testing in liquid hydrogen

Conclusions

- Thermal shock through fast cooling cryogenic cycling did not cause microcracking in toughened and untoughened epoxy resins
- This suggests the fibre-matrix CTE mismatch plays a larger role in composite matrix microcracking than thermal shock during fast cooling
- Elastomeric particle toughening led to better cryogenic performance by maintaining physical properties during thermal cycling

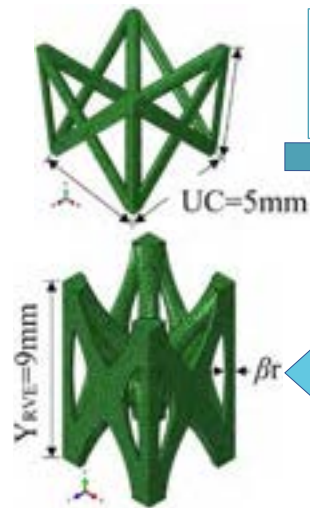
1. Technology Strategy 2022 - Destination Zero. 2022, Aerospace Technology Institute
2. Newbury, S., FZO-ACA-REP-0056 Academic Programme Research Findings. 2022, FlyZero, Aerospace Technology Institute.
3. Mallik, K., et al., Ultralight Linerless Composite Tanks for In-Space Applications, in Space 2004 Conference and Exhibit. 2004.
4. Sapi, Z. and R. Butler, Properties of cryogenic and low temperature composite materials – A review. Cryogenics, 2020. 111: p. 103190.

Multi-Objective Mechanical Optimisation of Lattice Cores

Athina Kontopoulou, Bing Zhang, Fabrizio Scarpa, Giuliano Allegri

Sandwich panels allow reducing structural weight by replacing traditional monolithic components. Our work aims to develop lattice cores with superior **mechanical** properties for high-performance sandwich panels. The topology of the lattice unit cell are crucial for the overall performance. Here, we aim to **maximise** the **compressive (E_2)** and **out-of-plane shear stiffness (G_{23})** of lattice cores using a **multi-objective genetic algorithm (GA)**. A representative unit cell (RUC) of lattice designs is used in **finite element (FE)** modelling framework which is incorporated with the GA-driven **optimisation**. Emphasis is given to the manufacturability of these lattice designs, considering layer by layer additive manufacturing constraints in the **variables bounds** used for the optimisation, as well as a **relative density constraint**. The optimised lattice cores are being tested numerically in full-scale models as well as experimentally.

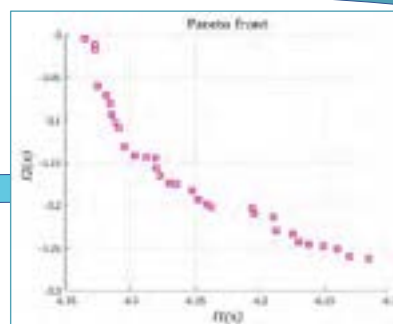
Micro-mechanical Optimisation



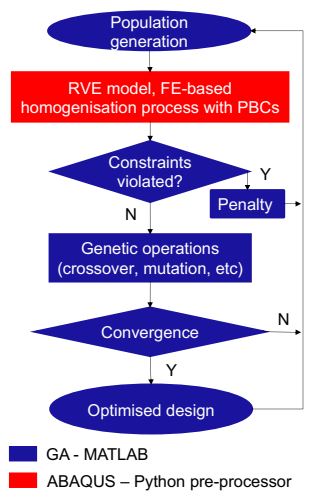
Objectives: minimise $f_1(x) = -\log(E_2)$
 minimise $f_2(x) = -\log(G_{23})$
 Subject to relative density (ρ_{rel}) **constraint:**

$$\rho_{rel} = \frac{\rho^*}{\rho_s} = \frac{V_{lat}}{V_{RVE}} \leq 0.4$$

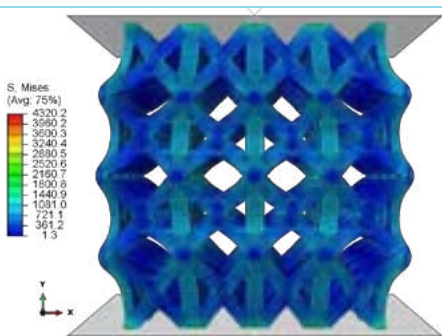
Variable	Lower bound	Upper bound
r	0.3 mm	0.7 mm
YRVE	5.0 mm	10.0 mm



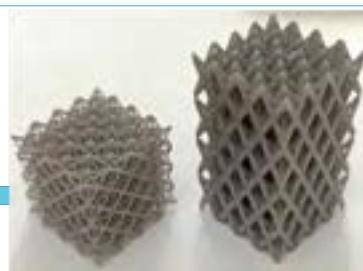
Computational Approach



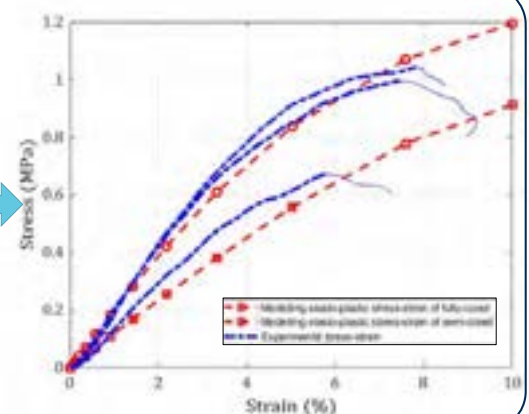
Macro-mechanical Validation



Elasto-plastic full-scale models under quasi-static compression load.



Additive manufactured samples through Stereolithography are tested under quasi-static compression load.



Conclusions

- By tapering the radius of the struts the stress concentration is also decreased close to the nodes of the lattice structure.
- With tapering parameter (β) equal to 0.43, we can increase the compressive stiffness by 12.5% and the out-of-plane shear stiffness by 7%.

Future work

- Investigate the dynamic properties of these lattice structures through numerical predictions and experimental validation.

Kinking in UD CFRPs Imaged In-Situ via High Resolution Synchrotron Radiography

K. Nelms, Y. Wang, Y. Chen, A. Rack, S. Rawson, Eric Maire, P. J. Withers

Background

The critical weakness of FRPs is their compression strength, which tends to be only 60% of their tensile strength [1] due to sudden failure by kink band formation. Kinks (fig. 1) are regions of fibers deflected at a significant angle relative to the loading direction and delineated by planes of fiber fractures. They are often accompanied by fiber microbuckling, fiber fractures, and longitudinal splitting [2]. However, how these failure modes interrelate, and their contribution to kink band initiation and propagation is debated.

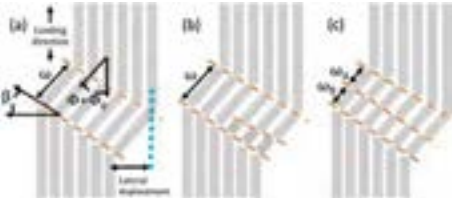


Fig. 1 : (a) key features are band width ω , band angle β , and the fiber angle, $\phi+\phi_0$. Multiple bands form as (c) complete bands "stacked" on one another or (b) smaller (sub-critical) bands

Much initial experimental work aiming to investigate kink band formation were limited to 2D studies post mortem. In-situ studies utilizing microscopy have only recently been published. Though insightful regarding propagation, these studies cannot capture 3D effects or kink initiation.

X-ray computed tomography is a non-destructive technique enabling imaging in 3D post mortem, in-situ or time-lapse sequences during loading [3]. A tomogram is reconstructed from 100s or 1000s of radiographs collected as the sample is rotated. This process limits the temporal resolution and requires that sample movement not occur during acquisition of radiographs.



Fig. 2: schematic of CT acquisition; a single radiograph plane is in focus at a time

The aim of this study was to use ultra-fast in-situ synchrotron radiography (20kHz frame rate) during compression of a unidirectional (UD) CFRP to capture the kink initiation and propagation mechanism in high temporal AND spatial resolution

Methods

UD FRPs were fabricated from Torayca T700 carbon fibre yarns and Huntsman Araldite LY 564/XB 3486 epoxy resin. A small-scale resin infusion (SSRI) method was developed to achieve cylindrical FRPs with high volume fraction and low porosity [4]. CFRPs were cured at 80°C for eight hours. The ends of the sample were inserted into steel end caps and a notch was made to encourage failure within the field of view of the synchrotron detector

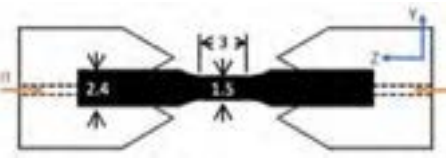


Fig. 3: Sample geometry and loading direction

In situ synchrotron x-ray radiography was conducted at the European Synchrotron Research Facility using a tension-compression loading rig developed at INSA-Lyon for in-situ CT studies [5]. Samples were compressed at 1 $\mu\text{m/s}$. Radiographs were collected at 20,000 fps using a Photron FASTCAM SAZ. The resulting voxel size was 1.1 μm and exposure time was 50 μs . The failure was recorded over 25 frames.

This specimen was scanned on a Zeiss Versa 520 X-ray scanner in the Henry Moseley X-ray Imaging Facility post mortem. A source voltage of 50 kV was used to produce 3201 projections taken over a rotation of 180°. The exposure time was 7 seconds per projection and voxel size was 1.28 μm . The Feldkamp-Davis-Kress (FDK) algorithm [6] was used for reconstruction and the reconstructed volume was viewed and segmented using Avizo 2019.

Acknowledgements

Huge thanks to my co-authors, Ying Wang, Yunhui Chen, Alex Rack, Shelley Rawson, Jerome Adrien, Eric Maire, and especially my advisors, Philip J. Withers and Neha Chandarana. Thanks to the ESRF ID19 team for the beamtime and support, and to CT-specialists Dr. Tristan Lowe and Dr. Billy Koe for their support and expertise. Finally, we acknowledge the EPSRC for funding via grants EP/R00661X/1, EP/S019367/1, EP/P025021/1, EP/P025498/1, EP/T02593X/1.

Results

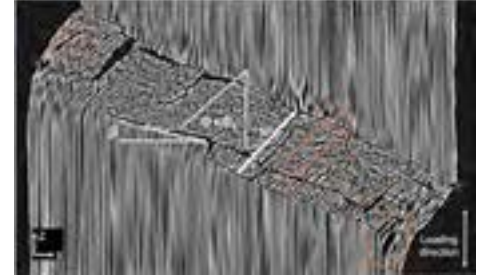


Fig. 4: Central CT slice of our sample after failure. Key geometric features tabulated below, orange lines represent sub-critical bands, and orange ellipses show longitudinal splits.

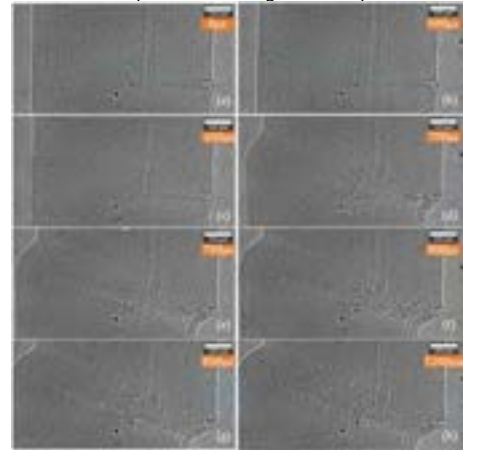


Fig. 5: X-ray radiographs leading up to and during failure for frames a) 1, b) 13, c) 14, d) 15, e) 16, f) 17, g) 18 and h) 25. The blue lines indicate length of the microbuckled region.

Fibers microbuckle elastically in concert (fig. 5a, 5b). The region appears to become reduced vertically as the fibers rotate with increased loading. For each frame, the largest fiber rotation angle is seen near the notch. This microbuckled region appears to propagate across the sample at a translation rate of 0.2 $\mu\text{m}/\mu\text{s}$ in 650 μs prior to kink initiation. The kink initiates at some point between frame 13 and frame 14 (Fig. 5c). This suggests that Majority of the kink band initiates and propagates within 50 μs (between fig. 5c and d), suggesting the band must travel laterally at a speed of at least 16.3 \pm 1.3 mm/msec.

REFERENCES

1. B. Budiansky and N. A. Fleck, *Journal of the Mechanics and Physics of Solids*, 1993.
2. B. Budiansky, et. al. *Journal of the Mechanics and Physics of Solids*, 1998.
3. S. C. Garcea, et. al. *Composites Science and Technology*, vol. 156, pp. 305-319, 2018.
4. Y. Wang, et. al. *ECCM17*, 2016.
5. E. Maire, et. al. *International Journal of Fracture*, 2016.
6. L. A. Feldkamp, et. al. *Journal of the Optical Society of America*, 1984.

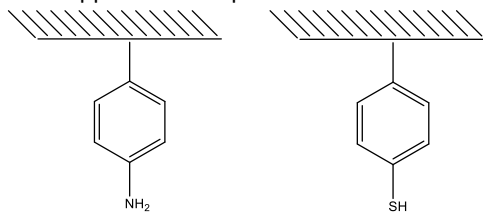
TMD and carbon nanocomposites for room temperature superconductivity.

Rikesh Patel, Prof Simon Hall, Prof Steve Eichorn, Dr Chris Bell

Superconductors are materials that, below a critical temperature, exhibit 0 DC resistance and expel an applied magnetic field from within itself. Often, the critical temperature is reached through cryogenic cooling. However, a mechanism of superconductivity, known as excitonic superconductivity, has been hypothesised to allow for room temperature superconductivity, through the compositing of transition metal dichalcogenides and carbon. No excitonic superconductor has yet been realised. This project aims to take the existing theory and make it a reality.

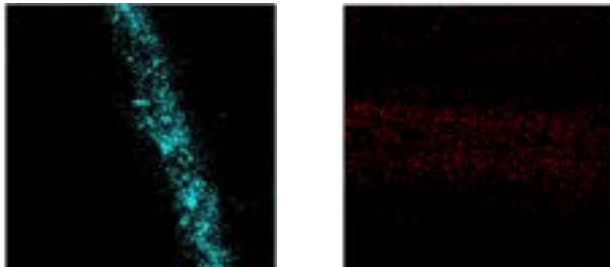
Method

Carbon fibers were functionalised with the metallophilic amine and thiol groups by Prof Luke Henderson's group at Deakin University. These fibers were then dipped in a suspension of 10 nm WSe₂ Nanoparticles in ethanol.

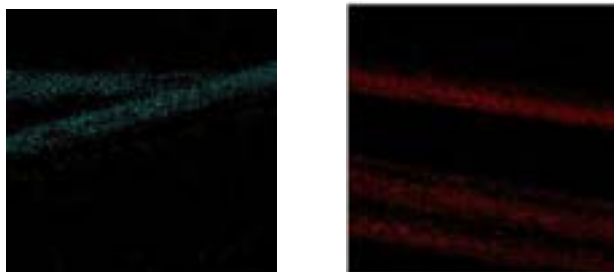


Time Of Flight Secondary Ion Mass Spectrometry

TOF-SIMS was used to determine the coverage of the applied coatings.



Thiol coated fibre without (left) and with (right) WSe₂ coating
Blue shows (C-S-H)⁺ fragments, red shows Se⁺ fragments

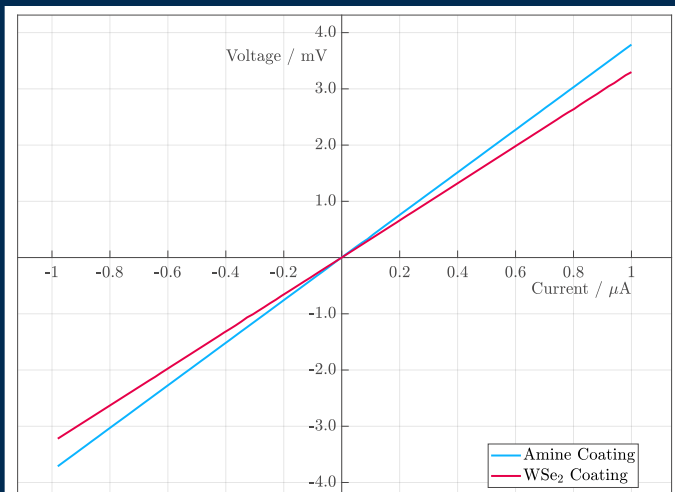


Amine coated fibre without (left) and with (right) WSe₂ coating
Blue shows (C-N-H₂)⁺ fragments, red shows Se⁺ fragments

Conclusions and Further Work

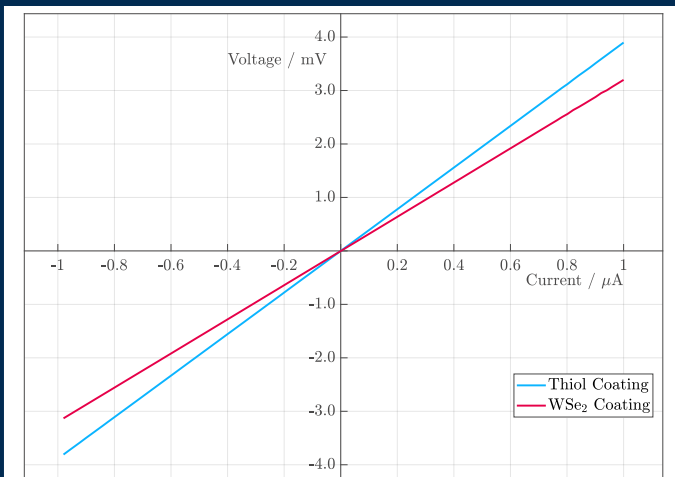
- Uniform coating of fibers after submission.
- Coated fibers are less resistive but superconductivity not seen.
- What is causing the change in resistance?
- Will superconductivity arise at lower temperatures?

Amino Coated Fibers 4 – Point Resistance Measurement



The addition of WSe₂ reduced the resistivity of the amino coated fibers by 1.81 μΩ m.

Thiol Coated Fibers 4 – Point Resistance Measurements



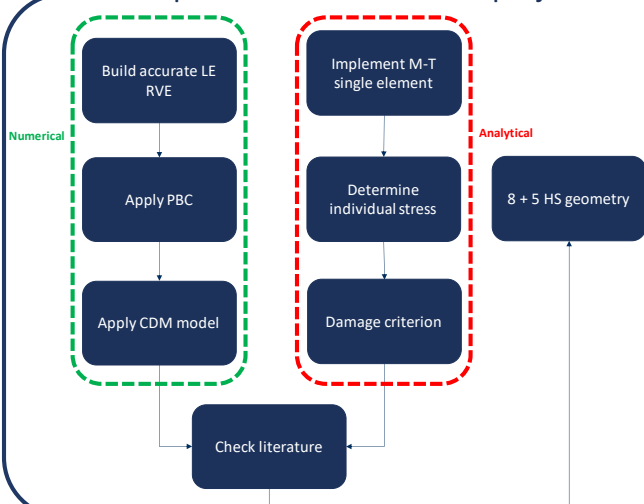
The addition of WSe₂ reduced the resistivity of the thiol fibers by 2.74 μΩ m

An analytical framework for fatigue simulation of Oxide/Oxide Ceramic Matrix Composites

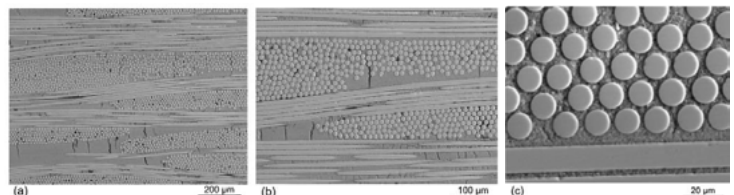
Alex Poyser, Giuliano Allegri, Stephen Hallett

This project aims to accurately predict the micromechanical behaviour of highly porous Oxide-Oxide Ceramic Matrix Composites (Ox/Ox-CMC), which can withstand the highly oxidative and corrosive environments in gas turbine engines. In Ox/Ox CMC, the fibres do not feature an interphase coating. The large volume fraction of porosity within the matrix controls the desired toughening behaviour. The mechanical behaviour of Ox/Ox-CMC is as unique as the underlying microstructure.

Proposed workflow for the project

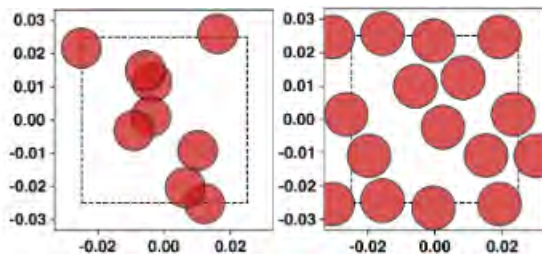


Data provided by Rolls-Royce will be used comparatively against mean-field homogenisation based on an Extended Mori-Tanaka (ExM-T) scheme and Representative Volume Elements generated by MicroTool. The micro-scale RVE. The numerical and analytical models will utilise Continuum Damage Mechanics (CDM) and a Damage criterion, respectively. The micro-scale results will generate an analytically based meso-scale RVE of 5 or 8 Harness Satin (HS) geometry. Below are varying SEM magnifications of Nextel 610 in a porous alumina matrix, as provided by Simon (2005)[1].



Simon 2005 International Journal of Applied Ceramic Technology 141 – 149 [1]

Random Fibre Placement inside an RVE



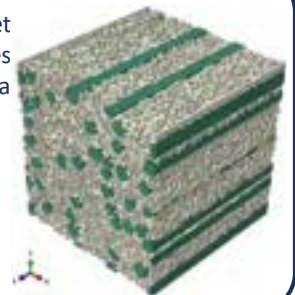
MicroTool uses Equations 1, 2 and 3 described by Pathan et al. (2017)[2] and Melro & Manno (2021)[3] to place fibres randomly in the RVE. Here there is a fibre v_f of 0.19 and a porosity v_p of 0.36.

$$F = \sum_{k=1}^{N_c} \alpha_k^2 \quad (1) \quad -R_i \leq \{x_i, y_i\} \leq L_{RVE} + R_i \quad \forall i \in N \quad (2)$$

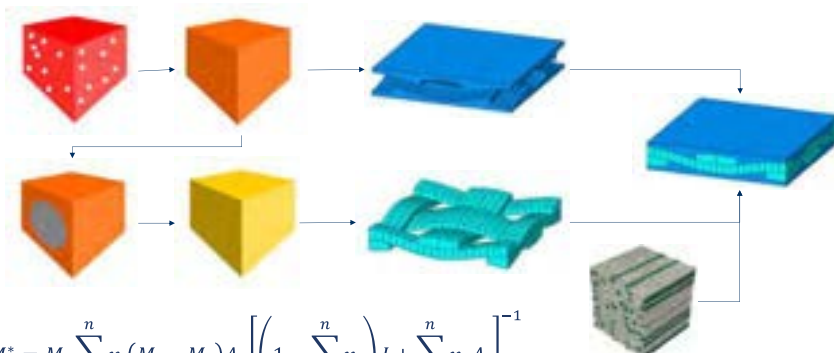
$$\sqrt{(x_i - x_j)^2 + (y_i - y_j)^2} \geq R_i + R_j + l_{min} \quad \forall i, j \in N \quad i \neq j \quad (3)$$

Pathan et al. 2017 Composites Part B 267 – 278 [2]

Melro & Manno 2021 Mechanics Modelling of Fibre-Reinforced Polymer Composites 31 – 54 [3]



Two-stage homogenisation of a porous matrix and a fibre inclusion



The first stage, homogenisation of the porous matrix forms the matrix characteristics in the meso-scale RVE. In the second stage, homogenisation of the fibre within the matrix forms the characteristics of the fibre tows at the meso-scale.

Benchmarking using the Micro-scale RVE and literature will validate the values of the two-stage ExM-T before fibre tow geometry is applied.

An iterative process utilising the Christensen damage criterion will then be applied to the RVE to replicate the onset of damage. Equation 4 shows Siboni & Benveniste's (1991) [4] multiphase homogenisation process.

Siboni & Benveniste 1991 Mechanics of Materials 107 – 122 [4]

$$M^* = M_1 \sum_{j=2}^n v_j (M_j - M_1) A_j \left[\left(1 - \sum_{j=2}^n v_j \right) I + \sum_{j=2}^n v_j A_j \right]^{-1} \quad (4)$$

Assessment of Subsurface Damage in Multi-directional Composite Structures using TSA

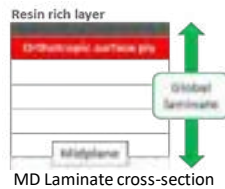
R. Ruiz Iglesias, G. Olafsson, O.T. Thomsen, J.M. Dulieu-Barton

Background of the project [1]

Resin Rich Layer Model: $\Delta \epsilon_{DIC} \rightarrow \Delta T_{RRL}$
The RRL is thermally isolated from the laminate stack

Global Laminate Model: $\Delta \epsilon_{DIC} \rightarrow \Delta T_{GL}$
 ΔT is generated by the strain experienced by the GL

Orthotropic Surface Ply Model: $\Delta \epsilon_{DIC} \rightarrow \Delta T_{SP}$
The SP is an isolated ply, so heat transfer effects are neglected



Aim & Objectives

Aim: Develop a novel full-field imaging methodology combining Thermoelastic Stress Analysis (TSA) and Digital Image Correlation (DIC) to identify subsurface damage as it evolves by creating non-adiabatic conditions in the composite laminate under cyclic loading.

Objectives:

- Analyse the thermoelastic response of laminated coupons after being damaged.
- Detect both surface and subsurface damage using a combination TSA and DIC.

Thermoelastic Stress Analysis and Digital Image Correlation

Thermoelastic Stress Analysis (TSA) is a full-field non-contact infra-red imaging technique that is based on measuring minor temperature variations (ΔT) on the surface of a component when is cyclically loaded.

$$\Delta T = \frac{-T}{\rho C_p} (\alpha_1 \Delta \sigma_1 + \alpha_2 \Delta \sigma_2) = \frac{-T}{\rho C_p} ([\alpha]_{1,2}^T [Q]_{1,2} [T] [\Delta \epsilon]_{xy})$$

Digital Image Correlation (DIC) is a full-field non-contact white light imaging technique tracing the movement of a speckle pattern applied on the material surface, calculating its displacement and strains.

*BFS-U3-5155P-C USB 3.1 Blackfly®

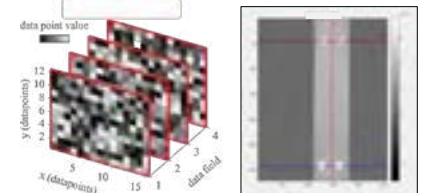


Telops FAST M3K



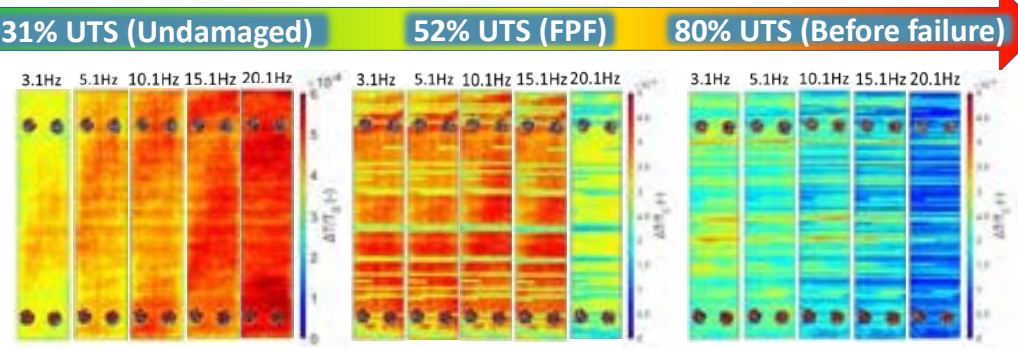
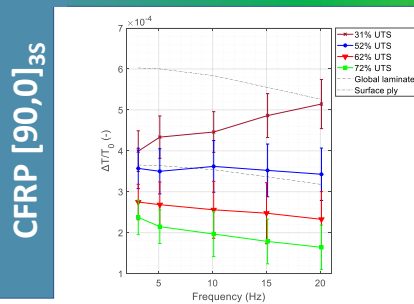
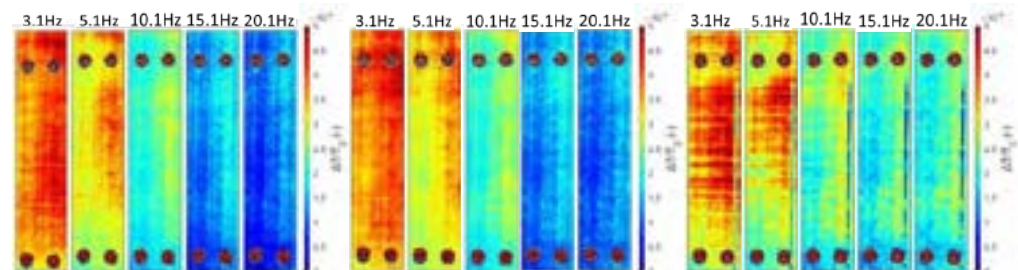
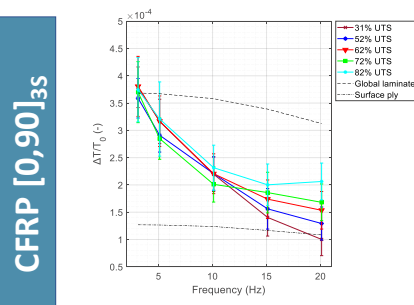
Blackfly® Cameras*

Full-field data fusion [2]



Enables comparing and quantitatively fusing full-field planar data by converting to a local spatial resolution.

Laminated Composites Subsurface Damage



31% UTS (Undamaged) 52% UTS (FPF) 80% UTS (Before failure)

CONCLUSIONS

- Subsurface thermoelastic response is visible at low loading frequencies, indicating that subsurface damage can be identified.
- Both surface and subsurface damage is visible for CFRP [0,90]_{3s} at low loading frequencies.
- CFRP [90,0]_{3s} adopts 0 ply thermoelastic response after inducing damage.

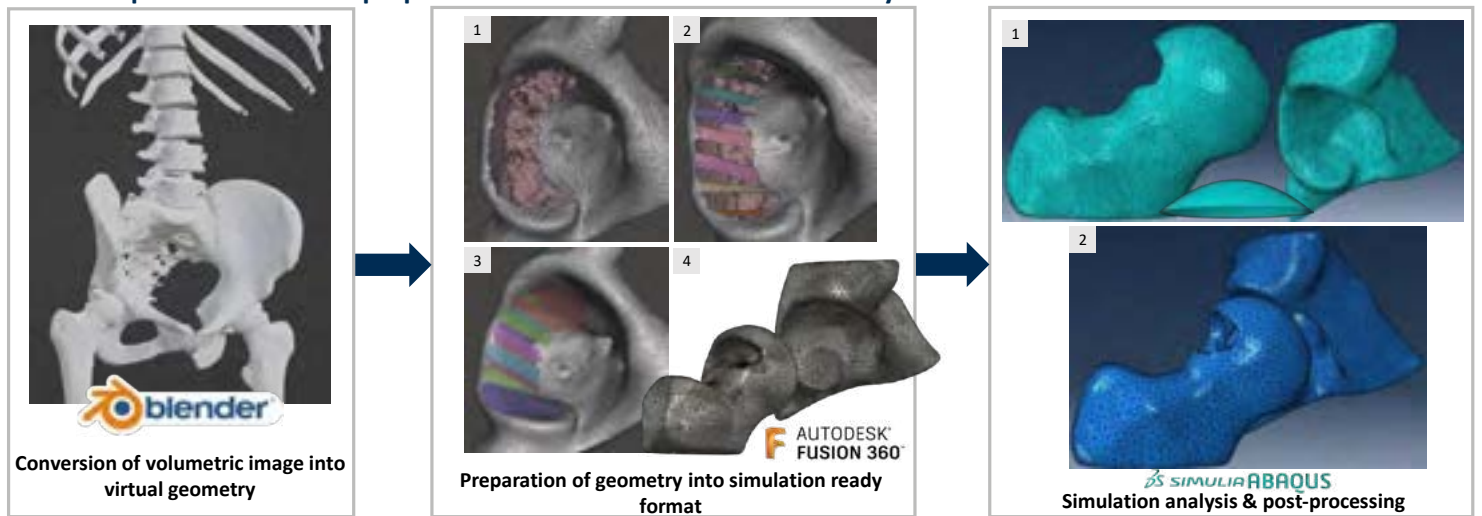
The optimisation of soft composite systems for biomedical applications

Joe Surmon¹, Sebastien Rochat², Kate Robson-Brown³, Richard Trask¹

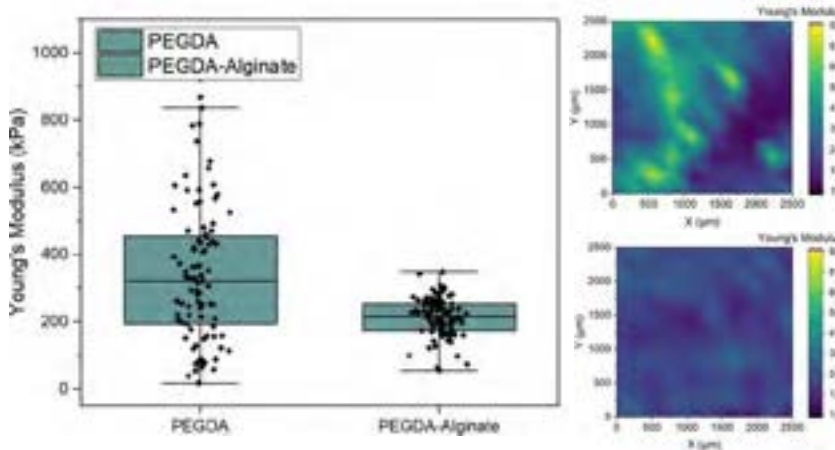
Medical CT-scans from the 'New Mexico Decedent Database' have been obtained and processed for modelling in Abaqus. The workflow is outlined below. Micro-indentation measurements have been taken on soft materials and will be compared to real human tissue. Pre-notched tensile testing has been used to assess the fracture resistance of the soft composite systems.



1. Complete workflow for preparation of CT-scans to simulation-ready format

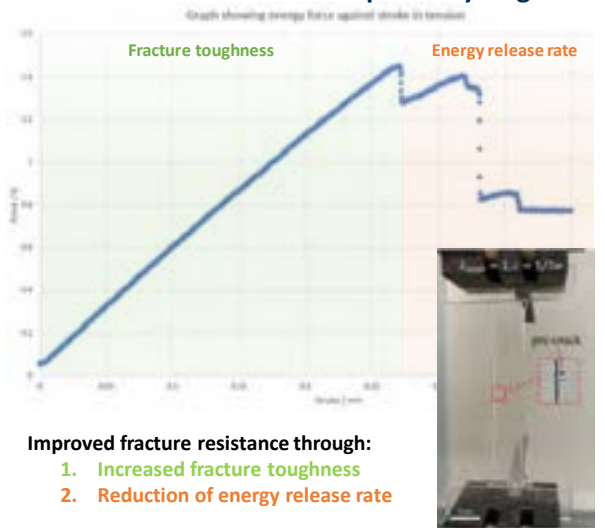


2. Microindentation of composite hydrogels



Microindentation of hydrogels over a 1 cm² test area with 10 x 10 measurements taken to produce a box plot and surface map of Young's Modulus values

3. Fracture resistance of composite hydrogels



Conclusion

- A range of methods are employed to optimise soft composite material systems for load-bearing applications
- Simulations have been used to validate experimental data and extrapolate to anatomical models

Future Work

- Full fracture resistance testing of hydrogel composite systems investigating: semi-IPN systems, hydroxyapatite and clay nanoparticles
- Complete hip-joint simulation testing

Investigation of the compressive behaviour of thin-ply composites with 4-point flexural test

Aree Tongloet, Xun Wu, Michael R. Wisnom

Introduction

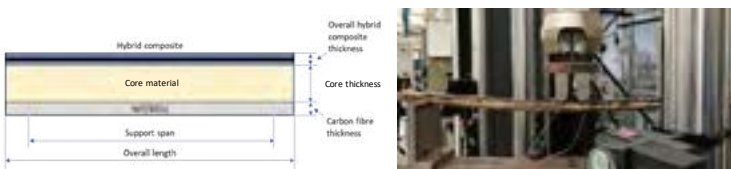
- Tensile failure of thin-ply hybrid composites has been presented in various studies.
- Compressive behaviour of the glass/thin carbon hybrid composites is still not well understood.
- Four-point flexural tests on sandwich beams have been introduced to achieve pure compressive failure in the gauge section and chosen to investigate the compressive behaviour of the S-glass/carbon hybrid composites and to obtain a baseline compressive strain.

The aims of the study

- Investigate the compressive failure strain of the carbon fibre hybrid composites.
- Investigate the failure mechanism of hybrid composites with different absolute carbon fibre ply thicknesses.

Experiment setup

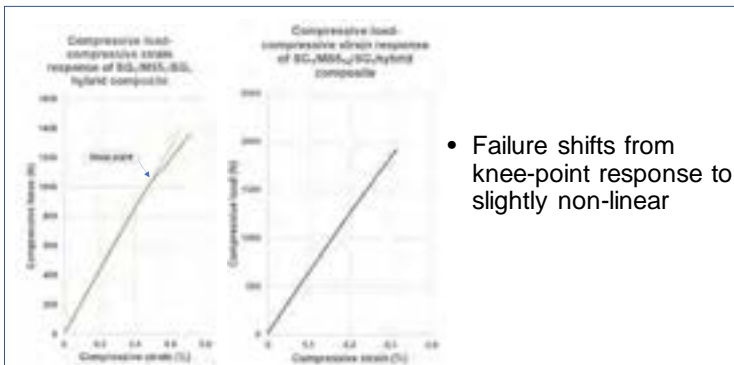
- 4-point bending fixture with Instron universal testing machine
- Attach strain gauges on top and bottom skin to measure compressive and tensile strains.



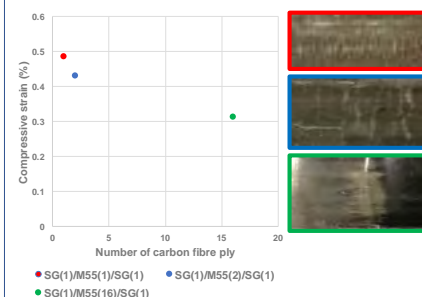
Hybrid configurations

Hybrid configurations	Carbon fibre thickness (mm)
SG ₁ /M55 ₁ /SG ₁	0.03
SG ₁ /M55 ₂ /SG ₁	0.06
SG ₁ /M55 ₁₆ /SG ₁	0.48
SG ₁ /TC33 ₁ /SG ₁	0.03
SG ₁ /TC33 ₂ /SG ₁	0.06
SG ₁ /TC33 ₁₆ /SG ₁	0.48

Load-strain response of SG₁/M55_n/SG₁ composites



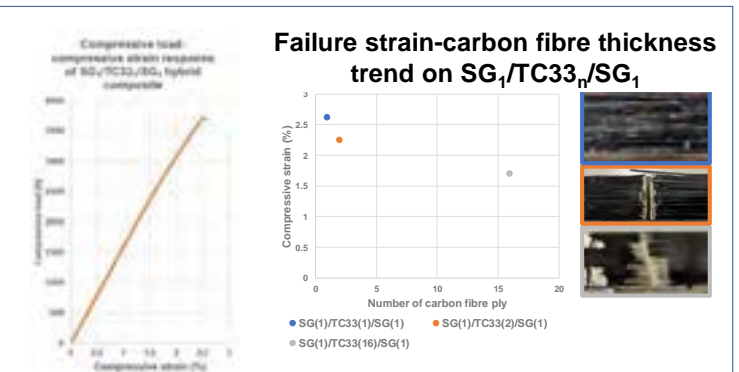
- Failure shifts from knee-point response to slightly non-linear



Failure strain-carbon fibre thickness trend on SG₁/M55_n/SG₁

- Shear instability is not the failure mechanism, as shown by small carbon fragmentations from SG₁/M55_n/SG₁ configuration.
- The absolute thickness of M55 carbon fibre controls the failure characteristics of the hybrid composites.

Load-strain response of SG₁/TC33_n/SG₁ composites



- Shear instability is the failure mechanism shown by sudden fibre failure.
- Very high strain can be achieved which offers greater advantage to enhance carbon fibre properties in these laminates.

Summary of the study

- Compressive behaviour and failure strain are affected by the thickness of low-strain fibre material.
- The failure of hybrid composites switched from fragmentation to shear instability type of failure for the M55 case.
- The proper high-strain/low-strain hybrid system could increase the compressive performance.

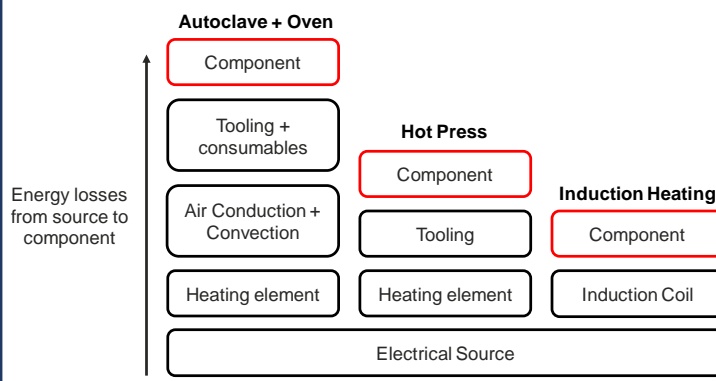
Inductive heating potential for energy efficient composites processing

J. Uzzell, L. R. Pickard, I. Hamerton, D.S. Ivanov

Energy efficiency is extremely important in regards to the future of composite manufacturing. Current methods such as autoclave and oven curing are highly inefficient as energy is wasted heating surrounding air, consumables and tooling with high thermal mass. Heating rate is also limited due to conductive heat transfer from the air through the thickness of a composite.

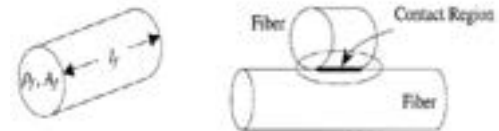
Electromagnetic (EM) induction provides rapid, volumetric and localised heating with minimal energy wasted. Heat is produced directly within electrically conductive carbon fibres reducing losses to tooling and allowing good temperature control and high heating rates.

Motivation:



Principle:

- Carbon fibres are sufficiently electrically conductive to produce eddy currents.
- Heating is produced in fibres due to resistance (Joule heating) and contact resistance at fibre junctions.



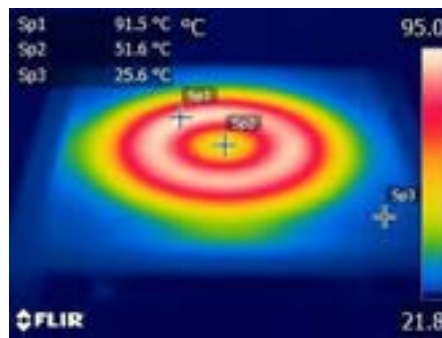
Advantages:

- Rapid – controlled by power input, high ramp rates as high as 10 deg/sec.
- Volumetric – Heat produced within laminate (fibres).
- Localised – Heating pattern directly matches EM field generation.

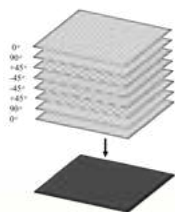


Challenge:

- Temperature distribution is highly non uniform.
- Low thermal conductivity both in plane and through thickness reduces heat spread from localised heating region.



Solutions: Material Architecture



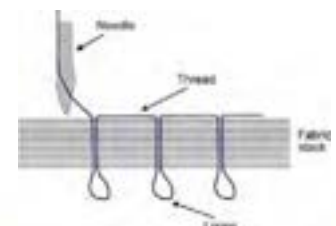
Layup, volume fraction and material properties

Coil Geometry



Novel coil design for inplane uniformity

Functionalisation



Through thickness tufting with metallic braids



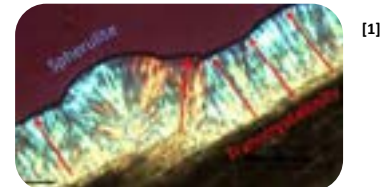
Crystallisation Modelling of Thermoplastics for interfacial strength predictions in composite over-moulding products

Maria Veyrat Cruz-Guzman

Dmitry Ivanov, Steve Eichhorn, Jonathan Belnoue, James Myers

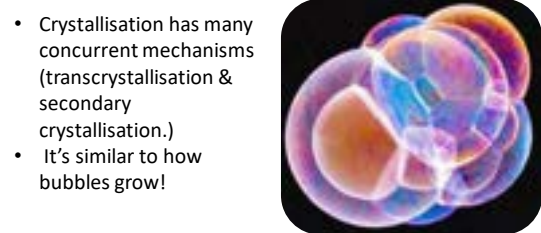
Composite over-moulding

- Increasingly viable solution for complex, multifunctional loaded structures
- Hybrid manufacturing process
- The quality of the heat-fused interface is important as there is a need for high-performance regenerated interfaces in thermoplastic composites



Crystallisation

- There is an important relationship between the two where **increasing crystallinity substantially decreases interfacial strength**.
- Crystallisation is complex to predict
- It is the most important phase transition to consider when processing thermoplastics



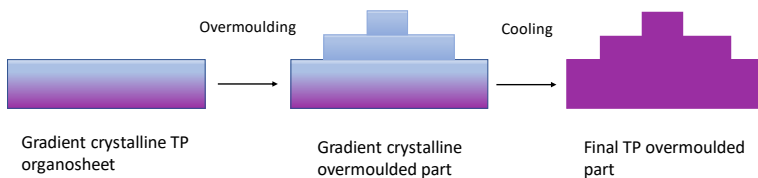
- Crystallisation has many concurrent mechanisms (transcrystallisation & secondary crystallisation.)
- It's similar to how bubbles grow!

- A simplistic 1D model was made as a tool to predict the crystallinity of a thermoplastic laminate & to explore the feasibility of alternative TP processing through the creation of a gradient crystallinity

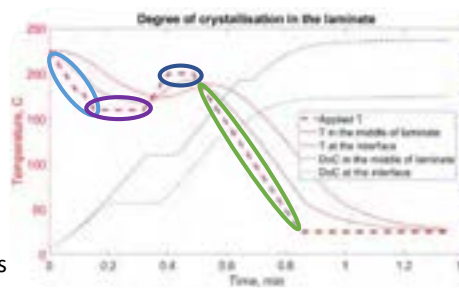
Currently, there are no clear nor defined models for the crystallisation process.

- The tool models a 1D coupled crystallisation and heat transfer problem.
- A differential Nakamura model was implemented via the line method in MATLAB.

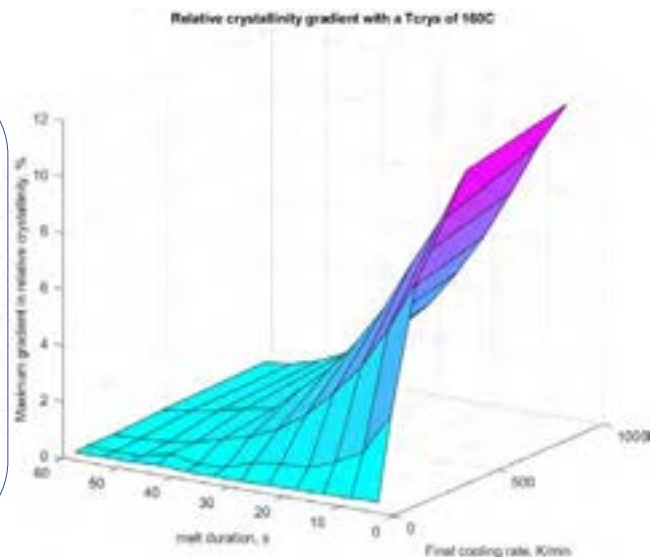
$$\frac{d\theta}{dt} = n * K(T) * (1 - \theta) * \left(\ln \left(\frac{1}{1 - \theta} \right) \right)^{\frac{n-1}{n}}$$



- The parameters looked at were: Initial and secondary cooling rate, the temperature of crystallisation, and the duration of the heating step (tm) [s] (labelled on the graph with the ellipses)
- A complex cooling cycle was designed and optimised to showcase the range of crystallinity gradients that can be achieved.



Example of a Relative crystallinity through-thickness graph with parameters labelled as below.
K1(initial cooling rate): blue; K2(Secondary cooling rate): green; Tc(Crystallisation temperature): Purple, and tm (duration of heating step): dark blue



Conclusions :

- A gradient structure is theoretically possible to obtain but only at very high cooling rates.
- More experimental understanding of crystallisation is required to fully model the crystallisation process of thermoplastics under a range of cooling cycles.

Digital Engineering of Composite Materials for Space Applications

George Worden, Kate Robson Brown & Ian Hamerton

Research problem and aim

- The environment in low Earth orbit (LEO) is hostile to materials, due to the presence of atomic oxygen, micrometeoroids, radiation. Testing materials in space is costly and time-consuming
- A novel benzoxazine based polymer has been developed to be resistant to the LEO environment with the addition of POSS nanoparticles.
- The aim of this project is to create a computational model of material components in LEO to provide a method to predict degradation and lifespan, with a physical twin of a number of material specimens exposed to LEO space on the ISS for validation of the model.



Figure 1: Bartolomeo LEO exposure module on the ISS

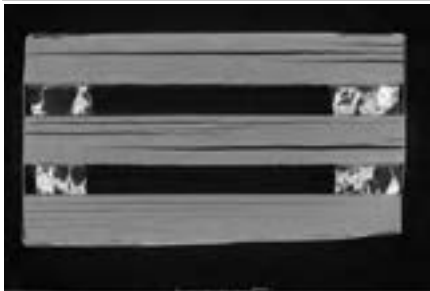


Figure 2: X-ray CT scan of original CFRP panel

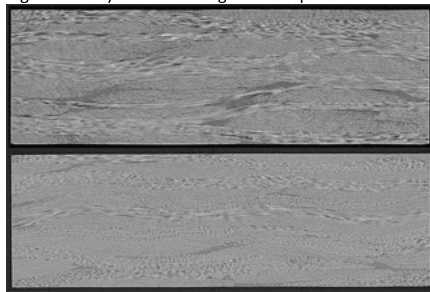


Figure 3: X-ray CT scan of newly manufactured CFRP panel

Material Characterisation

- Two panels of a new iteration of the benzoxazine based CFRP have been manufactured using resin transfer moulding (RTM). Only one panel contains POSS in order to determine how it affects material properties.
- X-ray CT scans of the previous and new CFRP panels have been carried out, shown in figures 2 and 3. These show an improvement in laminate quality for the newer panels, with much less delamination.
- A campaign of mechanical testing has been performed on samples of this new material to characterise it prior to LEO exposure. Some results from this is shown in figure 4.
- A framework for a finite element model for the mechanical performance of the material has been produced.

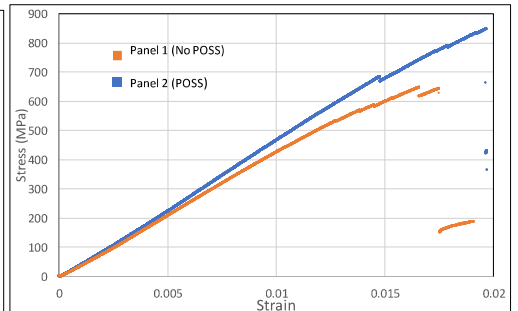


Figure 4: Stress/Strain response of CFRP panels in 3-point bending



Figure 5: CFRP panel manufactured using RTM

Current & future work

- Exposure of specimens from the newly manufacture panels to high energy atomic oxygen, followed by mechanical and thermal testing of the exposed samples to determine the property changes induced by the exposure.
- Refinement of the FEA model using the recent x-ray CT images and data produced through mechanical testing and AO exposure.
- Access to the GSI accelerator facility in Darmstadt has been secured through ESA. This will be used to expose samples of the novel CFRP to high energy radiation similar to galactic cosmic rays found in space. Materials exposed at GSI will be characterised before and after irradiation. The radiation shielding properties of the composites will be quantified in order to determine how well it could contribute to the radiation protection on a spacecraft.
- Finally, the success of these methods for prediction of degradation and lifespan will be assessed through their application to a real world design and deployment challenge. Ideally, this will use the ISS exposed specimens but time constraints may mean an alternative is required.



Figure 6: GSI accelerator facility

Investigation of porous composite materials for hydrogen storage

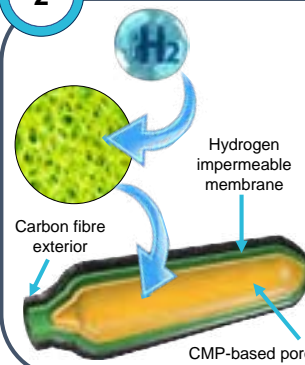
John Worth^{ab}, Prof C. F. J. Faul^a & Prof V. P. Ting^b

^a School of Chemistry, University of Bristol, Bristol, BS8 1TS, UK
^b Department of Mechanical Engineering, University of Bristol, Bristol, BS8 1TR, UK

1 Hydrogen (H₂) for renewable energy storage

- ✓ Clean combustion
 - ✗ Highly flammable
 - ✓ Globally abundant
 - ✗ Highly compressed (70 MPa)
 - ✓ High gravimetric energy density
 - ✗ High mechanically performing containment materials needed
 - ✗ Current storage technology is costly
- $$2\text{H}_2 + \text{O}_2 \longrightarrow 2\text{H}_2\text{O}$$

2 Conjugated microporous polymers



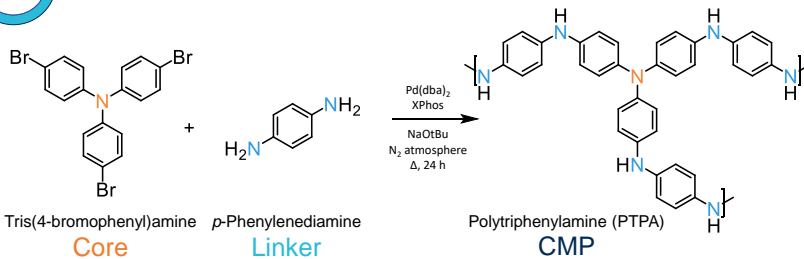
H₂ adsorption in pores combats current storage issues

Engineering micropores (< 2 nm) for optimal H₂ storage capacity¹

Conjugated microporous polymers (CMPs) are promising owing to their chemical and thermal stability and established synthetic routes

Potential for incorporation into composite tanks

3 Material synthesis and optimisation



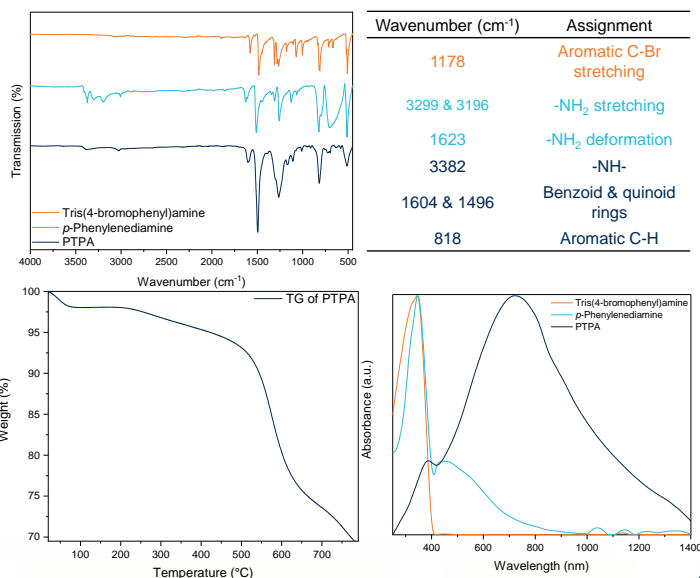
Buchwald-Hartwig cross-coupling amination reactions used to create porous CMPs²

Reaction conditions changed to create material with different properties

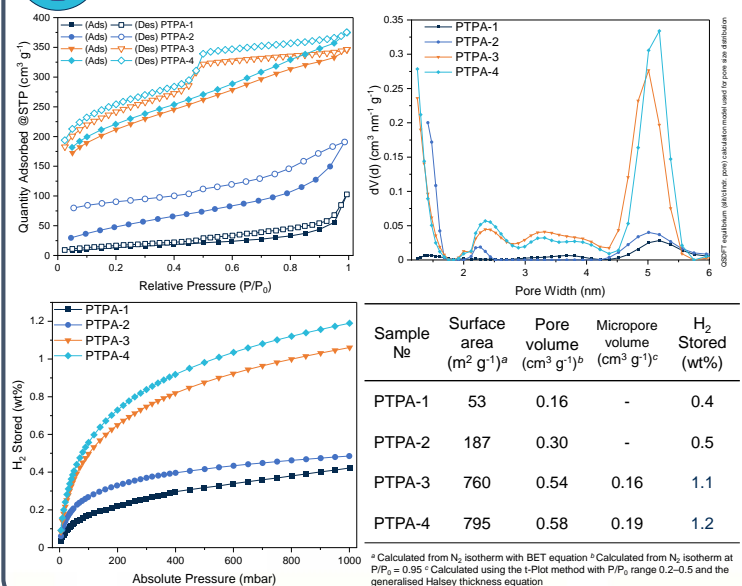
Bristol-Xi'an Jiaotong (BXJ) optimisation of Hansen Solubility Parameters (HSPs) to extend growth of CMP networks³

Sample №	Core:Linker	Solvent	Ionic salt
PTPA-1	1.00:1.50	Toluene	-
PTPA-2	1.00:1.50	Tetrahydrofuran	Sodium fluoride
PTPA-3	1.85:1.00	Tetrahydrofuran	Sodium fluoride
PTPA-4	1.95:1.00	Tetrahydrofuran	Sodium fluoride

4 Material characterisation



5 Gas sorption analysis



6 Conclusions

- Series of CMPs synthesised and characterised
- Synthetic modifications resulted in tuning of surface area, pore size distribution & pore volume
- Increased H₂ storage performance

7 Future work

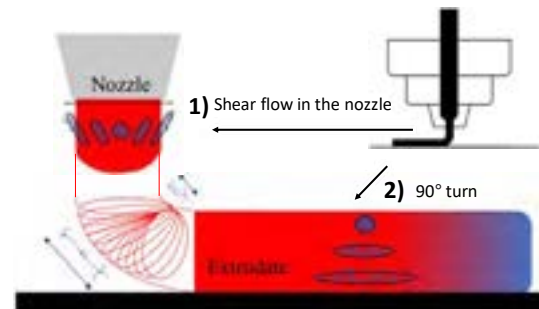
- Further optimisation of CMPs for H₂ storage
- Improve processibility via composite formation
- Mechanical testing of and characterisation of composite
- Gas sorption analysis of composite material

4D printing of single-layer thermoplastics: Quantifying the morphing mechanism

Erdem Yildiz, Byung Chul Kim, Richard Trask

Abstract

4D printed highly controllable self-morphing polymer and polymer composite structures will be created, exhibiting large deformation through the thermal shrinkage and control of the polymer material's Poisson's ratio. By exploiting this approach, the morphing mechanism will be governed by two main factors including the stored internal stresses during the deposition in the nozzle (shear flow) and 90° turn; the controlled release of the stress profile through heating above the polymer's glass transition temperature; and, by generating controlled shrinkage induced by the rearrangement (or relaxation) of the polymer molecular chains. Poly-lactic-acid (PLA) were used for the fused filament fabrication (FFF) process. The effect of these printing parameters such as raster angle, printing speed and layer thickness on the degree of the material morphing as well as the macroscopic properties and structural performance of the final part was analytically and experimentally investigated.



Modified from Hassan et al. (2021)
Hassan, N.M., Migler, K.B., Hight Walker, A.R. et al. Comparing polarized Raman spectroscopy and birefringence as probes of molecular scale alignment in 3D printed thermoplastics. MRS Communications 11, 157–167 (2021)

Printing Speed



❖ Specimens are designed with a raster angle of 0°, the results are completely different according to different printing speeds.

❖ Figure on the left shows deformed configurations for single layer printed between 20 mm/s to 100 mm/s printing speed after the heating-cooling cycle.

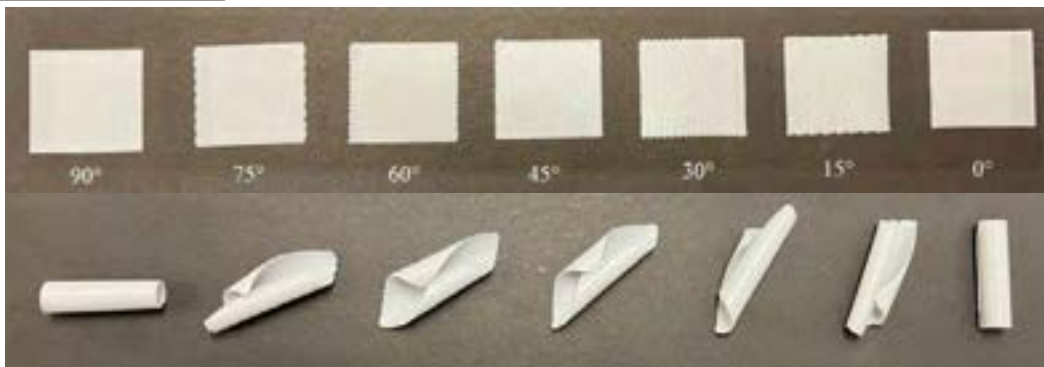
Nozzle Temperature



❖ To study the effect of nozzle temperature on shape transformation, square structures are fabricated for six different nozzle temperatures, namely, 185°C, 195°C, 205°C, 215°C, 225°C and 235°C with a printing speed of 80 mm/s and all other process parameters are set to same values.

❖ Figure on the left shows optical images of samples printed at different nozzle temperatures and then transformed into different shapes.

Raster Angle

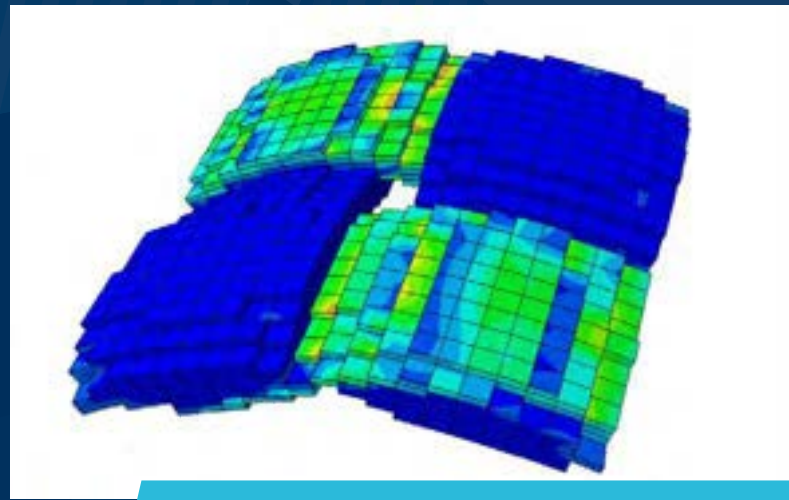
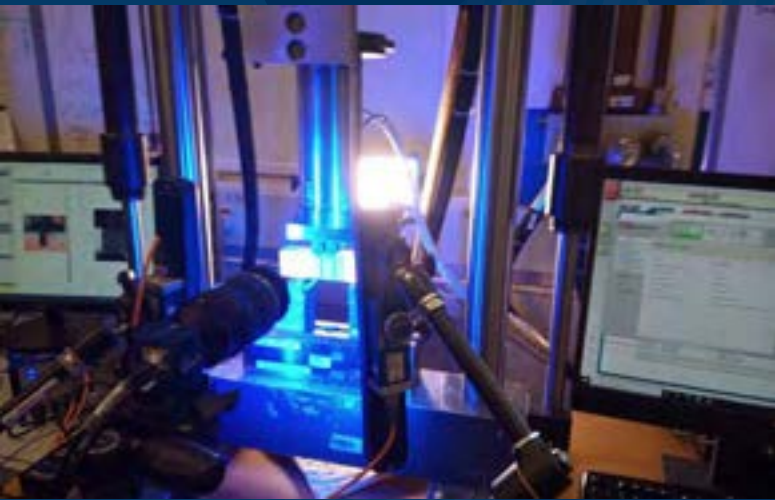
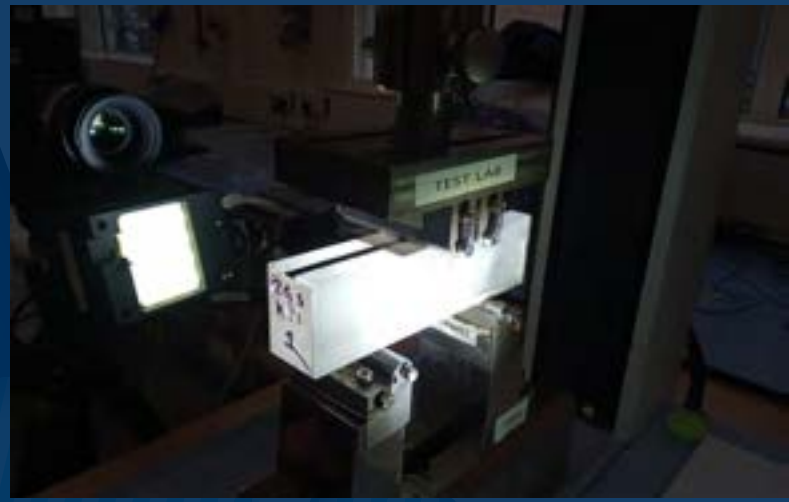
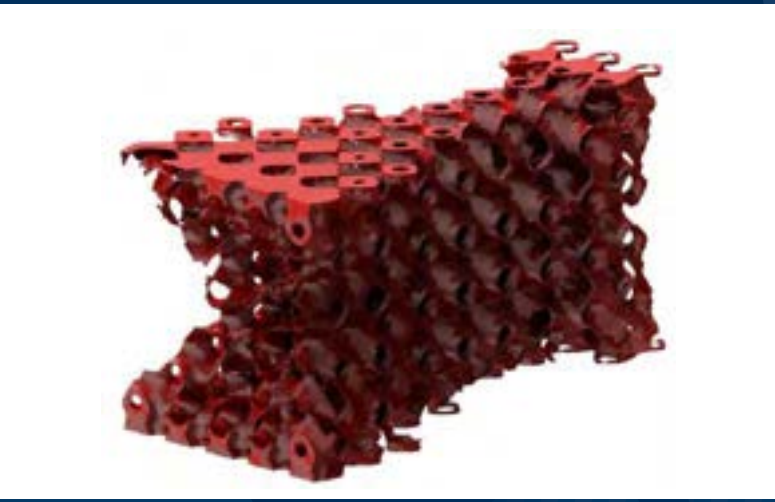


❖ Demonstration of a three-layer laminate (as printed) designed with raster angles follows: 90°, 75°, 60°, 45°, 30°, 15° and 0°.

❖ Figure on the left shows the deformation after the curvature becomes complex and nonuniform after heating over its $T_g + 20^\circ\text{C}$.

Future Works

- New material and printing combinations for attaining more complex geometries
- Targeting a wide range of potential applications in industry
- Creation of morphing high modulus and stiffness fibre reinforced lightweight structures
- Quick, cheap and sustainable mouldless composite manufacturing



STRUCTURES

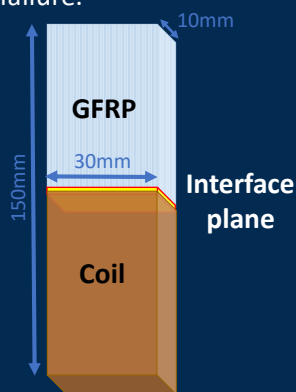
Investigation of the Strength of Adhesively Bonded Composite Joints Using a Modified Arcan Fixture

David J. Brearley, Ole T. Thomsen, Janice M. Dulieu-Barton, M'hamed Lakrimi

MRI machines, used for non-invasive medical imaging, comprise of a magnet storing >10MJ. The solenoids that make up the magnet induce large electromagnetic forces (~1MN) on composite spacers between them in cryogenic conditions. This leads to a complicated stress profile, due to the mechanical and thermal loads. From this loading a quench, where energy is released creating rapid helium boil off, might occur causing the magnet to become critically damaged. For analysis of the in-situ loaded state, and any possible fracture, thermomechanical and toughness properties in all constituent materials are necessary.

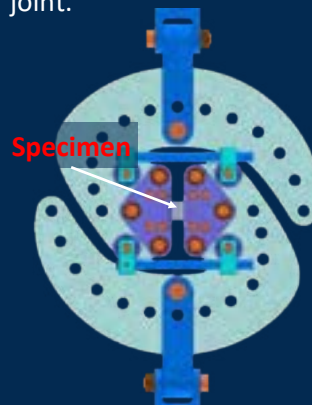


Identify feature of interest
Interface between dissimilar materials is a region with a large complex stress state and potential location of failure.



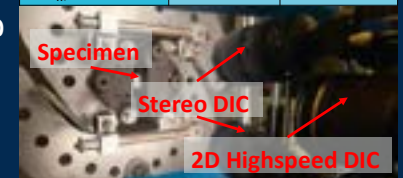
Quasi-static loading applying shear stress across the specimen to examine shear strength of the adhesive joint.

Modified Arcan Fixture

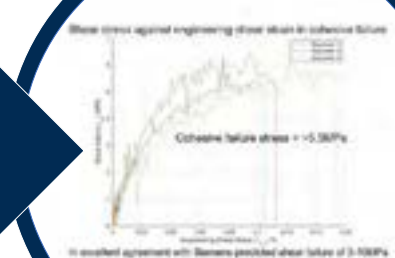
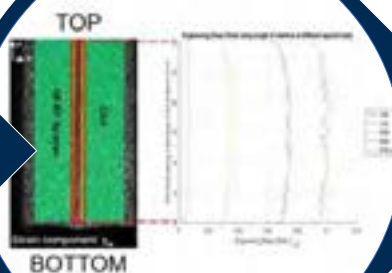
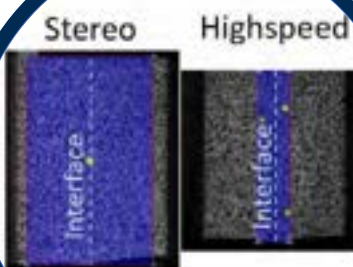


Digital Image Correlation

Hardware	Stereo DIC	Highspeed 2D DIC
Camera	Flir Blackfly S USB3	Photron FASTCAM SA-Z
Sensor	12 bit, 4096x3000	12 bit, 768x768
Lens	100mm	200mm
Pixel resolution	12.5mm/pixel	40.5mm/pixel
Frame rate	1Hz	30,000Hz
Subset size	31 pixels	21 pixels
Step Size	15 pixels	10 pixels
Noise floor (SD of ϵ_x)	9.64×10^{-5}	8.72×10^{-5}



PROCESSING



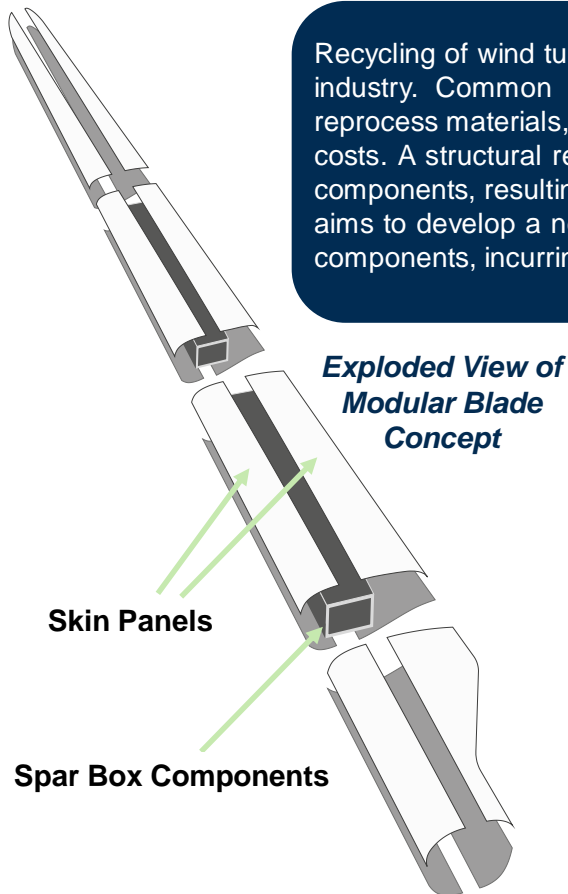
Future Work

To validate these results, specimens of adhesively bonded metallic specimens will be tested with the same method. An investigation on how changing the MAF rig loading, by adding counterweights onto the arms, effects the results. After satisfying that shear failure is occurring, the results will be compared to a cohesive zone model.

Recycling of Wind Turbine Blades: Design for Disassembly

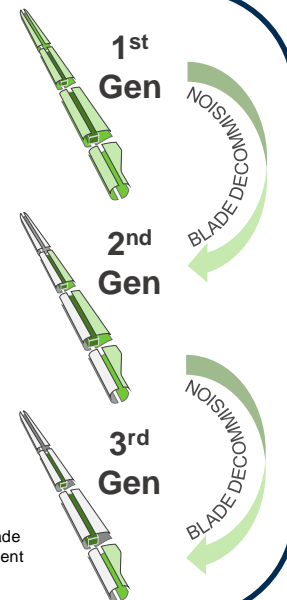
Tom Brereton, Dr Terence Macquart, Prof. Alberto Pirrera, Prof. Paul Weaver

Recycling of wind turbine blades at end-of-life is a significant challenge for the wind energy industry. Common research strategies in composite recycling focus on attempting to reprocess materials, often causing significant performance penalties as well as high energy costs. A structural re-design approach could facilitate the reuse of as-manufactured blade components, resulting in a much more energy efficient recycling solution. This current work aims to develop a new modular blade design to enable the reuse of high value composite components, incurring a lower energy cost than other recycling methodologies.

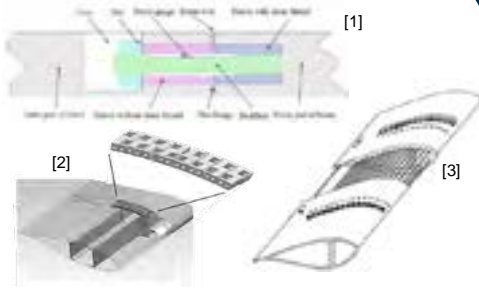


MODULARITY FOR BLADES

- Single-use blade designs require the whole blade to be decommissioned at end-of-life, even though some sections are still serviceable
- Modular blade design allows for the re-use of serviceable blade components
- Allowing for energy efficient recycling of high value composites such as carbon fibre spar box



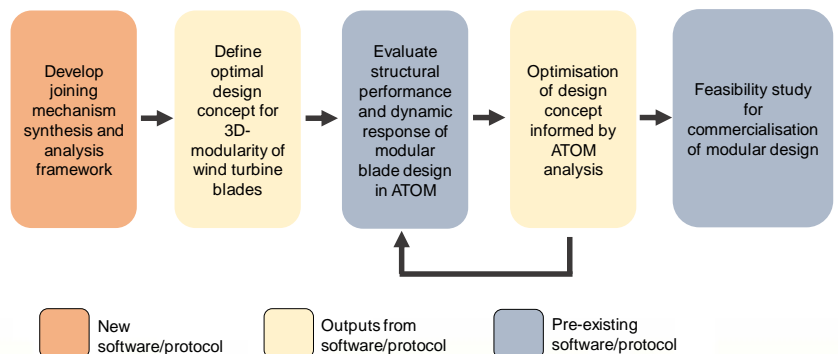
EXISTING DESIGNS



[1] Qin et al. (2018); <https://doi.org/10.1016/j.compstruct.2018.08.073>
 [2] Peeters et al. (2017); DOI: 10.3390/en10081112
 [3] Xu et al. (2016); DOI: 10.6052/j.issn.1000-4750.2014.06.0548

- ✗ Only 1D modularity – no skin/spar box separation
- ✗ Only suitable for small blades lengths
- ✗ Complex, intricate joint assemblies, unsuitable for on-site disassembly

DESIGN METHODOLOGY



Failure Analysis of Hybrid Laminates under Impact Using 2D Axisymmetric Model

An Chen, Xun Wu, Luiz Kawashita, Michael Wisnom

Background

- Carbon laminates are vulnerable to through-thickness impact loading due to low strain to failure.
- Hybrid laminates composed of carbon and high strain fibres such as glass have better impact performance.
- However, the underlying mechanism for the improvements are not well understood.
- Here an efficient 2D axisymmetric model is established to simulate the response of hybrid laminates against quasi-static indentation for the aim of understanding the factors controlling the response as well as the detailed damage mechanism under low-velocity impact.
- Emphasis is given to the interaction between fibre failure and delamination as well as how this controls the hybrid impact behaviour.

Method & Results

The model represents half of the through-thickness cross section of the test

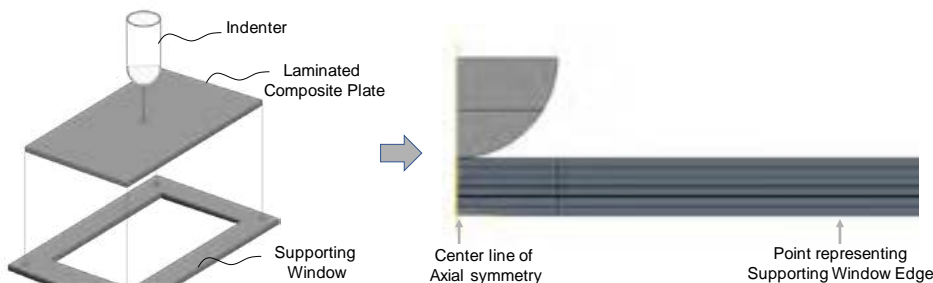


Figure.1 The schematic diagram of quasi-static indentation test (left) and the 2D axisymmetric model (right)

Two-dimensional solid elements and interface finite elements are employed to simulate intralaminar fibre failure and interlaminar delamination, respectively.

Accurate global response prediction

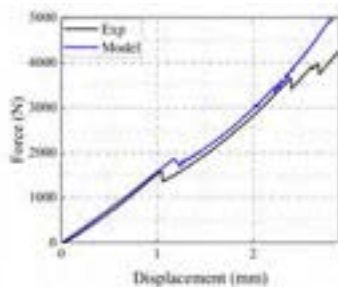


Figure.2 Load-displacement curves of baseline carbon laminate

The predicted local delamination correlates well with experiment

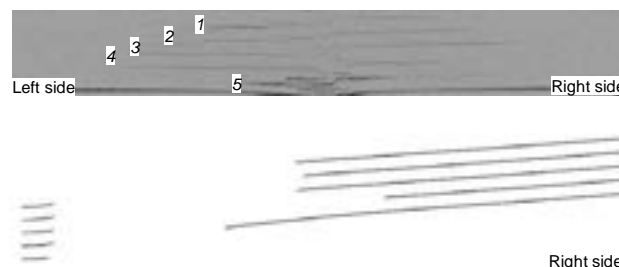


Figure.3 Delamination pattern from experiment (top) and from prediction (bottom) at displacement 2.75mm

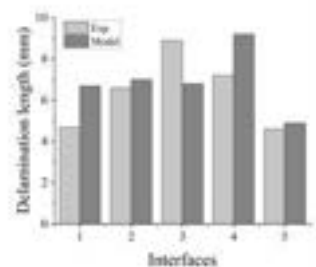


Figure.4 Delamination length at displacement 2.75mm

Delamination influences fibre loading state

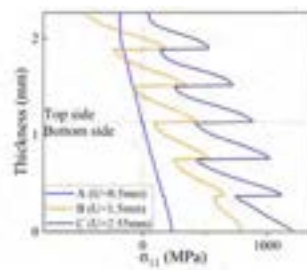
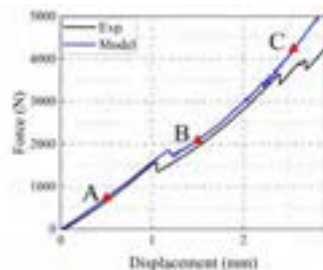


Figure.5 Through-thickness variation of σ_{11} at critical displacements

Along with delamination propagation, the compressive load at some upper plies changed to tensile load at large displacement.

Conclusions:

- 2D axisymmetric model is particularly efficient in the analysis of local events like penetration and it can reduce the high computational cost presented in the state-of-the-art 3D impact modelling.
- Failure analysis shows one effect of delamination is that at large displacement, the impact force is reacted to a larger extent by membrane rather than shear forces, putting more of the laminate into tension compared to the tension/compression in pure bending.

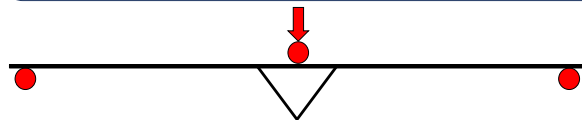
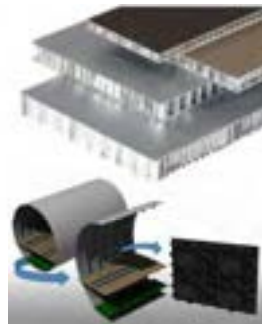
Experimental Testing of WrapToR Truss Stiffened Composite Panels

Chris Grace, Dr Mark Schenk, Dr Ben K.S. Woods

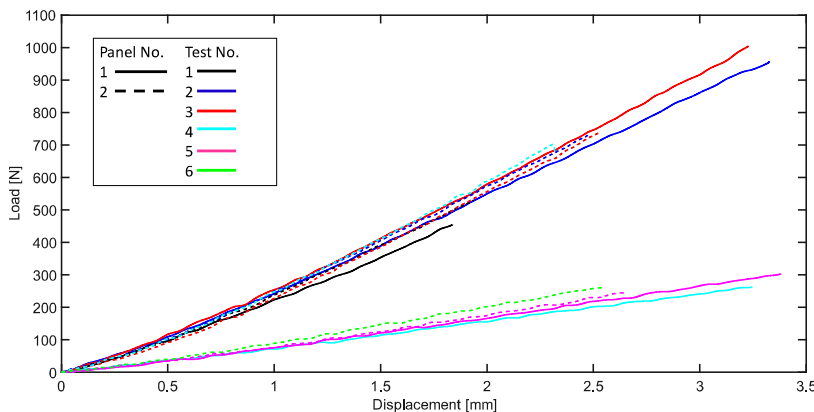
The Wrapped Tow Reinforced (WrapToR) truss fabrication technique produces truss beams from continuous wetted fibre using an adapted filament winding technique. It combines the excellent structural efficiency of truss geometry with the highly anisotropic properties of unidirectional fibre composites. This work investigates the performance of these truss structures as stiffeners for thin composite panels through experimentation and simulation.

background

- Stiffened panels are prevalent in industries that require lightweight, yet strong and stiff structures. Examples include sandwich panels and stringer stiffened panels used in aircraft wings and ship hulls.
- Truss beam structure increase their 2nd moment of area by moving material far from the bending axis and grouping material into stiff members that are predominantly axially loaded.
- The combination of unidirectional composites and truss structures is expected to provide superior stiffness and strength when utilised as a panel stiffener.



3-point bend experiment side view. truss shown on underside of panel with load and support rollers shown in red



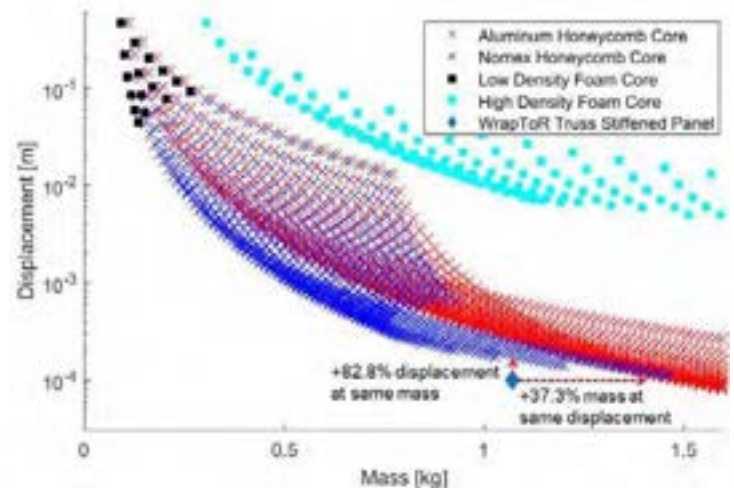
experiments

- A three-point bend test was completed on a unit cell panel with a central line load and two simply supported sides.
- Two sample panels were constructed (example shown above) and tested over several cycles to obtain their stiffness.
- Audible failure was observed after several cycles, shown by second grouping of lines on chart with reduced stiffness.
- Stiffness values for both panels pre-failure are shown below.

Panel 1	Panel 2
297.1 N/mm	326.3 N/mm

performance comparison

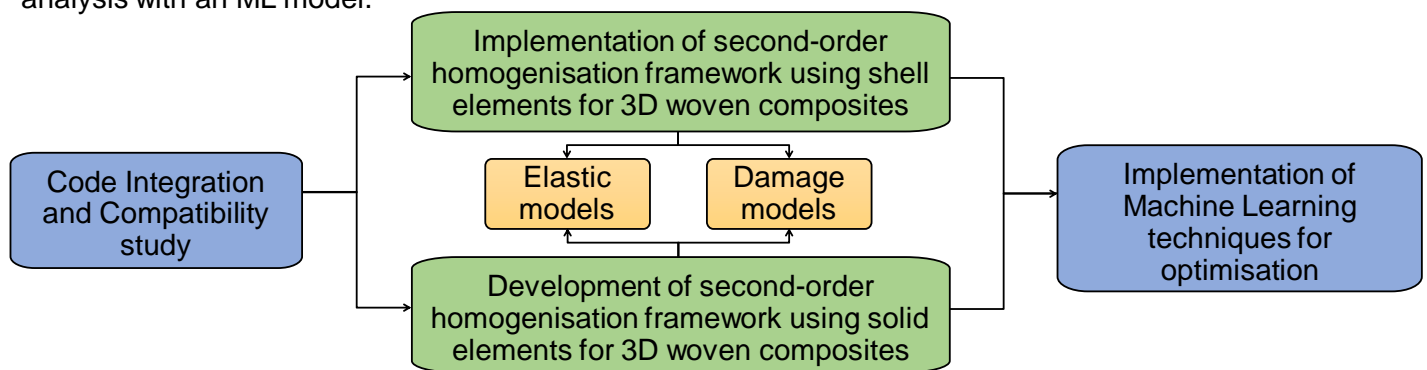
- A comparative analysis was performed against a large number of sandwich panel configurations (right) to compare performance.
- Four different core types were considered with different combinations of core and skin thickness.
- Sandwich bending theory was used to determine central displacement for a 200 N line load and plotted against the configuration mass.
- Data point for the truss stiffened panel was taken from experimental data (above), which provides comparable performance per unit mass.
- The graph shows the nearest sandwich configuration at the same mass has an 82% greater displacement while the nearest configuration with the same displacement has a nearly 38% greater mass.



Higher-Order Multiscale Modelling of 3D Woven Composites using Machine Learning

Athira Anil Kumar, Aewis Hii, Bassam El Said, Stephen Hallett

3D woven composites are becoming increasingly popular due to enhanced mechanical properties such as improved impact resistance and interlaminar fracture toughness, along with reduced manufacturing costs due to ease of fabricating complex geometries and alleviation of layup process. However, their internal architecture presents complex challenges in the computational modelling of these materials, whose mechanical behaviour spans over several length scales. In order to tackle this problem, users are employing computational homogenisation techniques, thus addressing the impracticality of a high-fidelity model. The classical first-order homogenisation framework, although well-established, has certain limitations, which are taken care of by using higher-order techniques such as the second-order homogenisation. This approach includes higher-order deformation modes, such as bending in the fine scale, and can account for the effects of strain localisation from the structural model. Machine learning (ML) techniques can be utilised further to effectively compute mechanical properties by replacing the fine-scale analysis with an ML model.



Code Integration study

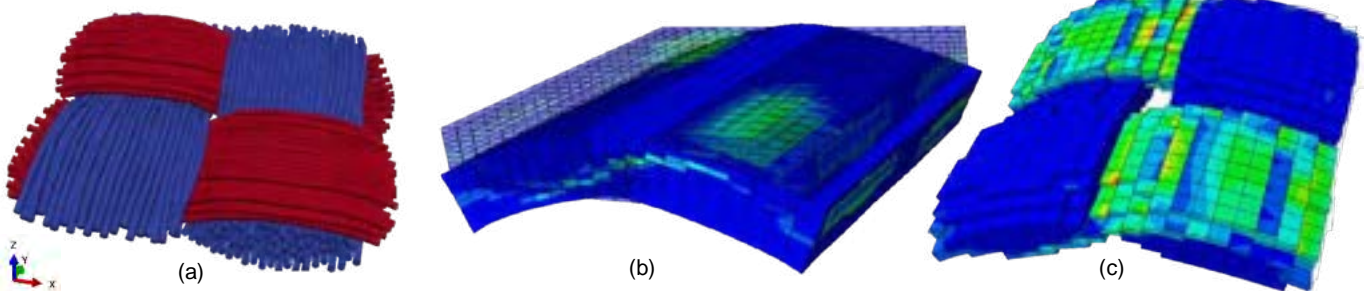


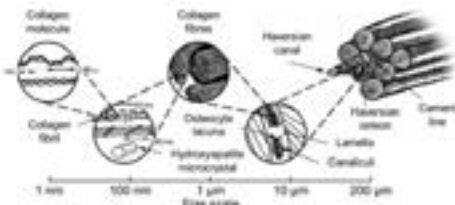
Figure (a): Weaving simulation and compaction, (b): plain weave composite meso-scale RVE undergoing bending, (c): voxelised yarn elements

Future Work

- Obtain homogenised elastic properties of a woven RVE and build a macro-scale model to execute the complete multi-scale FE² analysis.
- Development of a second-order homogenisation framework using solid elements.

Highly aligned, discontinuous fibre-composites for enhanced compressive performance

I.R. Lee, L.R. Pickard, I. Hamerton, G. Allegri



Adapted from Hierarchical structure in human compact bone from Materials with Structural Hierarchy, R Lakes, Nature, Vol. 361, Pages 511-515 (1993), DOI: 10.1038/361511a0

Compressive strengths of manufactured composite materials can be less than 60% of their tensile measurements. In contrast, natural composites such as bone, wood and shell, can exhibit significant compressive strength, despite being formed of intrinsically weak constituent materials. Key to this resilience are hierarchical systems of discrete structural elements, which couple mechanistic processes across length scales. This project is investigating the use of highly-aligned, short, discontinuous carbon-fibres as a reinforcing element within the next generation of manufactured composite systems aimed at mimicking such architectures.

METHOD

Discontinuous fibre composites generally exhibit lower strength values than equivalent continuous fibre materials. Good alignment of the short fibres however can significantly improve strength whilst retaining useful properties such as formability and the potential for re-use of reclaimed fibres. First steps in understanding the role they could play in a hierarchically structured system are characterisation and modelling of their typical properties under compressive loading.



MANUFACTURE

- Highly-aligned discontinuous fibre samples created using the patented HiPerDiF technology developed at University of Bristol



- 3 mm, 6 mm & 12 mm length fibres processed into 150 mm x 5 mm samples

- Continuous fibre samples generated for comparison

- Two commercial epoxy resin systems tested



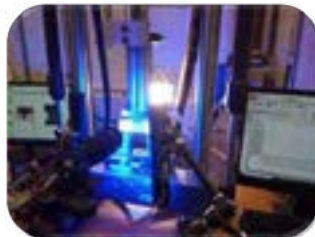
- Samples vacuum bagged and cured by autoclave

TESTING

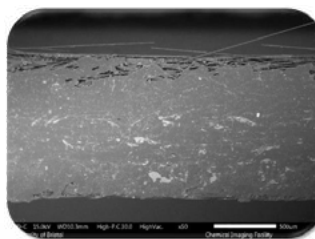


Adapted from Design of a bending experiment for mechanical characterization of pultruded rods under compression, G. Quino et al, ECCM20 Conference Proceedings, 26-30 June 2022

- Digital Image Correlation software used to capture mechanical properties and failure strengths



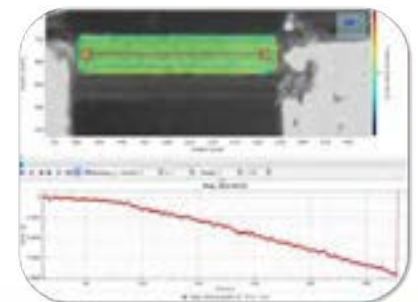
- Sample consolidation and failure surfaces imaged using SEM



- Novel four-point bend test developed by the NextCOMP project team

MODELLING

- Mori-Tanaka theory to be used to develop a model for effective compressive properties of short-fibre discontinuous composites
- M-T models based on Eshelby's equivalent inclusion theory, modified for particle phases within an homogenous matrix phase
- Model inputs to be based on collected test data
- Model refinement through consideration of probability distribution of fibre alignments



Detecting deboned regions through the face sheets of sandwich structures using mirror assisted imaging techniques

Hui Ling Leung*, Prof. Janice M. Dulieu-Barton and Prof. Ole T. Thomsen

* emily.leung@bristol.ac.uk

Motivation

Sandwich structures have been commonly used in automotive, aerospace and energy industries. Face/core debonding can reduce the stiffness and strength of the structure and can lead to a catastrophic failure with no/little prewarning. Large structures often have complicated geometry that limits the use of full field imaging techniques. During in-service inspection, it is difficult to inspect debonded regions of the structures (e.g. wind turbines) in a cross-sectional view, without disassembling/ cutting the part. Techniques are required that can monitor the damage initiation and progression from the exterior of the face sheet to gain an understanding of the actual sandwich structure performance.

Methodology



Figure 1: Sandwich specimens configuration

A 3-point bending set up was used to demonstrate that a front-coated mirror can be used to view inaccessible regions and extend the field of view of the cameras to collect the face sheet images for use in digital image correlation (DIC) and thermoelastic stress analysis (TSA). The specimens were loaded cyclically with a range of loading frequencies.

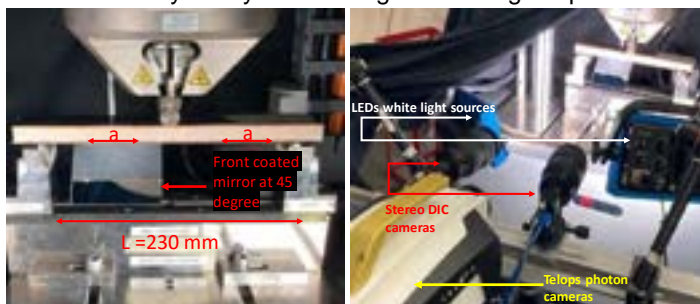


Figure 2: Experimental set up

TSA is based on the thermoelastic effect, which describes the coupling between mechanical deformation and thermal energy in an elastic solid. Based on the thermoelastic effect, when a strain induced temperature change occurs on an object surface, this can be used to derive changes in stresses.

References

[1] Fruehmann, R. K., Dulieu-Barton, J. M., Quinn, S. & Tyler, J. P. The use of a lock-in amplifier to apply digital image correlation to cyclically loaded components. *Opt Lasers Eng* 68, 149–159 (2015).

Results

Figure 3 shows the specimen loaded cyclically at 1.1 Hz, and that two regions of high ΔT of 0.04 - 0.02 K are evident at the edges of the debond. The regions of high ΔT reduce as the cyclic loading frequency increases. This indicates that heat transfer at low loading frequencies reveals the subsurface damaged region at the interface between the face sheet and the core.

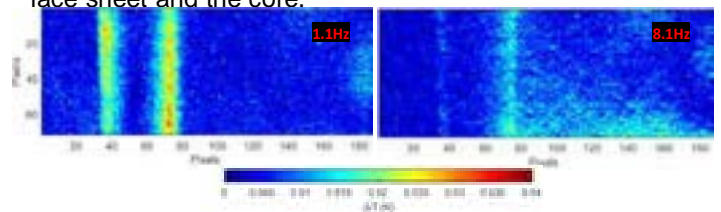


Figure 3: ΔT of 20 mm debond length specimen loaded at 1.1 Hz and 8.1 Hz

The change in strain, $\Delta \epsilon$, from DIC can be obtained using the lock-in algorithm [1]. The surface strain response was studied and compared with the FE predictions, and it shows that the experimental and FE results at the debonded region match reasonably well.

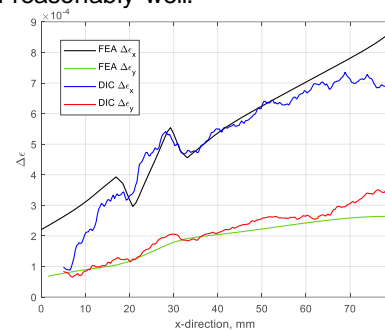


Figure 4: $\Delta \epsilon$ of the 10 mm debonded specimen

$\Delta \epsilon$ from DIC enabled ΔT to be calculated without any effects of heat transfer which can then be subtracted from ΔT obtained from the TSA to estimate the subsurface thermoelastic response.

Conclusion and future work

Interface debonding was observed through the face sheets using a thermal camera and a front-coated mirror. To observe the damaged region at the interface through the face sheets, a low loading frequency is required.

The interface ΔT may be inferred by subtracting the surface ply ΔT obtained from DIC. The stress intensity factor at the crack tip may be estimated, and the internal fracture behaviour can then be characterised through the face sheets of sandwich structures.

Compliant fairing for folding wingtips on commercial airliners

Student: Nuhaadh Mahid

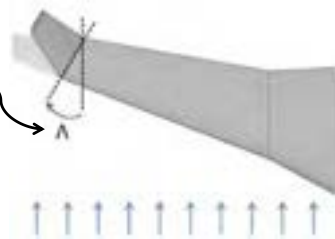
Supervisors: Dr Benjamin Woods, Dr Mark Schenk, Dr Branislav Titurus

1. Introduction

Extended wingspan in flight, folded wingtip when approaching airport gate

Flare angle helps to alleviate gust load

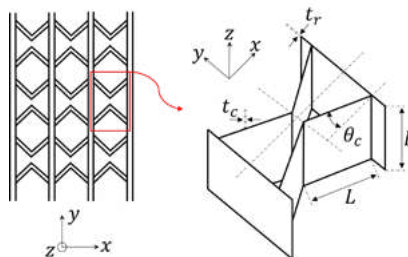
A morphing fairing needed to cover the hinge joint



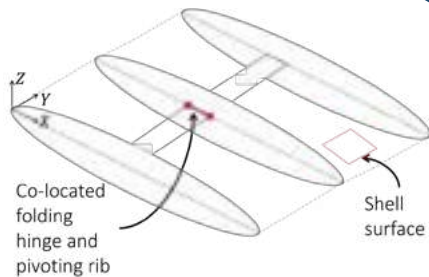
2. Modelling

Sandwich panel with a cellular core and elastomer facesheets

Analytical model used to evaluate equivalent shell stiffness matrix for the panel



Finite element model with equivalent thin-walled shell fairing and rigid ribs

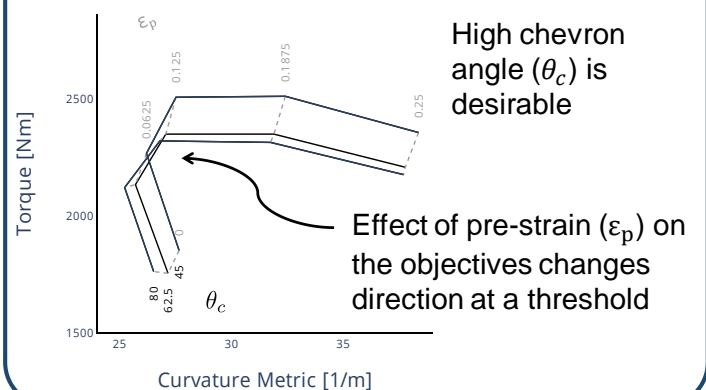
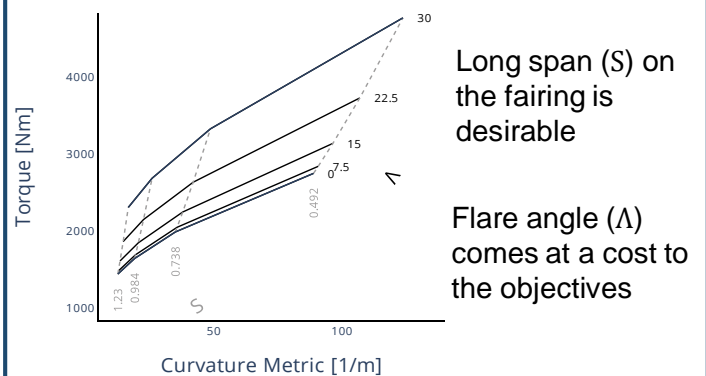
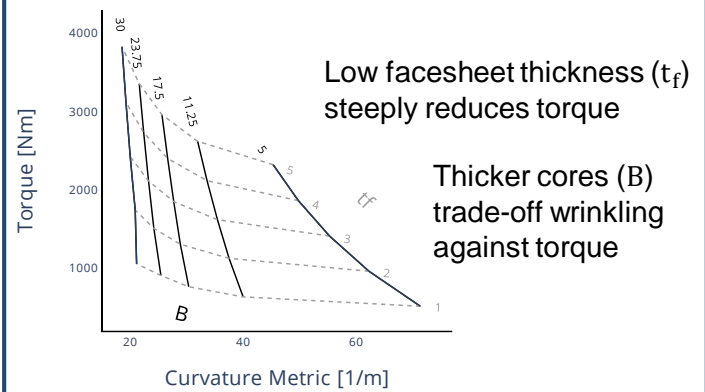
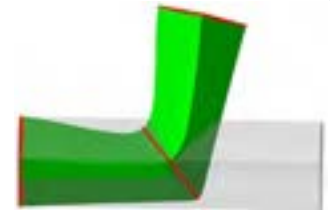


Parametric study presented for the design variables which are correlated with the objectives

Objectives are low torsional stiffness and low wrinkling on the wing surface as wingtip folds

3. Results

Shape of the folded and unfolded fairing (rear view)

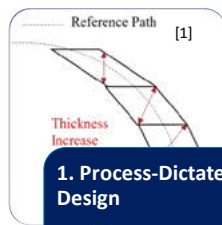


Elastic Tailoring of Composite Structures by Fibre Steering

Calum J. McInnes, Alberto Pirrera, Byung Chul Kim, Rainer M.J. Groh

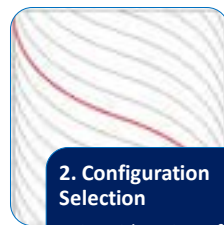
Aerospace design considers laminated structures to have fibres of constant orientation across the planform of a ply. With the advent of automated material deposition systems the concept of fibre steering, lamina in which the fibre orientation follows a curvilinear reference path, have been highlighted as a means of elastic tailoring to produce variable stiffness structures. This work aims to design mass-efficient solutions for a common aerospace load case, uniaxial compression under simply supported edge conditions. When optimising, we deviate from traditional linearised 'bucklephobic' design and allow instabilities in order to transition into the nonlinear region for safe exploitation of additional load-carrying capacity.

Research Methodology



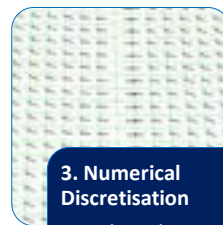
1. Process-Dictated Design

- Minimum allowable steering radius and geometry sets bounds to solution space



2. Configuration Selection

- Consideration of support conditions, loading and geometry



3. Numerical Discretisation

- Node and centroid-wise material orientation and thickness
- Asymmetry captured by solid-shell elements



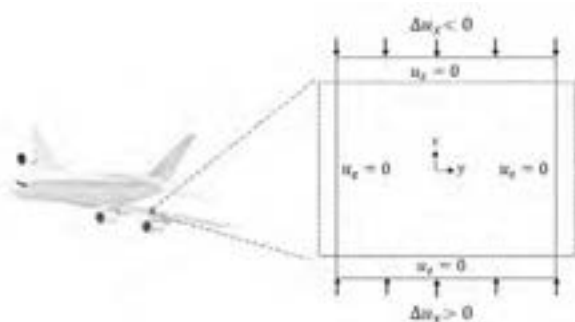
4. Structural Performance Quantification

- Linear Perturbation for eigenvalues and eigenmodes
- Riks to access post-bifurcation

Mass-Efficient Design Motivation

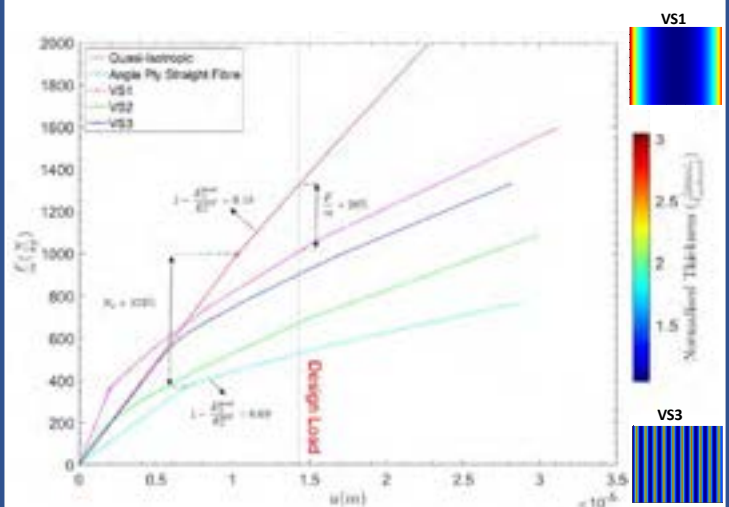
- **Concept 1:** For an applied strain can a fibre-steered panel take higher loading ($F/m \uparrow$ for equal Δu_x)?
- **Concept 2:** Can the stiffness drop due to global structural instability be mitigated by fibre steering ($\min\left(1 - \frac{E_x^{\text{post}}}{E_x^{\text{pre}}}\right)$)?

Design for Aerospace Load Case



- **Variable Stiffness 1 (VS1) – State-of-the-art**
 - Redistribution of stress to supported edges
- **Variable Stiffness 2 (VS2) – State-of-the-art**
 - Central tensile stress perpendicular to loading
- **Variable Stiffness 3 (VS3) – Enabled by CTS**
 - Reinforcement of supported edges

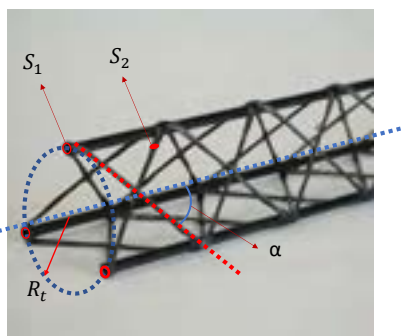
Tailorable Structural Performance



Trusstrusion: Continuously Extruded Wrapped Tow Reinforced Truss Beams

Francescogiuseppe Morabito, Dr Terence Macquart, Dr Mark Schenk, Dr Alberto Pirrera and Dr Benjamin Woods

Recent developments in advanced composite truss structures have shown very high levels of achievable structural efficiency by combining truss geometries, composite materials, and scalable manufacturing processes. On the one hand, filament winding-based approaches such as the Wrapped Tow Reinforced (WrapToR) truss manufacturing process allow for simpler machine design than other manufacturing techniques such as braiding or pultrusion; on the other hand, it is limited to batch production of truss beams with limited lengths. We present a new manufacturing concept to overcome this limitation known as WrapToR Trusstrusion. This concept uses coaxial winding heads to wrap multiple pre-wetted tows in opposite directions around continuously extruded longitudinal chord members to achieve a complete wound truss structure in one passage, avoiding the need for the reciprocating motion and fixed mandrel lengths of conventional winding machines. The WrapToR Trusstrusion concept is first introduced, and then a prototype Trusstruder machine is shown, followed by the numerical analysis and mechanical characterisation of specimens made by this machine. Trading off process and geometry versatility for standardisation and production rate, this new machine concept makes significant progress towards high throughput, continuous production of mechanically superlative WrapToR truss beams.

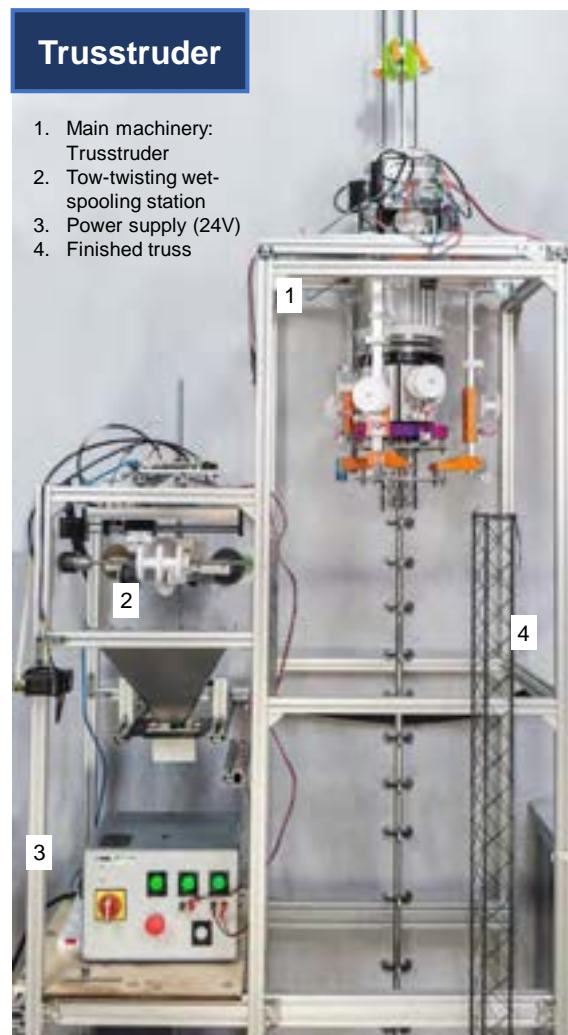


The current Trusstruder can produce WrapToR truss beams (figure above) with geometrical properties described in the table below.

	Property	Symbol. [unit]	Value / Range
R_t	Truss radius	R_t [mm]	40
α	Shear web angle	deg [-]	[15, 60]
S_1 - Chord member	R external	R_{ext} [mm]	6
	R internal	R_{int} [mm]	n.a.
S_2 - Shear web member	Web radius (6K to 48K)	R_{web} [mm]	[0.8, 1.25]

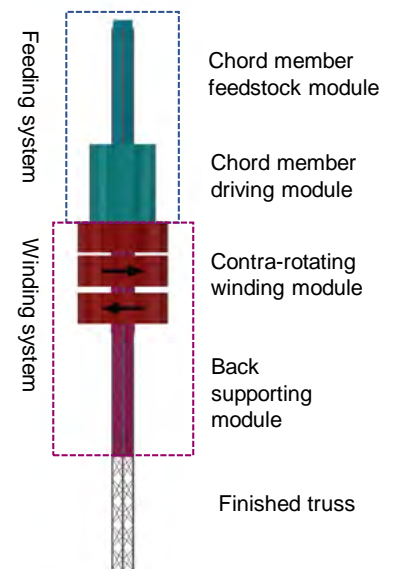


Contra-rotating module in operation



Trusstruder

1. Main machinery: Trusstruder
2. Tow-twisting wet-spooling station
3. Power supply (24V)
4. Finished truss



Trusstruder's modules schematic



WrapToR truss beam testing

[1] C J. Hunt, F. Morabito, C. Grace, Y. Zhao, and B.K.S. Woods, "A review of composite lattice structures," *Compos. Struct.*, vol. 284, p. 115120, 2022, doi:10.1016/j.compstruct.2021.115120.

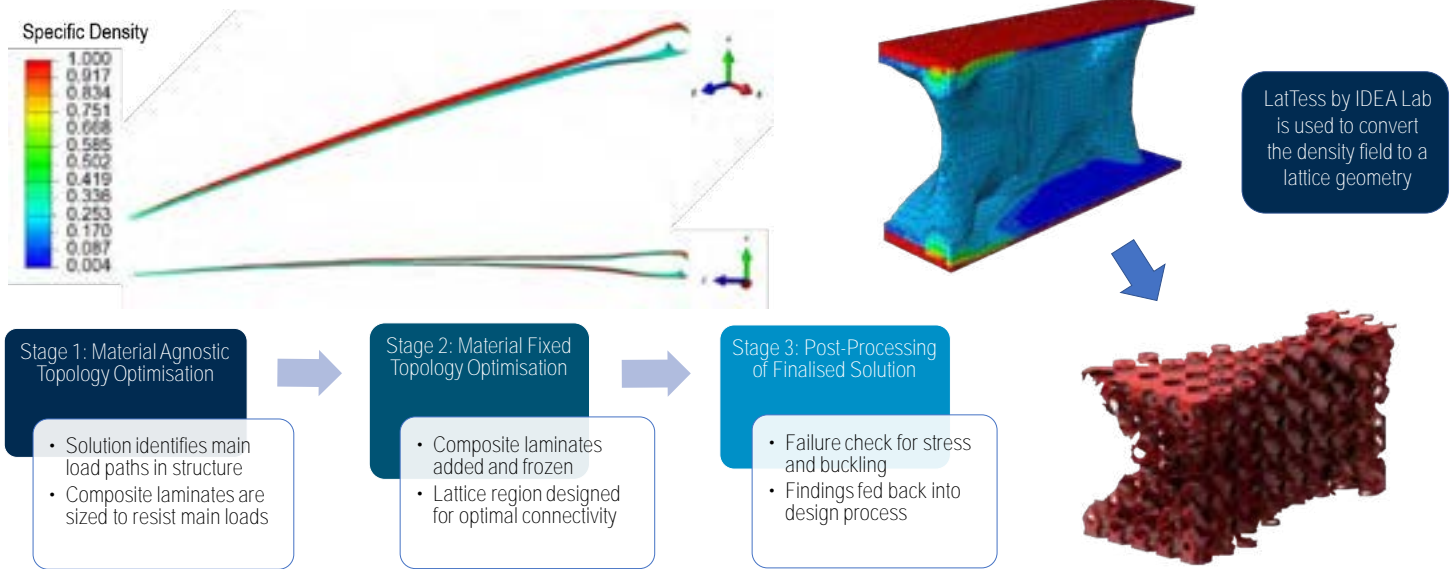
[2] B.K.S. Woods, I. Hill, and M. I. Friswell, "Ultra-efficient wound composite truss structures," *Compos. Part A Appl. Sci. Manuf.*, vol. 90, pp. 111–124, Nov. 2016, doi:10.1016/j.compositesa.2016.06.022.

Multi-Stage Topology Optimisation Design of 3D Printed Composite Structures

Alex Moss, Dr Ajit Panesar, Dr Terence Macquart, Dr Peter Greaves, Dr Mark Forrest, Dr Alberto Pirrera

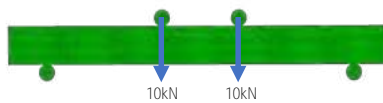
A novel multi-stage design process is proposed, which synergistically applies the benefits of composite laminates and additively manufactured graded lattices to improve structural efficiency. Before this methodology can be scaled up for applications such as wind turbine blades, it requires benchmarking against conventionally designed composite structures, e.g. panels, box beams and sandwich structures. A case study is presented, in which a wide box beam structure is optimised and the buckling performance at each stage of design is measured.

Design Methodology

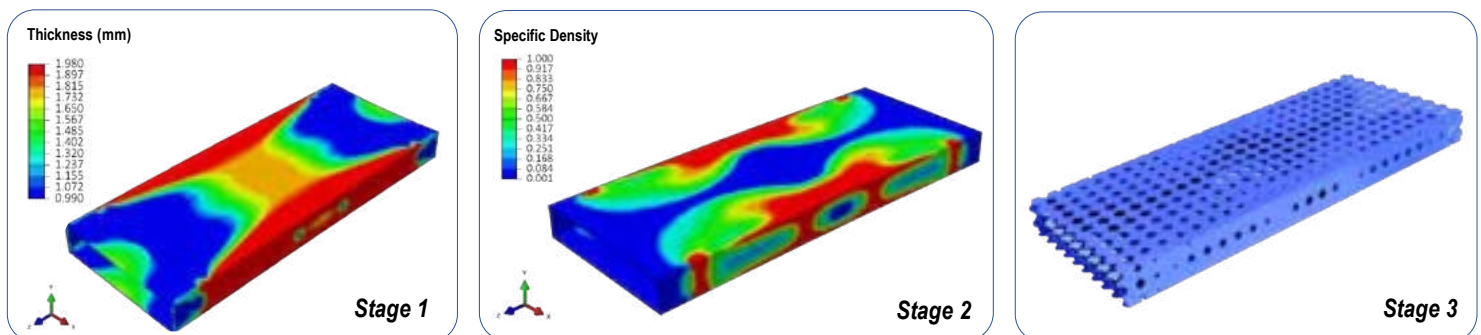


Panel Buckling Design Case Study

Four point bending of box beams results in multiple possible failure conditions, including panel buckling. The multi-stage topology optimisation design method was applied to this problem to identify possible non-intuitive solutions for this load case.



Design	Buckling RF
Stage 1	0.5
Stage 2	7
Stage 3	5



For this case study, a **thickness optimisation** was conducted on a shell box beam to design the composite laminates, followed up by a **topology optimisation** of the internal structure, producing an optimised lattice design which supports the laminates. The finalised design configuration utilises the high laminate stiffness to support the corners against **crippling failure** while the lattice mostly supports against **local crushing** due to the roller forces.

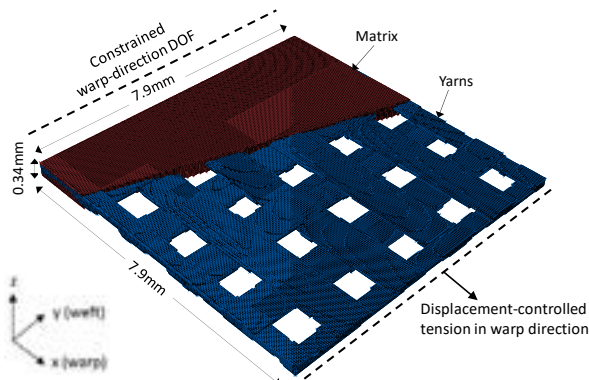
Challenges in Large-scale Modelling of Textile Damage: Implicit vs Explicit

Christian Stewart*, Bassam El Said and Stephen Hallett

*Christian.stewart@bristol.ac.uk

There is a growing use of textile composites across several industries due to their increased damage tolerance. This growth, however, is dependent on the ability to model their behaviour efficiently. This is especially true when modelling textiles at structural scales, due to the associated high computational cost. Implicit finite element (FE) methods can encounter convergence difficulties when solving highly non-linear material behaviour, such as progressive damage in textile composites. Explicit FE methods may provide a more robust alternative. In this study, an implicit and an equivalent explicit subroutine are compared through simulating a single layer of 5-harness satin (HS) weave under quasi-static, tensile loading. The long-term goal of the PhD is to develop a model capable of predicting the progression of damage in large-scale 3D woven composites under fatigue loading. Therefore, the work presented here informs about which FE solver is most suitable for use in the PhD project.

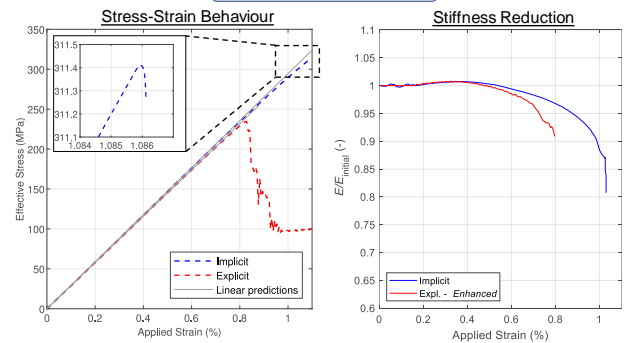
Numerical Model



- Single layer of 5HS weave discretised with voxel mesh, subjected to uniaxial tension
- Equivalent Implicit [1] and Explicit [2] subroutines implemented to capture matrix cracking (continuum damage mechanics) and shear nonlinearity within yarns
- Yarn debonding is not accounted for

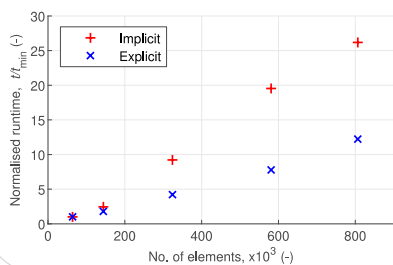
Results

Macroscale Behaviour



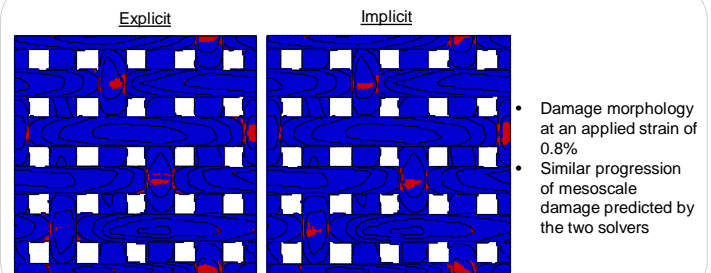
- Global stiffness from both solvers differs by only 1.6%
- Convergence difficulties in Implicit solver at vertical load drop
- Premature load drop in explicit solver, associated with runaway instabilities
 - The use of conformal mesh (instead of voxel mesh), enabling yarn debonding, should reduce this
- Delayed stiffness reduction in implicit solver due to material damping

Model Scalability



- Comparing runtime of both solvers with model size
- Runtimes normalised by the minimum runtime (coarsest mesh)
- Implicit runtime multiplier scales up with model size at faster rate than Explicit
- Larger (and more complex) models (e.g. 3D weaves), would have even more convergence issues for implicit

Mesoscale Behaviour



- Damage morphology at an applied strain of 0.8%
- Similar progression of mesoscale damage predicted by the two solvers

Conclusions

- Implicit solver exhibited convergence difficulties, whereas Explicit solver showed runaway instabilities in the macroscale behaviour
- Both solvers predicted similar progression of mesoscale damage
- Explicit solver is more computationally efficient for large-scale models (e.g. 3D weaves), thus, should be used in the PhD

Future Work

The work presented here informs the PhD project on the type of FE solver to be used. However, the long-term interest of the PhD project is the development of a model capable of predicting damage progression in 3D woven composites under pre-initiated damage under fatigue loading. Therefore, future work involves:

- Replacing voxel mesh with conformal mesh to be able to capture yarn debonding
- Experimental fatigue testing of notched 3D woven composites
- Development of model capable of predicting progression of meso-scale damage under fatigue
- Validation of the developed model against experimental data

Modal Nudging and Elastic Tailoring for Blade-Stiffened Wing Structures

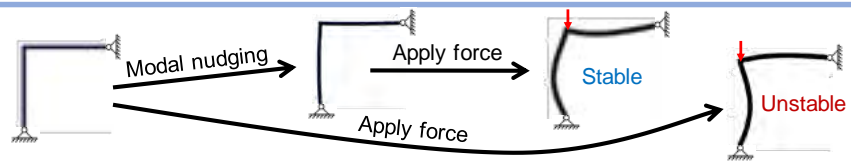
Lichang Zhu, Rainer Groh, Mark Schenk, Jiajia Shen and Alberto Pirrera

Abstract

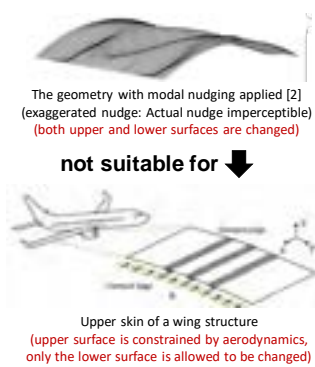
Modal nudging is a structural design technique [1] which can tailor the post-buckling response of slender or thin-wall structures without any significant increase in mass. It enhances control over the post-buckling behaviour to increase load-carrying capacity or reduce imperfection sensitivity. Modal nudging changes the geometry of all surfaces of a structure. The present work is a generalised modal nudging technique that works on thin-wall structures when the geometry of some of the surfaces is constrained, such as the upper skin of wing structures.

What is modal nudging?

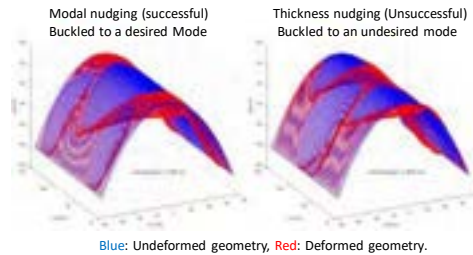
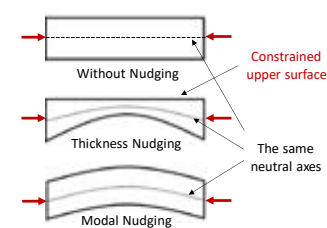
Modal nudging uses deformation modes on stable post-buckled paths to nudge the undeformed baseline geometry of the structure imperceptibly, thereby favouring the seeded post-buckling response over potential alternatives.



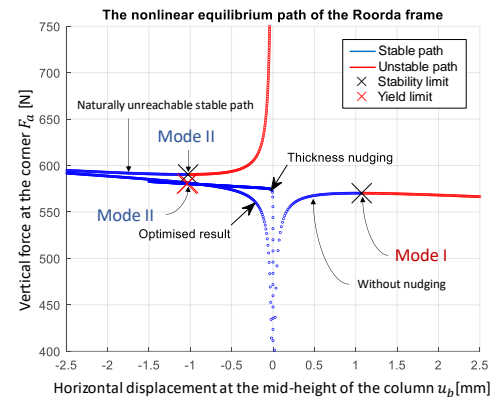
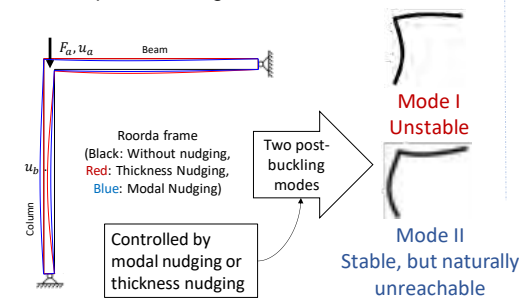
Current Work



Hypothesis: modal nudging and thickness nudging can both tailor the post-buckling behaviour.



Before investigating the effect of thickness nudging on a complex shell structure, we first study a simple 2D *Roorda frame* which still captures the essence of a nonlinear structure with two post-buckling modes.



Method	Force/volume [N/mm ²]	Cost [CPU core hour]
Modal Nudging	0.746	< 1
Thickness Nudging	0.740	< 1
Optimisation (2 variables)	0.742	12

Conclusions:

- Thickness nudging works in 2D
- It is less efficient than modal nudging
- It is equally efficient as a much more computationally expensive optimisation

Future Work

- develop a global optimiser featuring:
 - a MATLAB – ABAQUS interface
 - geometry defined by more than 2 control points, to increase design space
- comparing the efficiency between thickness nudging and the optimisation results
- developing thickness nudging in 3D structures

optimisation formulation:

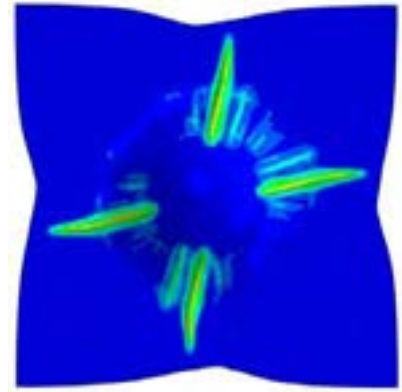
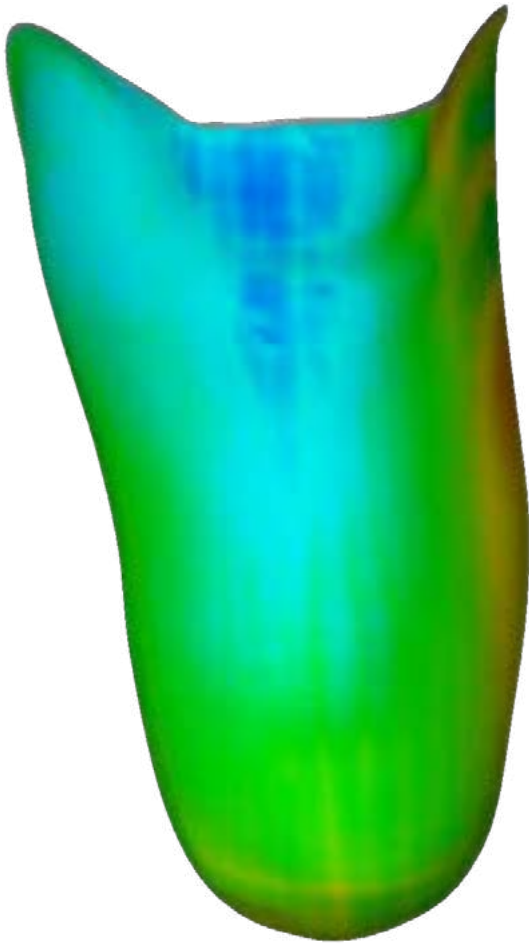
$$\min \left(\frac{A}{A_t} \left(1 + \frac{\|F - F_t\|}{\|F_t\|} \right)^\mu \right), \mu \in \mathbb{Z}$$

$$\text{subject to } \begin{cases} \sigma < \sigma_{\text{yield}} \\ \text{Post-buckling mode} = \text{Mode II} \end{cases}$$

- A: area
 A_t : area of the target nudged structure
 F : force at certain displacement
 F_t : force of the target nudged structure at certain disp.

Bibliography

- [1] Cox, B. S., Groh, R. M. J., Avitabile, D., & Pirrera, A. (2018). Modal nudging in nonlinear elasticity: Tailoring the elastic post-buckling behaviour of engineering structures. *Journal of the Mechanics and Physics of Solids*, 116, 135–149.
- [2] Cox, B. S., Groh, R. M. J., & Pirrera, A. (2019). Nudging Axially Compressed Cylindrical Panels Toward Imperfection Insensitivity. *Journal of Applied Mechanics, Transactions ASME*, 86(7).

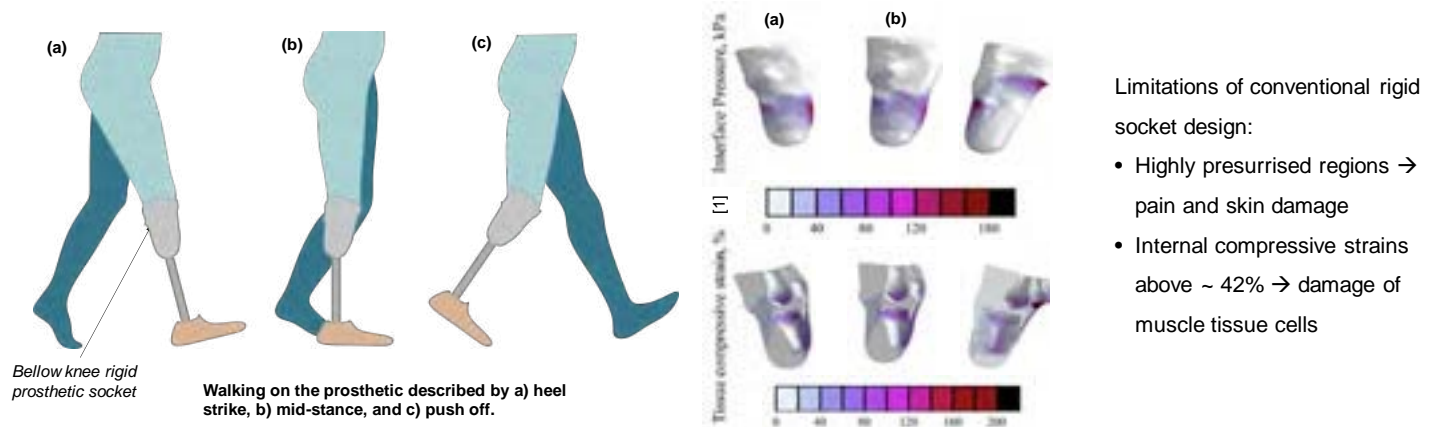


MANUFACTURING AND DESIGN

Design optimisation of an adaptive composite prosthetic socket

Kevin Alarcón, Alex Dickinson, Elena Seminati, Ole Thomson, ByungChul (Eric) Kim

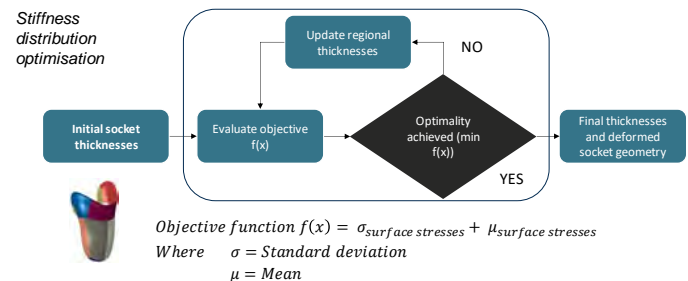
Introduction: Up to 82% of lower limb amputees report soft tissue injuries from using their prosthesis. Thus, up to 57% choose to abandon their prosthesis.



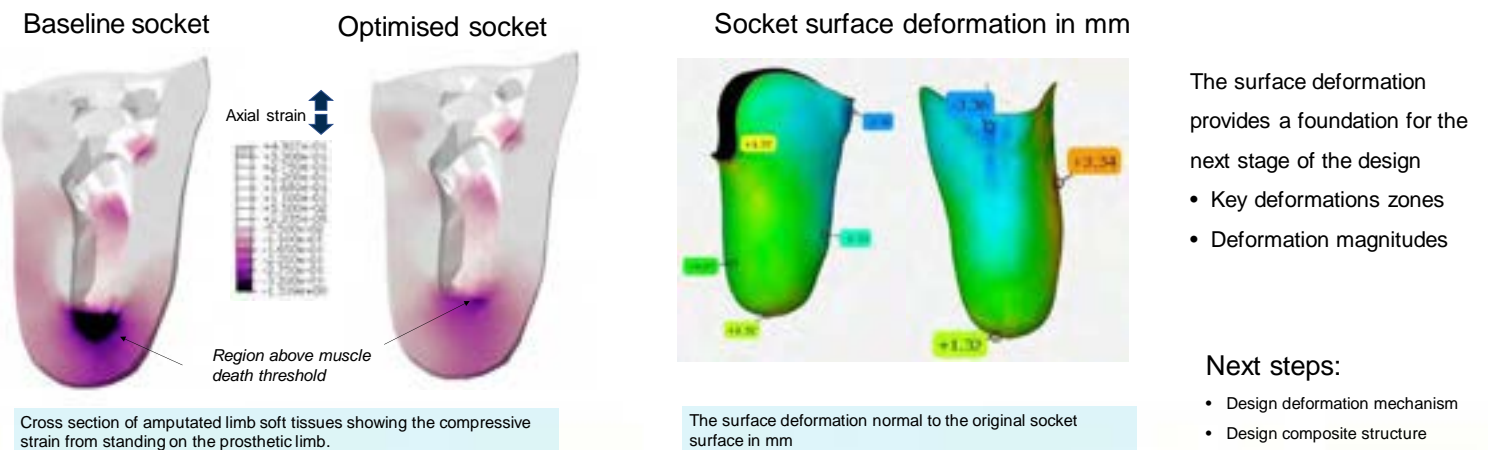
Methods: Design socket which self-deforms under load to avoid excessive soft tissue strains

Optimise stiffness distribution through FE-based optimisation

- CT-scan based FE model of socket and limb
- Model validation against experiment (digital volume correlation)



Results: The volume of soft tissue at risk of injury is significantly reduced by optimising the deformed socket shape.



References

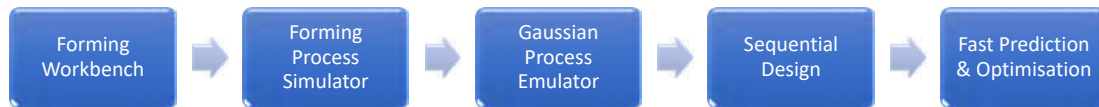
1. Kobayashi, T., Orendurff, M.S., Zhang, M. and Boone, D.A., 2016. Socket reaction moments in transtibial prostheses during walking at clinically perceived optimal alignment. *Prosthetics and Orthotics International*, 40(4), pp.503-508.
2. Rankin, K., Steer, J., Paton, J., Mavrogordato, M., Marter, A., Worsley, P., Browne, M. and Dickinson, A., 2020. Developing an analogue residual limb for comparative DVC analysis of transtibial prosthetic socket designs. *Materials*, 13(18), p.3955.

Fast Optimisation of the Formability of Dry Fabric Preforms: a Bayesian Approach

Siyuan Chen, Adam Thompson, Tim Dodwell (Exeter University), Stephen Hallett and Jonathan Belnoue

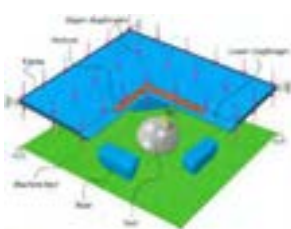
Composites are becoming increasingly important for light-weight solutions in the transport and energy sectors. In the field of composites manufacture, resin transform moulding (RTM) is a cheaper alternative to traditional manufacturing method. Before resin infusion, the fabric is to be formed into shape, however, the quality of forming is highly sensitive to wrinkles. These defects could induce considerable reduction to the quality of final parts. Simulation is a good way to understand the process and help to investigate the effect of the forming parameters (such as pressure and tensile forces) to wrinkle generation. Current BCI's forming process simulation tool can make high quality predictions but have long run times. On the other hand, we need large batches of simulations to find the forming conditions that minimise defects.

The project aims at exploring a new framework for the efficient optimisation of the processing conditions in the dry fibre forming process. This is achieved by building a Gaussian Process (GP) emulator that is trained from finite element (FE) simulation data. The work opens the door for digital twin. Longer term, a fully autonomous forming rig that allows defect mitigation by automatic adaptation of the process based on in-situ measurements and predictions from the GP will be built.



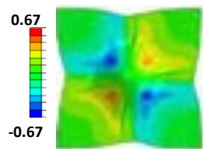
FE simulations

- Double-diaphragm forming.
- Single layer of dry NCF, hemisphere mould geometry.
- Risers used to provide tensions to eliminate wrinkles.
- UoB Hypodrape subroutine, mutually constrained membrane and shell elements, 2mm mesh.

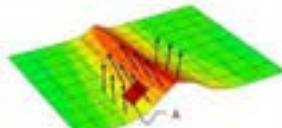


Scheme of the forming process [1]

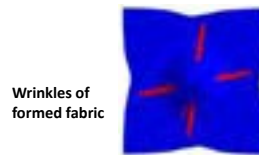
Shear angle (rad)



Experimental picture in [1]



WI = Variance of element normal of A and its adjacent elements



Wrinkles of formed fabric

Wrinkle index (WI)

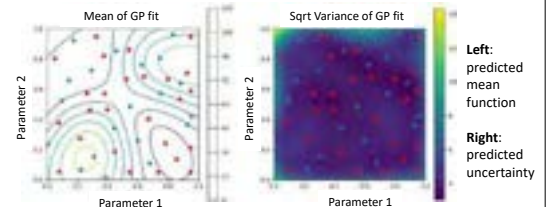
- A metric that measures the level of wrinkling near an element.
- **Sum of squared wrinkle index (SSWI)**
A value that reflects the overall wrinkling level of a formed fabric.

Gaussian Process (GP) emulator

- A machine learning method, mathematically tractable.
- Only needs a few data points to make **accurate predictions and uncertainty quantification**.
- **Input:** position of four risers **Output:** SSWI
- Each data point represents a simulation.

Sequential Design

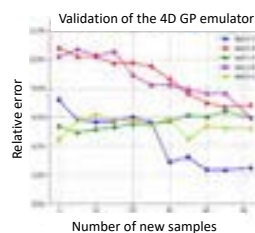
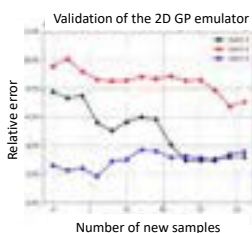
- Iterative addition of supplementary data points, to improve model predictive capabilities.



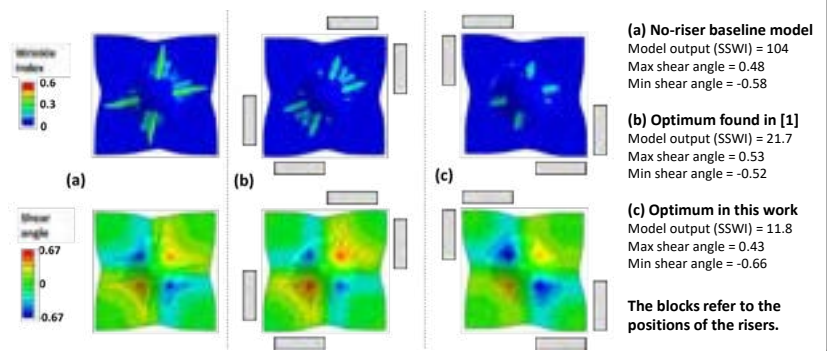
Blue points: initial training set (20 samples), by Latin Hypercubic Sampling
Red points: supplementary training set (26 samples), by sequential design

Validation of the GPs

- A 2D GP (two parameters) and a 4D GP trained
- For most validation batches, predictive deviations reduced during sequential design. Batch 5 and 7 are good initially.
- Final predictive error is lower than 10%.



Optimisation of forming process by GP: wrinkle level significantly reduced



[1] S. Chen, O. P. L. McGregor, L. T. Harper, A. Endruweit, and N. A. Warrior, "Optimisation of local in-plane constraining forces in double diaphragm forming," *Compos. Struct.*, vol. 201, no. January, pp. 570–581, 2018, doi: 10.1016/j.compstruct.2018.06.062
[2] S. Chen, A. Thompson, T. Dodwell, S. Hallett and J. Belnoue, Fast Optimisation of the Formability of Dry Fabric Preforms: A Bayesian Approach. Available at SSRN: <https://ssrn.com/abstract=4363693> or <http://dx.doi.org/10.2139/ssrn.4363693>

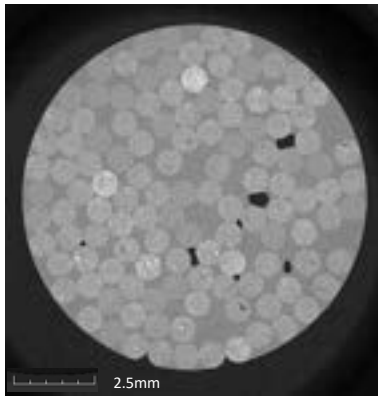
S. Chen in [1] is not me!

Manufacture of Struts with CFRP rod reinforcements

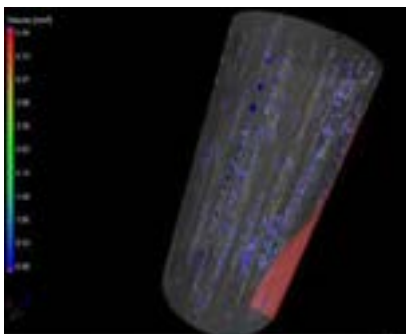
Nicolas Darras, Laura Rhian Pickard, Giuliano Allegri, Richard Trask and Michael Wisnom

One of the main limitations of Fibre Reinforced Polymer (FRP) composites is low compressive strength due to kink bands, which are greatly affected by misalignment of the fibres. One way to improve their alignment is to manufacture the composite by pultrusion, the original tension applied to the fiber leads to a better alignment. Furthermore, hierarchical composites can delay the kink band, thanks to obstacles within the structure preventing the propagation of the failure. One potential route for hierarchical composites is to integrate rods into bundle systems such as thick plies or struts. Nevertheless, the manufacture of circular cross-sections and void-free struts is not trivial but can be achieved with Resin Transfer Moulding (RTM). This work seeks to investigate how to overcome the challenges of manufacturing struts reinforced with pultruded Carbon Fibre Reinforced Polymer (CFRP) rods, from the diminution of voids to the demolding of the parts.

CHALLENGES

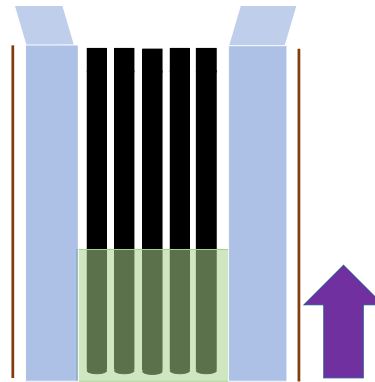


High porosity (0.82%) and nonhomogeneous distribution of 0.8mm rods within the sample. Injection of resin made with low pressure.



CT scan of strut demolded from pipe with Dremel, sample damaged during process.

CURRENT SOLUTION

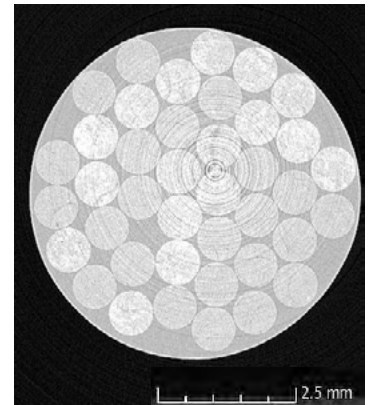


Drawing of the RTM set-up: the hose is in blue, the copper pipe in brown, the rods in black and the resin in green.

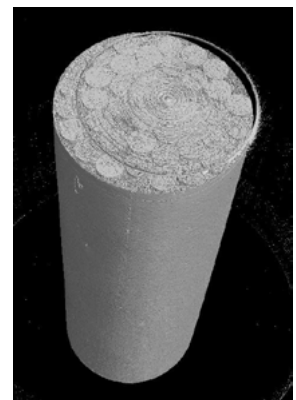


Picture of the set-up performed at the National Composite Centre (NCC)

RESULTS



CT Scans of the struts made with 0.8mm rods and following the new process at the NCC.



No porosity has been detected with a CT scan. Voids are too small to be detected.

The strut is created by integrating the pultruded rods in a silicon hose for resin injection. A copper pipe is used as a mould to constrain a circular cross-section during the process. Low pressure is first applied, before increasing it little by little, to remove as much as possible the air from struts and preventing the creation of voids and decreasing its porosity. Rings have been placed from each side of the copper pipe tube to pinch the hose and prevent the rods from moving during resin injection.

Design strategy for 4D printed flax fibre PLA composite biomimicking humidity triggered actuators

C. de Kergariou*, A. Le Duigou, A. Perriman, F. Scarpa

*corresponding author:charles.dekergariou@bristol.ac.uk

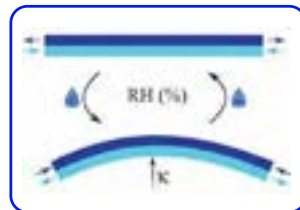
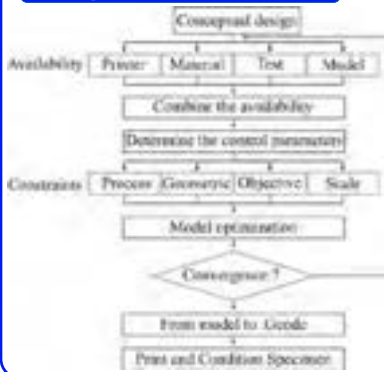
[0]-Abstract

We have proposed a holistic review and a set of design guidelines [1] for 4D-printed macroscale composite actuators triggered by humidity (**hygromorphs**). The design guidelines discussed in the review were implemented to explore the design space for 4D printed continuous flax fibre reinforced poly(lactic acid) hygromorph structures. Material properties like porosity [2], mechanical [3] and hygro-expansion [4] have been measured first and the used to convert 3D printing G-codes in Finite Element models [5]. Sets of materials and printing geometry have been derived from the design space [6] to create Calla lily and leaf biomimicking structures [7].

Paper

de Kergariou et al., "The Design of 4D-Printed Hygromorphs: State-of-the-Art and Future Challenges," Adv. Func. Mat., vol. 33, 2023.

Design Process



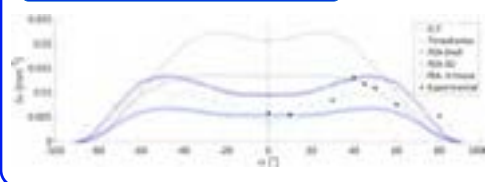
[1]-Review

- ✓ Design guidelines
- ✓ Optimize, condition, produce, model

[6]-Design Space

- ✓ Greater responsiveness
- ✓ No anticlastic double curvature

Models vs Experiment



Improved actuation?



Paper

de Kergariou, et al., "Design space and manufacturing of programmable 4D printed continuous flax fibre poly(lactic acid) composite hygromorphs," Mat. Des., vol. 225, 2023.

Parameters influencing actuation

- Porosity
- Mechanical
- Hygro-expansion
- Fibre Path

[2]-Porosity

- ✓ Define best strategy for porosity measurement



Paper

Kergariou, et al., "Measure of porosity in flax fibres reinforced poly(lactic acid) biocomposites," Compos. Part A, vol. 141, 2021.

[3]-Mechanical

- ✓ Influence of humidity on mechanical properties



Paper

de Kergariou, et al., "The influence of the humidity on the mechanical properties of 3D printed continuous flax fibre reinforced poly(lactic acid) composites," Compos. Part A, vol. 155, 2022.

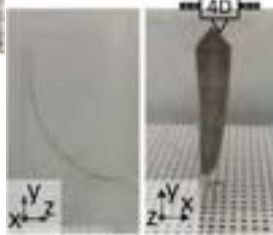
[4]-Hygro-expansion

- ✓ Thickness, length, width dimensions

[7]-Biomimicking



Calla Lily

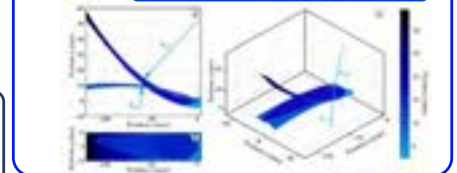


Leaf

[5]-Model

- ✓ Create model for continuous filament
- ✓ Validation model with experiment

Actuation



In house model



Paper

de Kergariou et al., "Design of 3D and 4D printed continuous fibre composites via an evolutionary algorithm and voxel-based Finite Elements: Application to natural fibre hygromorphs," Add. Manuf., vol. 59, 2022.

DcAFF

Discontinuous Aligned Fibre Filament for 3D Printing :Production, Printing and Performance

Narongkorn Krajangsawadi, Ian Hamerton, Benjamin K.S. Woods, Dmitry S. Ivanov, and Marco L. Longana

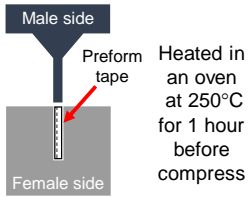
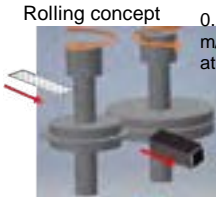
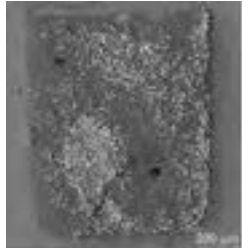

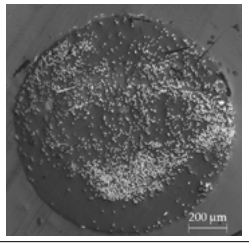



DcAFF (Discontinuous Aligned Fibre Filament) is a novel composite material for 3D printing or, fused filament fabrication (FFF), where highly aligned discontinuous fibres, produced using the High Performance Discontinuous Fibre (HiPerDiF) technology, reinforce a thermoplastic matrix to provide high mechanical performance while retaining high formability.

Production

The main challenge of filament production is to form the HiPerDiF thin composite tape into a circular cross-section filament while preserving fibre length and a high level of alignment.

There are two main steps in filament-forming:

1. Bulking tape into a square-like cross-section;
2. Hot-pultrusion through several nozzles to form a circular cross-section filament

	Initial trial with manual moulding	Semi-automated method
Bulking Tool	 <p>Male side Preform tape Heated in an oven at 250°C for 1 hour before compress Female side</p>	 <p>Rolling concept 0.2-0.5 m/min at 130 °C</p>
After Initial Forming		
After Nozzle Pultrusion		
	 Controllable bulked shape (low voids)	High production rate (~50 cm/min)
	 Slow process (< a meter per hour)	Inconsistence pressure (small internal voids)

Printing

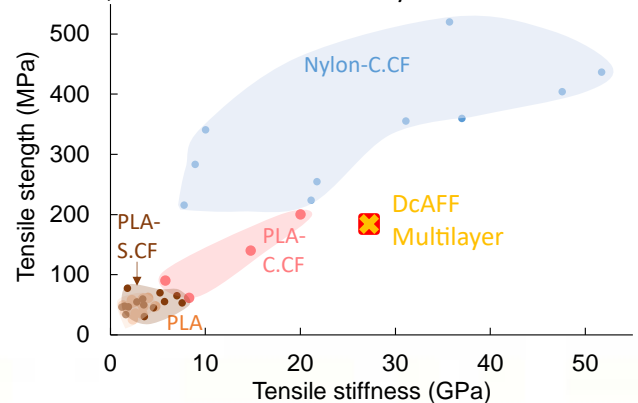
- ✓ Accurate deposition when printing of straight line, or low curvature geometry
- ✗ Poor accuracy when printing tight radius corners, or high curvature turning



Performance

Tensile properties of DcAFF (PLA-carbon fibre) compared to other composite 3D printing materials: PLA, PLA-short carbon fibre (PLA-S.CF), PLA-continuous carbon fibre (PLA-C.CF), and nylon-continuous carbon fibre (nylon-C.CF)

DcAFF is better than other PLA composites, particularly PLA-C.CF, but it is still lower than nylon-C.CF



Investigating the performance of HiPerDiF 3G composites using a hybrid design

Chantal Lewis¹, Rhys Tapper², Mark Harriman², Marco Longana³, Carwyn Ward⁴ and Ian Hamerton¹

¹Bristol Composites Institute, University of Bristol

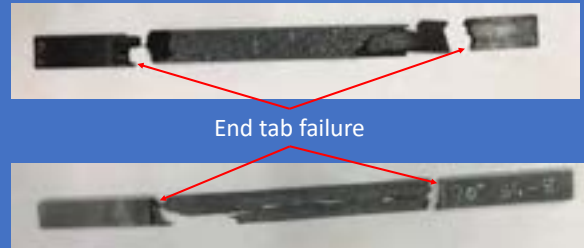
³Department of Chemistry, Politecnico di Milano

²Solvay Composite Materials

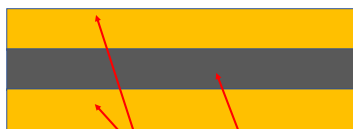
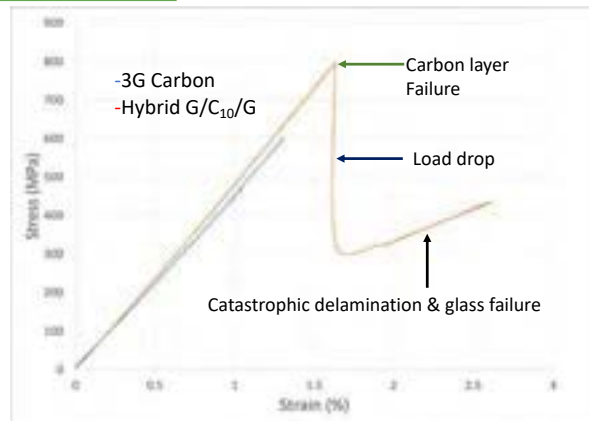
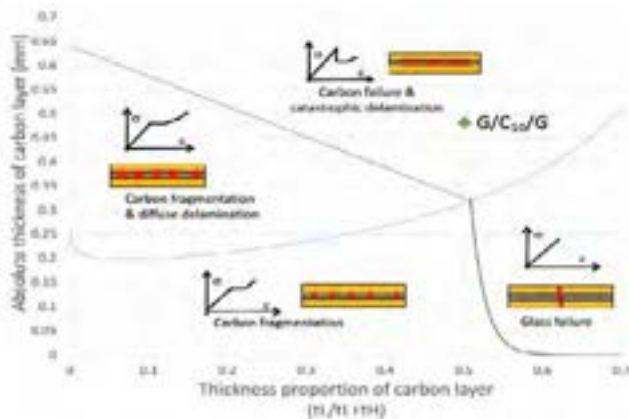
⁴School of Engineering, UWE Bristol

Introduction

Unidirectional aligned discontinuous fibre reinforced composite (ADFRC) samples made using the HiPerDiF 3G machine exhibited premature failure due to the stress concentration at the end tabs. To avoid this, Interlaminated hybrid specimens were produced and mechanically tested to obtain a more accurate value for the failure strain of the ADFRC material.



Specimen design & testing



High strain material
(MTM49 glass)

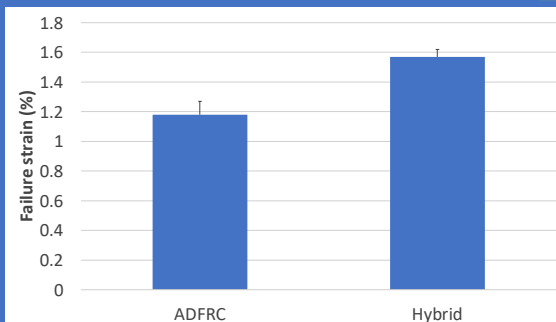
Low strain material
(ADFRC 3G carbon)

- Altering the absolute and relative thickness controls the failure behaviour
- Desired failure mode = carbon layer failure and catastrophic delamination



- Tensile testing as per ASTM D3039/3039M

Conclusion & future work



- Using Interlaminated specimen identified failure strain with **higher confidence**
- Next steps is to apply the same methodology to the characterisation of other specimen types:
 - 3G Specimen with 6mm fibres
 - UD-Continuous prepreg

Characterising the reflow behaviour of semi-cure laminates

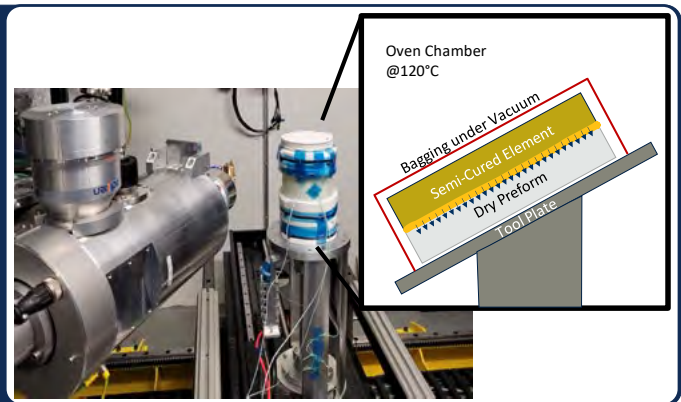
M. O'Leary, A. Radhakrishnan, K. Gaska, E. Nazemi, F. A. Borger, M. Mavrogordato, I. Sinclair T. McMahon, and J. Kratz

Introduction:

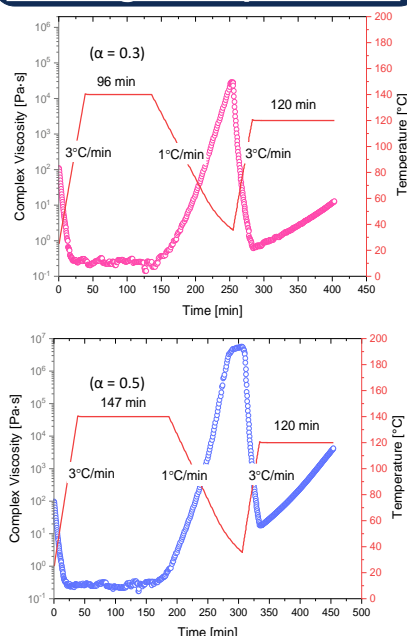
Semi-Curing is an emerging manufacturing technology, and when applied to Liquid Composite Moulding (LCM), involves the initial infusion and partial cure of elements which are then integrated into a wider structure for further LCM steps. These further infusions and cures are often done at temperatures where there is the potential for the initially semi-cured material to reflow. This poster outlines how we have explored the potential for reflow in the semi-cured material through *in-situ* and *ex-situ* CT scanning.

CT Setup

- Semi-cured elements with α of 0.3, 0.6, 0.7, 0.8 were cut into 25x25mm and paired with matching 25x25mm dry fabric preforms
- Initial oven trials allowed for *ex-situ* samples to be produced
- The *in situ* rig developed by P. Galvez Hernandez was used in the Custom 450/225 kVp Hutch at the university of Southampton 25 μ m resolution was achieved in these scans
- 1 scan was taken every 2 minutes
- *Ex-situ* scans were taken in the diondo d5 with 10 μ m resolution



Rheological Experiments



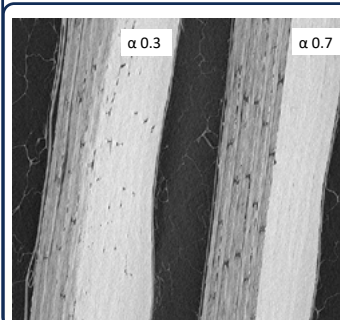
Initial rheological tests were run on neat resin samples to explore if there was any indication of the potential for reflow prior to exploring reflow *in-situ*

Thermal Profiles Explored

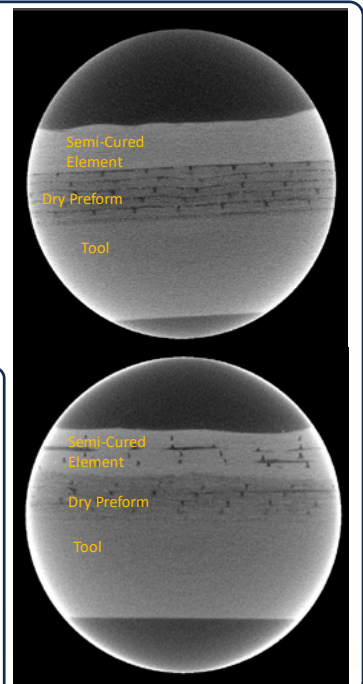
In each of the *in-situ* scans, the samples were ramped to injection temperature and held there for a period of 2 hours before being cooled back down. This was done to simulate an initially semi-cured part coming to temperature prior to infusion.

Scan Results

- The adjacent CT slices show the first and last scan of the experiment in the middle of the sample
- This is a low degree of cure sample of $\alpha = 0.3$
- The initially void free semi-cured element can clearly be seen to have new void formations within it
- Further work must be done to explore the formation of these void areas.



These samples were thermally cycled prior to CT scanning. The 0.3 samples can clearly be seen to exhibit reflow while the higher degree of cure sample has not flowed.



Thermal Management Techniques in FRP Composites for Applications in Rotorcraft

Toby Wilcox^{a*}, Richard Trask^a, Ian Bond^a, Julian Booker^b, Ian Farrow^a

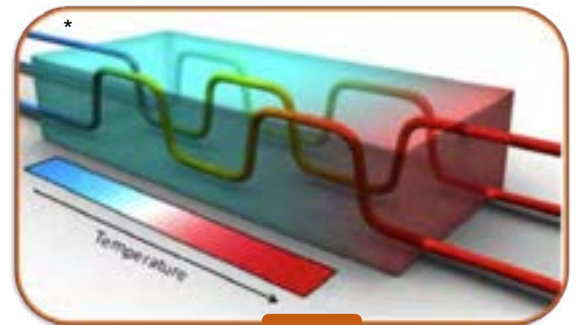
^aBristol Composites Institute, Queens Building, Bristol, BS8 1TR ^bElectrical Energy Management Group, Queens Building, Bristol, BS8 1TR *Author (toby.wilcox@bristol.ac.uk)

Overview

As rotorcraft move gradually away from conventional drives and mechanisms and more towards electronic components and hybridisation, the need for effective regulation of heat has never been higher. Fibre Reinforced Polymers (FRPs) already have widespread applications in the aerospace industry for both primary and secondary structures. They are however poor thermal conductors and have relatively low working temperatures, making them unsuitable for use in areas of elevated temperature or where significant heat removal is required. If these thermal properties could be improved, the potential applications could be numerous. Two techniques are being investigated in this project: A passive system using Z-pins to improve the through-thickness conductivity of an FRP laminate, and an active technique involving a system of embedded microchannels through which a coolant can be passed to aid heat removal through the laminate. The aim of this project is to determine if one or both of these techniques can be used to significantly improve the thermal characteristics of the FRP composites without having a marked effect on their mechanical properties. This will be investigated through thermal testing of manufactured samples, relevant mechanical testing, and the development of a numerical model to analyse the optimum process parameters and to predict thermal profiles.

Passive

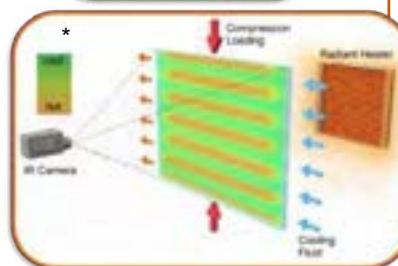
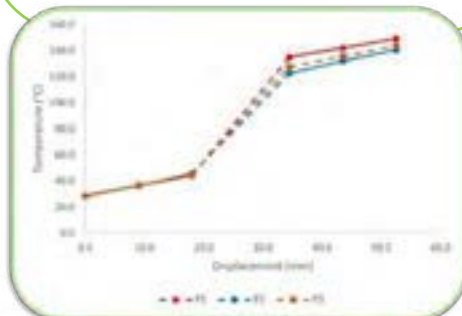
- Carbon Z-pins inserted into FRP prepreg before cure to create array
- Pins create channels to conduct heat through the sample
- Samples undergo Heat Flow Meter testing
- Samples held in compression in material stack between steel blocks
- Heat applied from bottom; cooling applied from top
- Temperature recorded across the stack at various displacements
- Temperature ranges are used to calculate the thermal conductivity of the samples
- Results show improved thermal conductivity in pinned samples when compared to unpinned samples
- Overall, a 12% increase was achieved
- Contact conductance also showed a similar improvement
- Further testing is need to investigate the optimum pins material, dimensions, and array



Active

- Microchannels can be inserted into dry fibre preform using one of several techniques
- Creates a network of interconnected channels across multiple planes
- Coolant can be pumped through the system to facilitate heat removal
- Samples can be thermally tested to determine the improved rate of heat removal
- Mechanical testing can also be carried out to determine knock-down factors and effects on survivability at elevated temperatures
- Studies have shown a marked improvement in thermal performance
- Much more work needed to optimise channel parameters and integrate system
- Numerical model can be developed to study channel properties and to validate experiments

* Images courtesy of Anthony M. Coppola, Ph.D.



On-line consolidation of thermoset prepregs : Analysis of laminate quality

Axel Wowogno, Iryna Tretiak, Stephen R. Hallett and James Kratz

This work aims to assess the behaviour of thermoset based prepregs in an Automated Fibre Placement (AFP) process context, where the added material is being heated while being laid. After having analysed the effect of the process parameters (time, temperature, pressure) on thickness evolution, attention is brought on the process related imperfections: voids and defects.

Materials

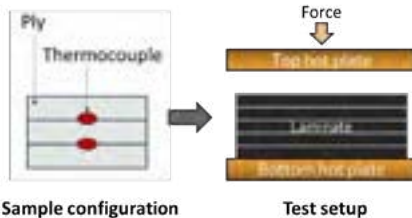
➤ **Out of Autoclave prepreg (OOA):** Hexcel M56/IM7 and **Snap Cure Resin prepreg (SCR):** Hexcel M78.1

Methods

➤ **Material Characterisation :** Analyse the influence of AFP parameters on laminate thickness
➤ **CT-scan :** Analyse porosity

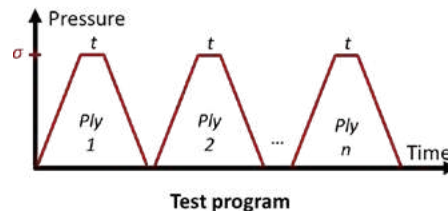
Sample preparation

- Cross-ply configuration
- Embedded thermocouples



Testing program

- Ply-by-Ply compaction :
5, 10, 20 plies



Key Process Variables

- **Pressure magnitude**
Fixed at 0.1 MPa
- **Pressure application time**
1s – 10s
- **OOA Temperatures**
120 – 210°C
- **SCR Temperatures**
100 – 160°C

Results

➤ **OOA prepreg** ➔ Noticeable impact of temperature on porosity and thickness

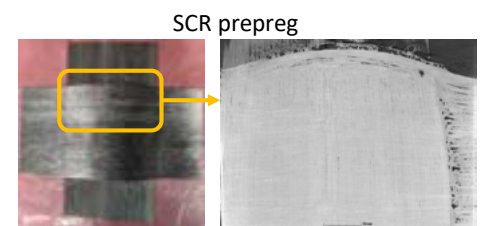
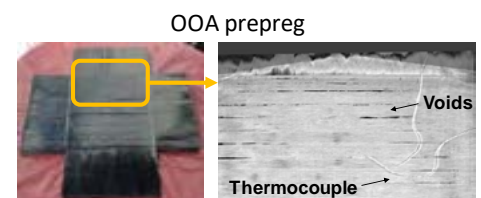


➤ **SCR prepreg samples** ➔ Observation of defects during the compaction test



- **Higher T°**
= Faster curing
= More defects
= Inter-ply voids
- **Best T° = 130°C**
- Least defects

➤ **Effect of process parameters:**
10 plies @ 120°C & 0.1Mpa – 2.5s/ply
(Scans = top view of the central plies' interface)



Conclusions

➤ **Out of Autoclave prepreg (M56)**

Time ↑ = Void level ↓
Temperature ↑ = Thickness ↓

➤ Usual cure cycle = 2h dwell @ 180 °C ➔ AFP with higher temperatures would permit high-quality preform production

➤ **Snap cure resin prepreg (M78.1)**

Time ↑ = Void level ↓ then ↑
Temperature ↑ = Thickness ↓

➤ Creation of high-quality laminates at lower temperatures
➤ Offers opportunities for shorter consolidation processes

Tensile Characterisation of HiPerDiF PLA/Short Carbon Fibre Tape Under Processing Conditions with Micromechanical Model

Burak Ogun Yavuz, Ian Hamerton, Marco L. Longana and Jonathan P.-H. Belnoue

Aim: Material characterisation for forming simulations of aligned discontinuous fibre thermoplastic (HiPerDiF) prepreg by using micromechanical model

Manufacturing Method

1

Impregnation

① Vacuum Mould
② Vacuum Bag
③ Pre-impregnated PLA Tape
④ HiPerDiF Prepreg
⑤ Vacuum Part
⑥ Sealant

@ 195 °C
Under Vacuum Pressure For 4 Hours

One batch of production

Specimen

Cross section

Fibre Volume fraction ≈ 35%

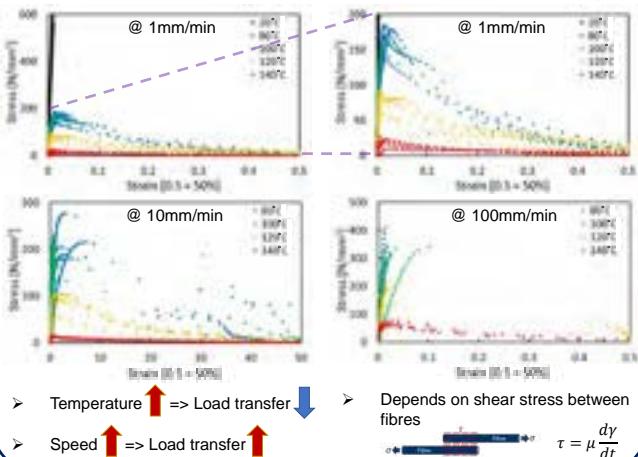
Tensile Characterisation under Processing Conditions

2

Test setup

- @ 20 °C, 80 °C, 100 °C, 120 °C, and 140 °C
- @ 1mm/min, 10mm/min, 100mm/min crosshead speeds
- Shimadzu electromechanical test machine
- Thermal Chamber
- 10 kN load-cell
- 5MP Stereo DIC
- Strong LED light source

Tensile behaviour temperature and speed dependency



Rheology and DSC of PLA

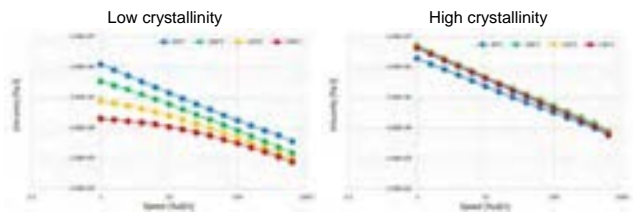
3

Rheology test setup

- 170 °C contact temperature
- Oscillations
- From 1 rad/s to 628 rad/s
- @ 80 °C, 100 °C, 120 °C, 140 °C
- 0.5mm thickness

Temperature history

Viscosities with two different temperature history



Differential scanning calorimetry (DSC)

- 1°C/min ramp rate
- 20°C>190°C>20°C>190°C>20°C>110°C>20°C>190°C
- PLA and PLA/Carbon fibre
- Low temperature crystallization is stronger than recrystallization and ends about 100 °C
- Annealing up to 110 °C creates high level of crystallinity

Micromechanical Model

4

- Shear rate dependent storage modulus ($G(\dot{\gamma})$) and corresponding viscosity ($\eta(\dot{\gamma})$) data taken from rheology experiment with high crystallinity
- Fibre length (L)=3mm, Diameter (D)=7μm, Fibre volume fraction (f)=0.35, Overlap length (δ)=1.5mm, Fiber volume fraction parameter (K)=2.64

$$\sigma = 2\tau f \frac{\delta}{D}$$

Shear stress to Tensile stress

$$\sigma = \left(2G(\dot{\epsilon}) \left(\frac{L-\delta}{D} [K-1] f \frac{\delta}{D} \right) \dot{\epsilon} - \left(\frac{G(\dot{\epsilon})}{\eta(\dot{\epsilon})} \right) \sigma \right)$$

Micromechanical model

$$\tau + \frac{\eta}{G} \dot{\tau} = \eta \dot{\gamma}$$

Maxwell viscoelastic model

$$\dot{\gamma} = \frac{L-\delta}{D} [K-1] \dot{\epsilon}$$

Shear strain to Tensile strain

Future work: Implementing material behaviour into forming simulations → Forming defect free parts experimentally



DESIGN, BUILD AND TEST

CDT22 – Design, Build and Test. Sequential Instabilities for Actuating Aerodynamic Surfaces

Asaad Biqai, Ragnar Birgisson, Jacopo Lavazza, Matthew Leeder, Matthew Lillywhite, Will Mahoney, Joe Rifai, Gökhan Sancak, Jan Uszko, Anna Williams

Embracing structural instability, not as a possible failure mode, but as a route to new functionality, can lead to promising applications in morphing structures. One possible application is in passively actuated wing spoilers, where sequential instability can be exploited to trigger the rapid deployment of a bistable composite spoiler panel after a spanwise beam has buckled due to gust-induced wing deformation. This sequential instability interaction between an Euler beam and a bistable composite shell has been previously modelled using finite element analysis [1]. In this project, the previous analysis will be validated with the manufacturing and testing of a physical prototype.

AIM

By buckling an Euler beam, in contact with an antisymmetric, bistable composite laminate shaped to the upper surface of an aerofoil, we seek to instigate a sequential, interacting instability to demonstrate utility for passively actuated wing surfaces.

MODELLING

Finite element model used to inform design of experiment and to predict behaviour.

Displacement response of model will be compared with gathered experimental data.

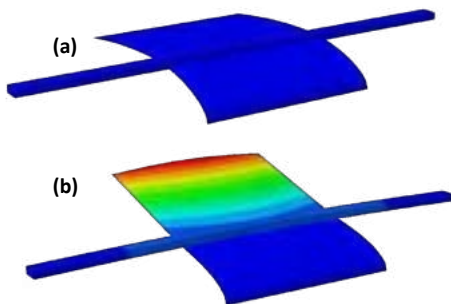


Fig.1. (a): Undeformed model. (b): Deformed model with displacement contours.

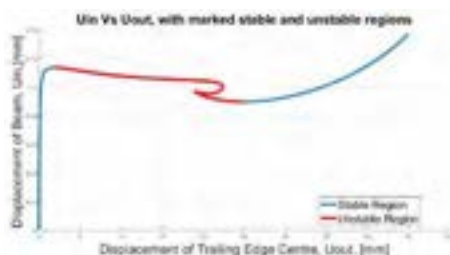


Fig.2. Displacement response of the FE model.

MANUFACTURE

Laminate Details:

- 2/3 chord length of NACA 4312 aerofoil.
- Width: 150 mm.
- Layup: [+45,-45,0,+45,-45].
- Two laminates produced from two prepreg systems.

Hand layup with vacuum bag.

Manufactured on an aerofoil profile tool.

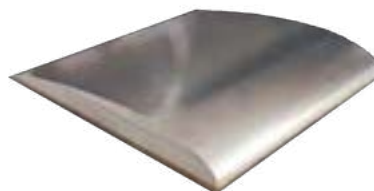


Fig.3. Aerofoil tooling block.

Oven cure for first system.

Autoclave cure for second system.

Beam Details:

- Steel
- 15 mm x 5 mm x 400 mm

TESTING

Beam will be compressed under displacement control to instigate sequential instability.

Stereo DIC will be used to record displacement response as the beam and laminate buckle.

Thin force sensor used to measure contact between beam and laminate.

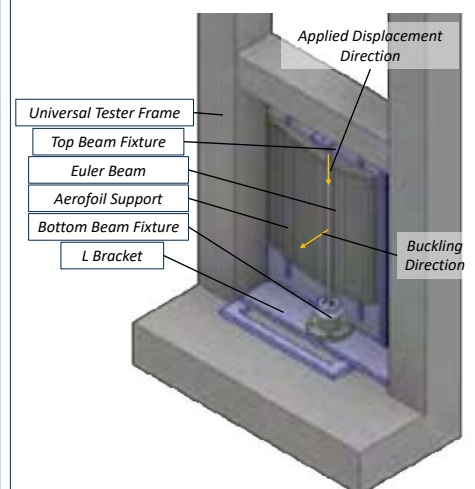


Fig.4. Schematic of test setup.

composites-institute@bristol.ac.uk

 @UoBrisComposite

Queens Building,
University Walk,
Bristol, BS1 8TR